PREFACE

We would like to introduce the report of the scientific activity of the Frank Laboratory of Neutron Physics for 1996. The first part is a brief review of the experimental and theoretical results of investigations in condensed matter physics, nuclear physics and applied research. The second part presents the investigations which characterize the main directions of research in greater detail. The reader can receive a more complete picture of the research carried out in the Laboratory from the list of publications for 1996 following Part 2.

A technical project for the IBR-2 modernization has been developed. "Agreement on realization of the plan for upgrading the IBR-2 reactor in 1996-2005" has been drawn up and approved. If we manage to successfully implement the modernization project, by 2005 a new unique reactor which will exhibit record parameters wiil work for 25-30 years wiil be created.

Further development of the User Policy continued, aimed at attracting a larger number of physicists, chemists, biologists, and specialists in materials science to carry out experiments at the IBR-2 reactor. In 1996, the number of submitted proposals for experiments was 153, the largest for the recent 3 years. The proposals came from 23 countries, including nonmember-states of JINR. On the average, the requested beam time was 2.5 times larger than that available.

The financial situation in the Laboratory changes drastically compare with the previous years. Deficit financing and delays in funding the IBR-2 modernization project (about 25% of the plan) resulted in the suspension of work in all directions of the modernization project, because of deficit financing, a considerable delay in fulfilment of the IREN project has to be noted. Instrument upgrades and the scientific program were provided for mainly from financial contributions in the frame of JINR-FRG and JINR-Hungary agreements for cooperation, as well as from other programs and funds.

The Frank Laboratory of Neutron Physics is one of the leading neutron centers of Europe and continues to develop in spite of the difficulties its host country is currently experiencing.

V.L.Aksenov
Director

28 February 1997

1.1. CONDENSED MATTER PHYSICS

General situation at the IBR-2. Fourteen neutron beams are extracted to the experimental halls of the IBR-2 reactor. On nine of them, neutron spectrometers for investigations in condensed matter physics are positioned. Three of nine beams are split into two by means of optical systems and as a result, the experimenters have twelve spectrometers (see the Table). After the replacement of the movable reflector in March 1995, the reactor operates stably and as a rule, in accordance with the adopted schedule.

Spectrometers for investigations in condensed matter physics. To conduct condensed matter investigations at IBR-2, four main techniques are applied: diffraction, small-angle scattering, inelastic scattering, and polarized neutron optics.

The group of diffractometers includes **HRFD**, the high resolution Fourier diffractometer for analyzing the structures of polycrystal substances, as well as internal stresses in bulk samples for industrial application products, **DN-2**, the multipurpose diffractometer for investigations of single crystals and long-range structures and for experiments in real-time mode, **DN-12**, the diffractometer for investigations of microsamples primarily at high pressures, and **NSVR**, the multidetector diffractometer for texture investigations.

Also, one small-angle scattering spectrometer, **YuMO**, exists and allows a diverse program of investigations into large-scale inhomogeneities (macromolecules in solutions, micelles, density fluctuations in hardening concretes, etc.) to be carried out.

The group of inelastic scattering spectrometers includes **DIN**, the direct geometry spectrometer with a fast chopper mainly designed for investigations of liquids (quantum and classical), **KDSOG**, the inverted geometry multidetector spectrometer-diffractometer for investigations of the phonon density of states and phase transitions, and **NERA**, the inverted geometry spectrometer with crystal analyzers for investigations of inelastic and quasielastic scattering in hydrogen containing substances, as well as for molecular spectroscopy.

The group of neutron-optical instruments includes **SPN**, the polarized neutron spectrometer operating both in the transmission mode (depolarization) and reflectometer modes, **REFLEX-P**, the polarized neutron reflectometer, and **REFLEX-N**, the nonpolarized neutron spectrometer. The experiments with the reflectometers are conducted with the beams reflected in the horizontal plane.

User program. The 1996 list of the IBR-2 spectrometers operating in the user mode includes 9 instruments: HRFD, DN-2, NSVR, YuMO, SPN, REFLEX-P, KDSOG, NERA, and DIN. The beam time is distributed in accordance with experts recommendations on the submitted proposals and the existing long-term agreements for cooperation. The new spectrometer on the list is the REFLEX-P with its first stage commissioned for test operation in the spring. At present, DN-12 is under radical modernization to be completed by the middle of 1997. The formation of the neutron beam on REFLEX-N was completed, but its operation has been temporarily suspended in connection with the necessity to concentrate efforts on the provision of the experimental program for REFLEX-P. The SNIM spectrometer was closed in 1996 in accordance with the recommendations of the Program Advisory Committee.

The main parameters of the spectrometers and their sample environment systems meet the world level standards. The number of countries from where applications for beam time were received has increased to 23. The application for the 1996-II round is 1.6 times larger than for the 1996-I round. This is connected with that the user program is being continually developed, as well as with the increased activity of the spectrometer leaders. The user program can be extended by increasing the number of experiments on DN-2, REFLEX-P, DN-12, and DIN.

Execution of the scientific program. The formation of the program was determined by the parameters of the existing spectrometers and users' demands. The main directions of research have been almost the same for a few recent years.

Diffraction. At the IBR-2, neutron diffraction is used to investigate the atomic structure of polycrystalline materials, phase transitions in crystals under the action of external fields, crystals with incommensurable structure modulation, structure of novel materials (HTSC, GMR-compounds, superprotonics, etc.), multilayer lipid membranes, orientational magnetic phase transitions, texture of rocks, metals and alloys, and internal stresses in bulk samples, composite and gradient materials.

In 1996, the program for investigations of mercury-based superconductors by neutron diffraction continued. In the HRFD experiments, precision structural data were obtained. These allowed the dependence of the superconducting transition temperature on the excess oxygen content to be determined. This dependence appeared to be a parabolic one with the maximum at about 0.20 free charge carriers per CuO_2 layer, in agreement with the established idea of the formation mechanism of superconducting properties in layered copper oxides (V.L.Aksenov, E.V.Antipov, A.M.Balagurov et al., Phys. Rev. 1997). Experiments to determine the symmetry of a low temperature superconducting phase (Fmmm or Cmca from the data in the literature)

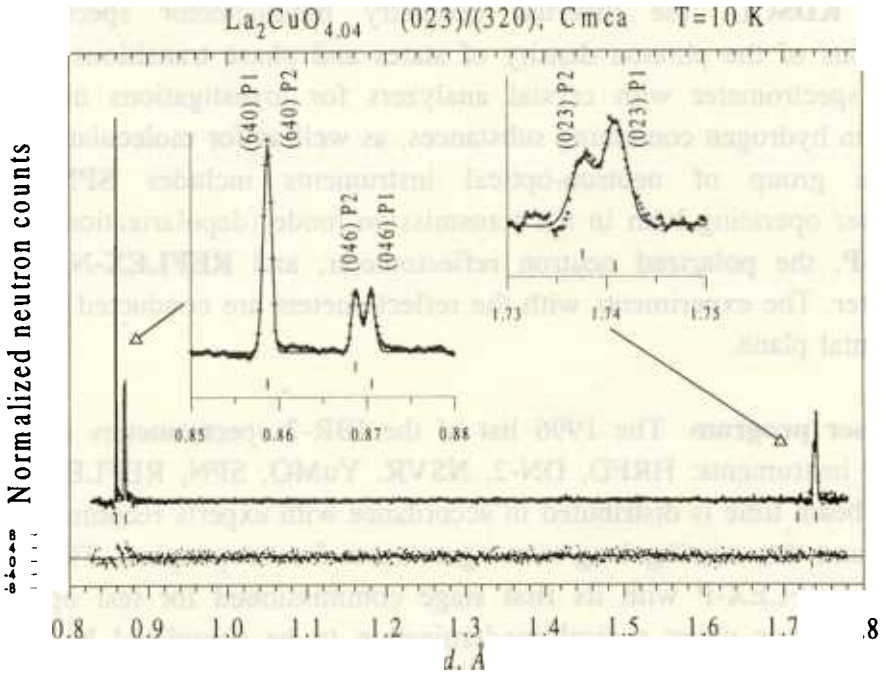

Fig.1. The diffraction spectrum of $La_2CuO_{4.04}$ measured for the [023] reciprocal lattice direction

were conducted with a $La_2CuO_{4.04}$ single crystal containing extra oxygen in the miscibility gap region. Figure 1 illustrates the HRFD diffraction spectrum for the [023] direction of the reciprocal lattice of the crystal. At T=10 K, one can easily see that peak (023) splits into two components corresponding to the oxygen-poor (P1) and oxygen-rich (P2) phases. The existence of the (023) peak is the evidence of the Cmca symmetry of the P2 phase because for the Fmmm space group this peak is forbidden (A.M.Balagurov, V.Yu.Pomjakushin, V.G.Simkin et al. Physica C, 1997).

In cooperation with Institute of Crystallography RAS (Moscow) and LLB (Saclay), investigations of the magnetic structure of the system $U(Pd_{1-x}Fe_x)_2Ge_2$ with a complicated magnetic behavior at T<140 K were initiated. The experiments were conducted with the HRFD diffractometer in Dubna and with the G4.1 diffractometer in Saclay. A radical change in the character of ordering of the magnetic moments of uranium atoms in dependence on the temperature has been detected already at lowest levels of iron doping. So, at temperatures lower than 65 K in compounds with x=0.02, instead of the initial sinusoidally modulated structure a simple antiferromagnetic structure appears and at temperatures above ~65 K, the z-component of the propagation vector decreases with a jump from k_z=1 to k_z≈0.76 and continues to decrease as the temperature increases (Figure 2).

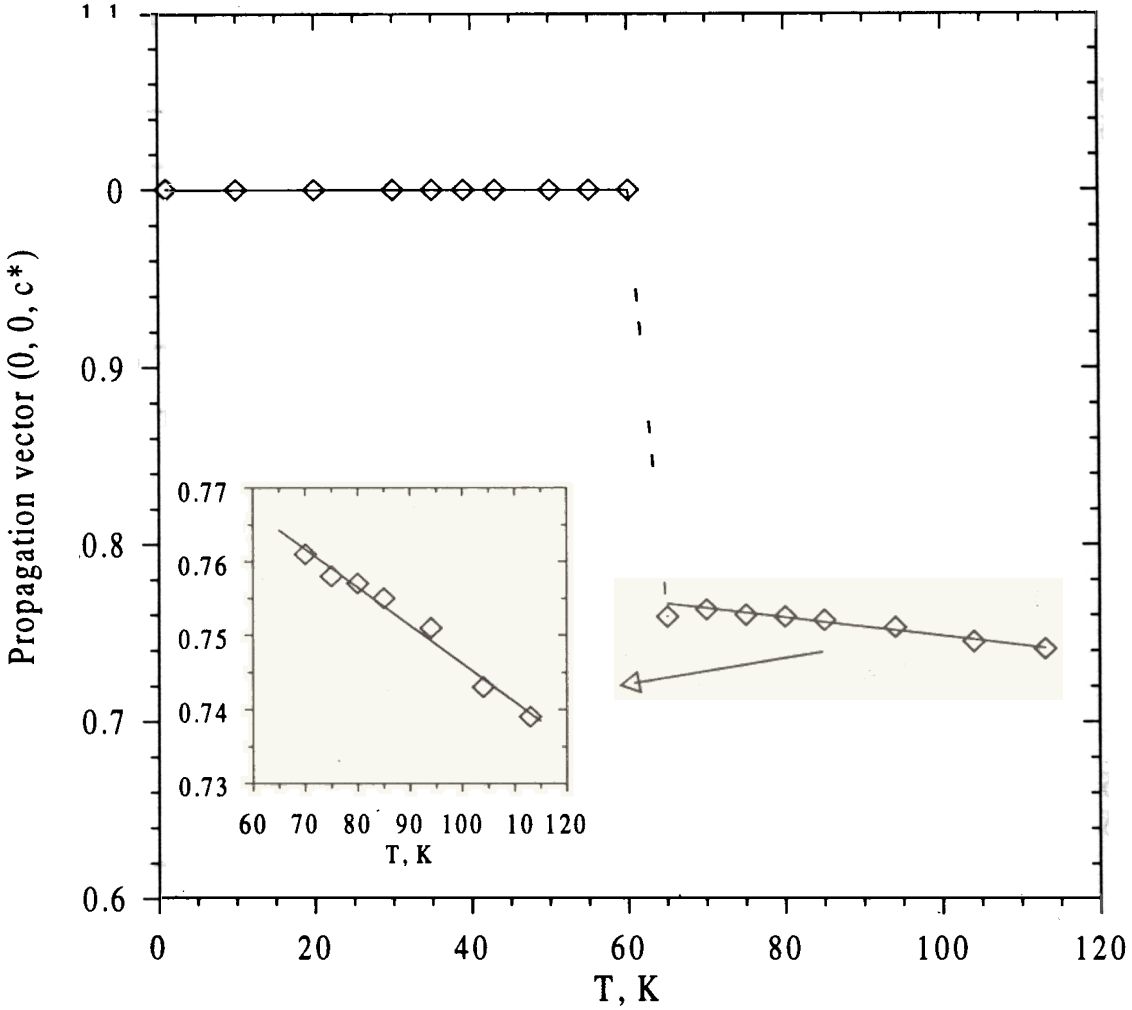

Fig.2. The temperature dependence of the z-component of the propagation vector of the $U(Pd_{0.98}Fe_{0.02})_2Ge_2$ structure

In the first half of the year (just before the start of modernization) in cooperation with the RNC "KI", on the DN-12 diffractometer for investigations of microsamples at high pressures, a series of experiments with ammonium gallogenids ND_4Cl and ND_4Br was completed (earlier, the results for NH_4Cl were obtained and published (A.M.Balagurov et al, High Press. Res. 14 (1995) 55)). The measurements were performed up to the pressure 35 kbar for ND_4Cl and 45 kbar for ND_4Br (Fig. 3). The equations of state, as well as the dependence of the position parameter of the structure and interatomic distances on the pressure, were obtained.

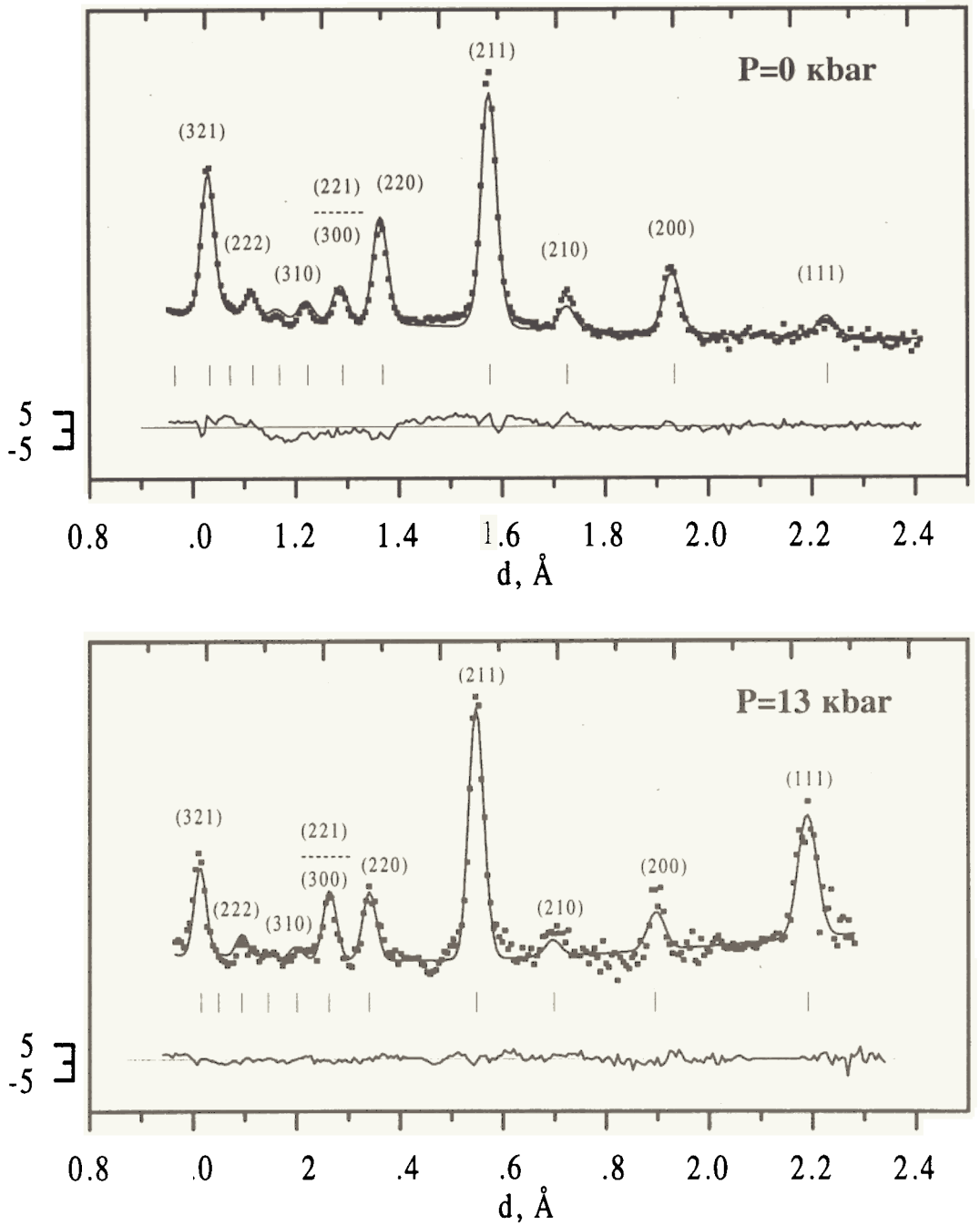

Fig.3. Diffraction patterns of ND_4Cl, measured at 0 and 13 kbar and processed by the Rietveld method. The scattering angle $2\theta=90°$. The experimental points, calculated profile, and the difference curve are shown

The conclusion can be made that the behavior of all the investigated systems is similar in many respects. The configuration of ammonium atoms does not practically change (the length of the *N-D/H* bond remains constant), the distance between halide atoms and ammonium decreases about linearly with pressure and at a certain pressure, the structural phase transition connected with ordering of the ammonium orientation in the lattice ($P_c \approx 25$ kbar for ND_4Br) takes place. The important observation was that the molecularity of these compounds decreases as the pressure increases and at some pressure, the hypothetical phase transition to a pure ion structure might take place.

On HRFD, a program for residual stress investigations was realized in the frame of the agreement for cooperation between FLNP and Fraunhofer Institute for Nondestructive Testing, Saarbruken, Germany. Though this is a quite new direction for HRFD, a lot of studies were performed in a short time. For details see the experimental report by V.L.Aksenov et al. in this book.

Small-angle neutron scattering. The method is applied for investigations of polyelectrolyte solutions, polymers, micellar formations, metallic glasses, concretes, and fractals. The goal of the investigations is to determine the parameters of large scale inhomogeneities and their behavior in dependence on the external conditions in these substances.

In collaboration with the Institute of Macromolecular Chemistry (Prague), the program of investigations of amphiphile polymers with the YuMO small-angle scattering spectrometer continued. As is known, in water, block copolymers consisting of hydrophile and hydrophobic molecules form micelles with a surprisingly homogeneous size distribution and, in addition, can solubilize different organic molecules. In the conducted experiments, the dynamics of the solubilization process was studied. This appeared possible thanks to an exclusively high efficiency of the YuMO spectrometer. Separate small-angle scattering spectra were measured in 10 min (and sometimes, in 2 min). It appeared that in the process of chloroform solubilization, the change of the radius of a PMMA-PAAc micelle in the course of time strongly depends on the extent of the initial neutralization of the solution (Fig. 4) (J.Kritz et al, Macromolecules, 1996).

In the experiment with DMPC lipid membrane multilayers, the reason for an increase in their repetition period in the vicinity of the phase transition temperature which is close to the critical temperature for lipid membranes, has been clarified. It has been shown that the effect is mainly connected with an increase in the intermembrane space, i. e., with an increase in the entropic repulsion in the critical region.

Detailed precision data on the temperature dependence of the length of cylindrical self-organizing TDMAO (tetradecyldimethylaminoxide) micelles in water solution were obtained. As it was to be expected, first the micelle lengths increased as the temperature increased, then reached some plateau and, what was totally unexpected, started to decrease at the temperature above 50°C. The obtained results, as well as the block copolymer results, have yet to be interpreted (N.Gorski et al, J.Appl.Cryst., 1997).

A large volume of work to study structural changes in tylacoid membranes during the formation process has been carried out. Dark tylacoid membranes are directly connected with the fundamental biochemical process of photosynthesis and therefore, to study their structure and, specifically, the influence of external factors on the structural parameters is an urgent problem. In the conducted experiments, the technique for obtaining standard samples of tylacoid membranes has been finished off. With these samples, we managed to prove the existence of

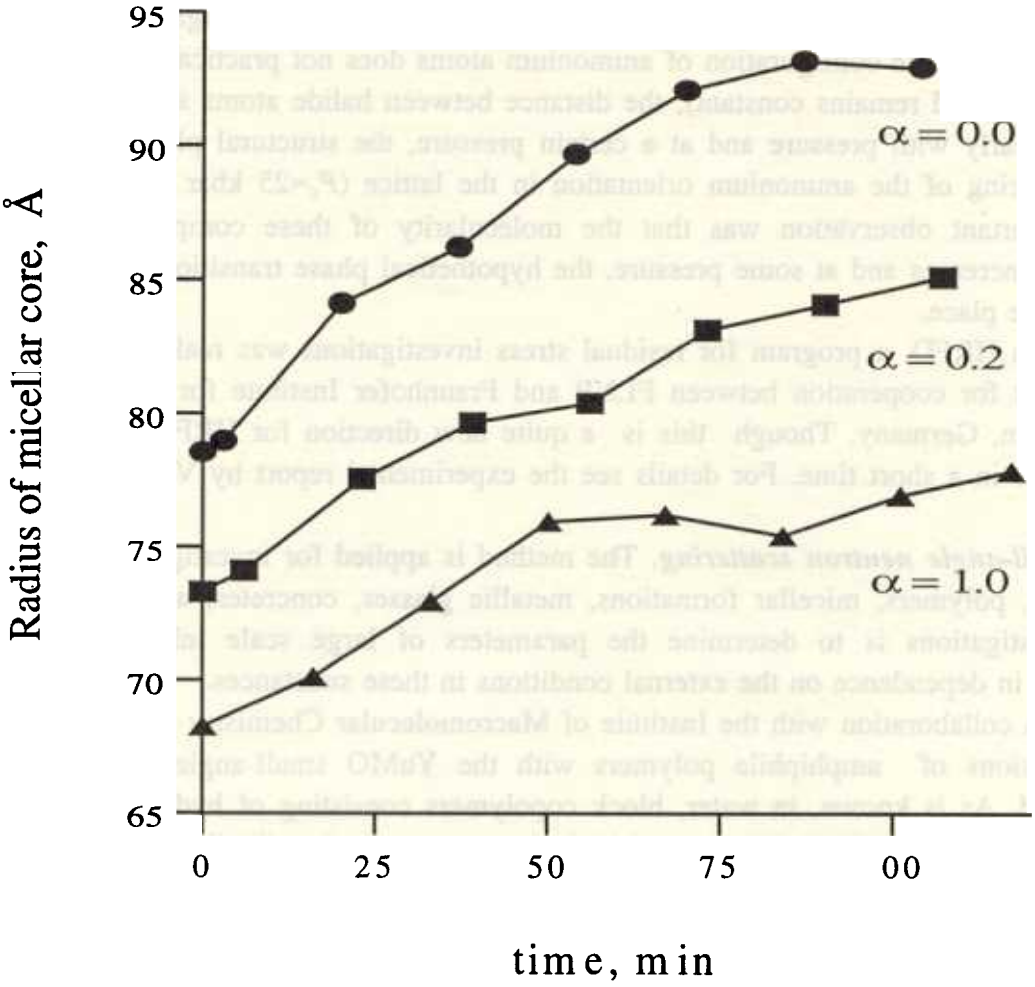

Fig.4. Variation of the micellar radius during the solubilization of chloroform into PMMA/PAAc micelles for the chosen degree of neutralization α. The mean radius was determined by fitting the SANS experimental data to the theoretical scattering curve of homogeneous spheres with a Schulz-Zimm distribution of radii.

structural changes caused by a long exposition to light. The measured effects were analyzed in the framework of the model of topological structural rearrangement. This allowed us to make the conclusion that the rearrangement involves the formation of quasicylindrical domains in the membrane and in the process of formation, the scattering density near the surface of the tylacoid membrane increases (A.D.Tugan-Baranovskaya et al, Biochem. and Mol. Biol., 38 (1996) 485).

Neutron optics with polarized neutrons. The purpose of the experiments is the investigation of the micromagnetic properties of matter, determination of the characteristics of the magnetic field interaction with matter, investigation of thin mono- and multilayer films, and investigations of open surfaces and hidden interfaces.

Earlier experiments to investigate small-angle scattering and polarized neutron depolarization in a $Fe_{70}Ni_{30}$ alloy revealed the existence of two magnetic correlation lengths different by a few tens of times in the vicinity of the Curie point (T_c=287 K) for this alloy. On the SPN spectrometer, the first experiments to discover the effects connected with the possible dependence of the phenomenon on the neutron wavelength were conducted. The measurements were carried out over a wide temperature range in the vicinity of the transition point at several

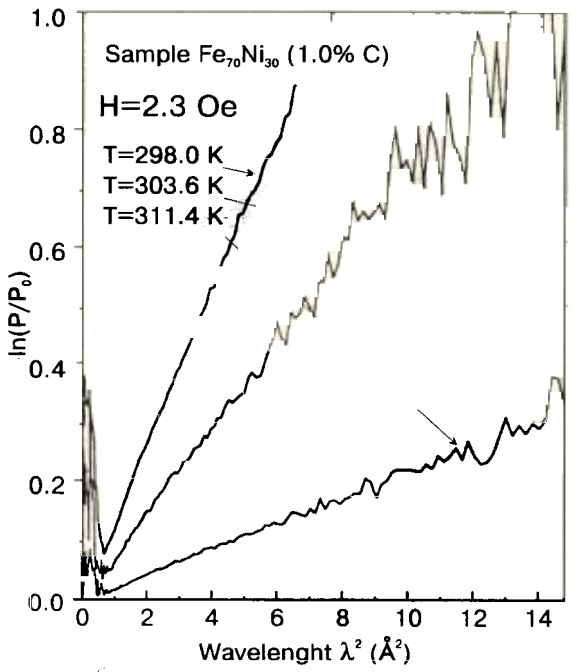

Fig.5. The dependence of the logarithm of the function $P(\lambda)/P_0(\lambda)$ on λ^2 shows its linear character without noticeable oscillation effects

external magnetic fields. Clear evidence for the temperature hysteresis of a magnetically disordered state above T_c and its dependence on the magnetic field has been found. Figure 5 shows the neutron depolarization as a function of λ measured for three temperatures near T_c. The data are well described by the function $P(\lambda)=P_0(\lambda)exp(-\alpha\lambda^2)$ without any oscillations. This is the evidence for a complete disorder of the magnetic induction vector inside the sample.

As it was planned for 1996, the first stage of the REFLEX-P polarized neutron reflectometer was put into operation and the first test and physical experiments were conducted. The neutron beam is polarized by means of an optical system of two high-quality mirrors positioned in parallel. The mirrors are made by sputtering *Fe-Co* alloy on a *Ti-Gd* substrate. The achieved beam polarization over a wide wavelength range is one of the best in the world for instruments of its type (Fig. 6). One of the first REFLEX-P experiments was conducted to investigate neutron reflection from self-organizing polymeric films, polysteinsulfonate and polyallilamine with deuterization of each alternate layer. The stability of these systems, as well as the possibility to exert an influence on their structural parameters by introducing small molecules into the interlayer space, was estimated. It was shown that, in spite of the essential rigidity of the system, this influence exists, i.e., steeping in salt solution will noticeably change the repetition period of the structure.

Inelastic neutron scattering. On the IBR-2 spectrometers, the method of inelastic neutron scattering is used to study the dynamics of atomic motion in molecular crystals, the dynamics of hydrogen in metals, the dynamics of atoms and molecules adsorbed on the surface of substances, magnetic excitations in rare-earth intermetallic compounds, the density of phonon states in novel materials and adsorbed layers, generalized frequency spectra, and stochastic dynamics in metals and alloys. Investigations of the spectra of elementary excitations in superfluid ^4He are of fundamental interest in connection with recent theoretical predictions of their properties not studied experimentally before.

In 1996, the main direction of research with NERA was the investigation of the dynamics of methyl and ammonium groups in compounds $(NH_4)_2SO_4$, $(ND_4)_2SCN$, $C(NH_3)_6I_2$, and $(CH_3)_2C_6H_4$ and solid solutions $(NH_4)_{1-x}K_xSO_4$ and $(NH_4)_{1-x}Rb_xSCN$ in cooperation of the Institute of Nuclear Physics, Krakow. For solid p-xylenes, incoherent inelastic scattering spectra were measures for different substitutions of hydrogen by deuterium: $D0=(CH_3)_2C_6H_4$, $D4=(CH_3)_2C_6D_4$, $D6=(CD_3)_2C_6H_4$, and $D10=(CD_3)_2C_6D_4$. This allowed modeling of the rotational potential of methyl groups and the quantum mechanical calculation of the structure of molecules and their vibrational spectra to be performed. In the first approximation, it appeared possible to describe satisfactorily the results for all four molecules using one set of atom-atom interaction potentials (Fig.7) (I.Natkaniec, J.Kalus et al, ECNS-96, Interlaken).

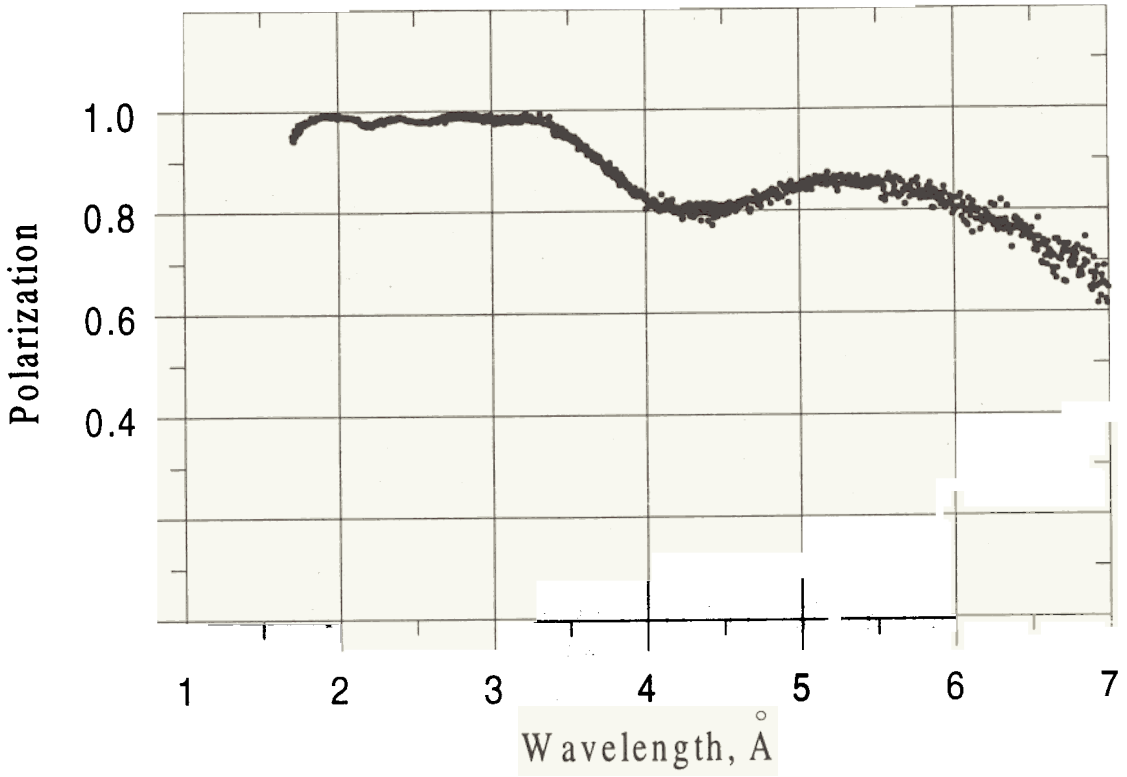

Fig.6. The wavelength dependence of the neutron polarization at REFLEX-P

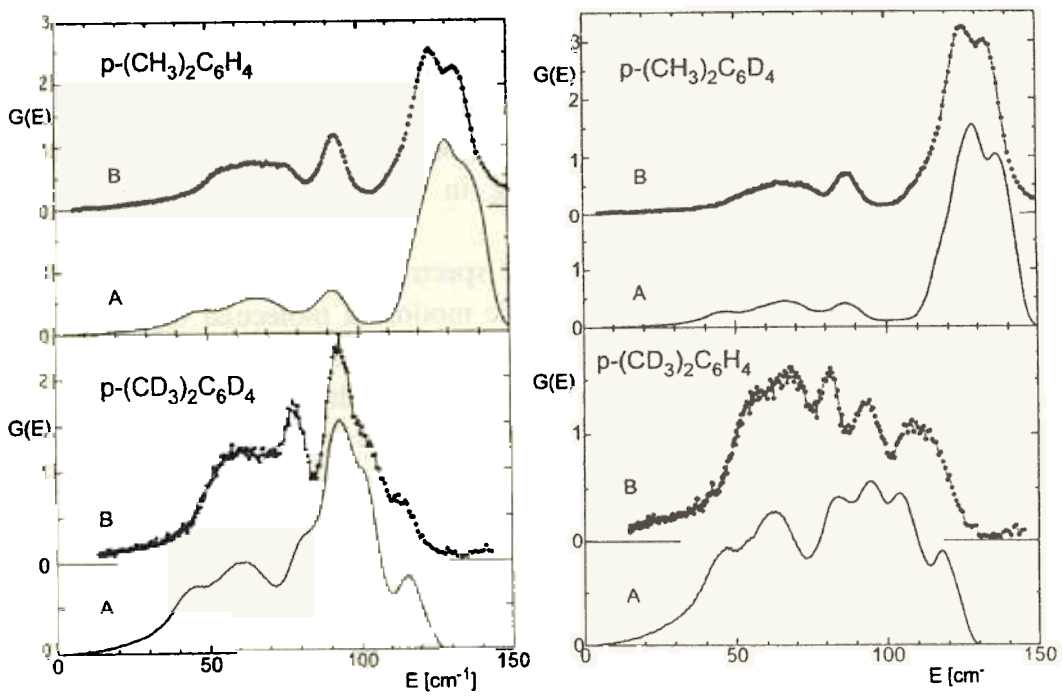

Fig.7. The calculated (A) and measured (B) phonon spectra of solid p-xylenes at 10 K for various deuterium contents

With the KDSOG spectrometer, inelastic neutron scattering spectra (INS) of hydrogeneted fullerite C_{60} samples were measured in cooperation with the Institute of Solid State Physics RAS. The samples were synthesized in hydrogen atmosphere at 620 K under the

pressure 0.6 GPa with subsequent quenching to the temperature 85 K. After taking the INS spectra, the sample was annealed at 300 K to have the composition $C_{60}H_{24}$ and its INS spectra were measured again. In the process of annealing *~1.4*H_2 per C_{60} molecule were removed. It appeared possible to obtain the information about intra- and intermolecular vibrations in the $C_{60}H_{24}$ molecule, while the difference spectrum provided the information about the transition energies between the rotational states of the hydrogen molecule, in particular, splitting of the level *(0→1)* at 14.7 meV due to interaction of H_2 with the neighbor molecules $C_{60}H_{24}$ was observed (A.I.Kolesnikov et al, ECNS-96, Interlaken).

On the DIN spectrometer, experiments to study the effects of ion and hydrophobic hydration, in particular, diffusive and vibrational-rotational motion of water molecules hydtrating the Li^+ ions in comparison to the motion of molecules of pure water, continued. The comparison has shown that the intensity of the first translational mode ($\varepsilon \approx 6$ meV) decreases, the intensity of the second mode ($\varepsilon \approx 20$ meV) increases, and the region of librations remains practically without changes (A.G.Novikov et al, ECNS-96, Interlaken).

Further investigations of localized states of hydrogen and oxygen in dilute solid solutions VH_x, VO_y, and VH_xO_y aimed at the determination of the interinfluence of *p*- and *s*-doping elements on the local structure of the defect space showed that at low doping concentrations, in a triple system *V-O-H,* hydrogen is localized in the tetrahedral or "displaced" tetrahedral positions. For the triple system, a considerable increase of quasielastic scattering possibly connected with its delocalized hydrogen state was observed.

On DIN-2PI, trial experiments to measure dispersion curves for single crystals of simple compounds were performed in the cooperation with the Physical Energetic Institute (Obninsk). For a nitrogen-free sample of steel (18% *Cr*, 15% *Ni*, 10% *Mn*), the positions of phonons in the [110] direction were measured. The results were approximated by the model of central forces taking into account the second coordination sphere. It is seen that the model describes well the experimental data for the branch *Tl* over the entire range of momentum transfers and for the *L* branch up to $q/q_m \approx 0.3$ at least. The experiments have shown that conditions for dispersion relation measurements in the low-frequency region of excitation spectra exist.

Development activities. In addition to work on the completion of the first stage of the REFLEX-P spectrometer, intense effort was concentrated on the reconstruction of the DN-12 diffractometer (project SUPERMAN). By the end of 1996, we managed to complete the preparation for positioning of the mirror neutron guide manufactured by the Hungarian firm "Mirrotron". In the first quarter of 1997, the neutron guide will be put into operation and this will allow the background conditions of the diffractometer to be essentially improved, as well as the neutron flux in the region of long waves to be increased.

At HRFD, work to modernize the instrument and extend its possibilities continued. In the system for control of Fourier chopper rotation, a magnetic type encoder capable of holding higher radiation load than optical encoders was installed. This will make it possible to increase the neutron beam aperture, as well as increase the neutron flux on the sample by ~2 times. A large +90° detector with 20 photomultipliers was installed, tuned, and put into operation. This detector in combination with the -90° detector put into operation at the end of 1995 will allow the radial and tangential components of the tensor of internal stresses to be measured simultaneously without changing the orientation of the sample. At the beginning of 1997, the second detector at a large scattering angle (2θ=152°) will be put into operation and this will allow the data collection rate from polycrystal samples to be doubled. With support of the

Institute of Nondestructive Testing (Saarbruecken, Germany), the necessary equipment for increasing the efficiency of internal stress experiments was purchased and include a loading machine, a tensor scanner, and a nitride boron slit system. At present, experiments with the loading machine are being carried out. The scanner and the slit system will be put into operation at the beginning of 1997.

The two-dimensional detector with a position resolution ~3 mm for both axes started operations at DN-2. This detector allows the realization of the three-dimensional neutron diffractometry of single crystals, i.e. the collection of information in the volume of the reciprocal space of the crystal without rotating the sample or the detector.

The new position sensitive detector for the SPN spectrometer was tested in real conditions and will be put into operation in near future. The parameters of the detector (the resolution ~1.5 mm and the registration area 40x120 mm) will ensure effective investigations of the diffusion scattering of neutrons following reflection and small-angle scattering for small momentum transfers (10^{-4}-10^{-2}Å^{-1}).

For DIN, an essential decrease in the background over the low energy region has been obtained with the help of a rotating double collimator operating in phase with the IBR-2 power pulses.

Scientific program of the Condensed Matter Physics Division in 1996 was performed in cooperation with the following institutes and organizations:

Bulgaria	University; Institute for Nuclear Research and Nuclear Energy (Sofia)
Czech Republic	Polytechnical Institute (Prague)
Egypt	Atomic Energy Authority of Egypt (Cairo)
Finland	Technical Center (Espoo)
France	Laboratoire Leon Brillouin (Saclay); Institut Laue-Langevin (Grenoble)
Georgia	University (Tbilisi)
Germany	Hahn-Meitner Institute (Berlin); Research Center (Rossendorf); University (Bayreuth); Technical University (Kemnitz); Research Center (Darmstadt); GKSS (Geesthacht)
Hungary	Research Institute for Solid State Physics (Budapest)
D.P. Republic of Korea	University (Pyongyang)
Poland	Institute of Nuclear Physics (Cracow); University (Poznan);
Romania	Atomic Physics Institute (Bucharest)
Russia	Kurchatov Institute; Institute of Solid State Physics; Institute of Theoretical and Experimental Physics; Petersburg Nuclear Physics Institute; Institute of Physics of Metals; Moscow State University; Institute of Crystallography
Slovakia	University (Bratislava)
Sweden	University (Goteborg)
Switzerland	Paul Scherrer Institute (Villigen)
U.K.	Rutherford Appleton Laboratory (Abingdon)
Uzbekistan	Institute of Nuclear Physics (Tashkent)
Vietnam	Institute of Physics (Hanoi)

In greater detail, this cooperation is described in the "Topical plan for JINR research and international cooperation" (Dubna, 11-7160 or http://www.jinr.ru/jinr/plan/).

1.2. NEUTRON NUCLEAR PHYSICS

In 1996, nuclear physics investigations with slow neutrons were carried out on seven beams of the IBR-30 + LUE-40 neutron source, on the eleventh beam of the IBR-2 reactor and on the neutron beams of other sources in Russia, Germany, France, the USA, and China. It is necessary to note that the new, valuable opportunities which opened after Russia jointed ILL, Grenoble, have been used effectively: some measurements with cold and ultracold neutrons were successfully performed. The research program for IBR-30 was formed, taking into account the time schedule of creating the new neutron source for nuclear physics investigations — the IREN project. In accordance with this schedule, the IBR-30 + LUE-40 complex has to be shutdown by the middle of 1997, so it was necessary to concentrate all available resources on the most important experiments. An extensive program for investigations of resonance neutron induced fission was realized, as well as traditional investigations of the properties of highly excited states of heavy nuclei, parity violation effects, and reactions with the emission of charged particles.

1.2.1. EXPERIMENTAL

Parity Violation and Time-Noninvariance Effects in the Interaction of Resonance Neutrons with Nuclei

The first measurements of some neutron resonances (E_n< 20 eV) of the pseudo-scalar correlation $(\sigma_n k_f)$ between the neutron spin σ_n direction and the fission fragment momentum k_n were performed on the POLYANA setup with the polarized neutron beam of the IBR-30. The specially designed ionization chamber and high intensity of the neutron source allowed us to measure the energy dependence of the effect for the ^{235}U target shown in Fig.1. For the first time, the *P*-odd effect in the cross-section demonstrated interference in the energy dependence. The quantitative analysis of the obtained results was closely related to the multi-level, many-channel treatment of other interference effects investigated in FLNP for the resonance neutron induced fission of the same target nucleus (see section **Nuclear Fission** for more details).

In the framework of the TRIPLE collaboration, the investigation of the mass dependence of the mean-square matrix element M_W of the weak neutron-nucleus interaction continued on the polarized neutron beam of LANSCE, Los Alamos. The measurements of the $(\sigma_n k_n)$ correlation were done by the method of capture gamma-ray registration for the ^{117}Sn and ^{103}Rh isotope targets. For neutron energies E_n < 1000 eV, there are 15 and 17 known *p*-wave neutron resonances for ^{117}Sn and ^{103}Rh nuclei, respectively. Only in three of them for *Sn* and in two for *Rh*, the meaningful *P*-odd effects (on the level of three standard deviations or higher) were observed. The results are being analyzed now. The recently completed analysis of the experimental results obtained in 1995 for the ^{107}Ag target nucleus yielded the respective M_W value 2.4+1.7-1.1 meV. This indicates that the mean-square matrix element M_W has equal values for nuclei with close level densities.

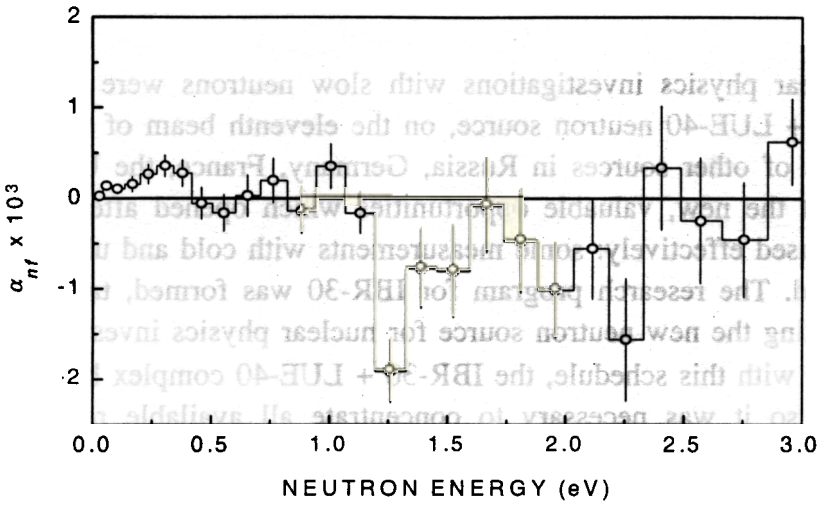

Fig.1. The parity violating interference effect of fission fragment emission in the neutron induced fission of ^{235}U

A very actual problem for some leading neutron centres is the study of time–non invariant (*T*-odd) effects in resonance neutron induced reactions. The key difficulty is large polarized nuclear targets. Up to the end of 1995, when the high *P*-odd effect was discovered near E_n = 3.2 eV for a natural *Xe* gas target, the only real candidate for a polarized target was a ^{139}La nucleus. However, the possibility of utilizing a polarized *Xe* target is feasible only if the *Xe* isotope responsible for the observed *P*-odd effect is odd. In this case, it is conceivable, in principle, to polarize a *Xe* gas target by a circular polarized laser beam. The first isotope of the *p*-wave neutron resonance at E_n = 3.2 eV was identified in the measurement of the (*n*, gamma)-reaction for a natural *Xe* target on the IBR-30 pulsed neutron source. It is ^{131}Xe with the spin 3/2. This result opens new possibilities for the experiments.

A new method of studying the time–noninvariant effect in the transmission of polarized neutrons through a polarized target was proposed at FLNP. It consists of rotating the neutron polarizer round the target by 180°. The estimated accuracy of the ratio of *T*-odd to *P*-odd matrix elements is on the level of 10^{-4} if the above-mentioned rotation is realized with a rather reasonable precision of 10^{-5} rad. The method requires one neutron polarizing device and is free at many false effects inherent in other known experimental schemes. The only feasible neutron polarizer for the proposed method is a ^3He polarized filter. In collaboration with the Lebedev Institute, a prototype of such a polarizer is being created. It consists of two aligned aluminosilicate glass cells filled with ^3He at the pressure 10 atm. The active volume of one cell is 40 cm^3 with the cross-section 5.3 cm^2. The first experiments with this device on the neutron beam of the IBR-30 source are planned for the end of 1997.

Nuclear Fission

Angular correlations of fission fragments in resonance neutron induced fission of the ^{235}U nucleus

Essential progress has been achieved in the realization of "full" experiments for investigating resonance neutron induced fission of the ^{235}U target nucleus. Due to improvement of the experimental technique at low sample temperature (T~0.1 K), the statistics for measuring the angular anisotropy of fission fragments $A_2(E_n)$ with respect to the target spin orientation was increased more than twice. Thus, the experimental data for $A_2(E_n)$ are now available in energy bins of 0.05 eV with an accuracy of 3–10 %, up to E_n < 30 eV. With the aid of the original code for multi-level, many-channel R-matrix analysis, as well as with the specially modified standard code SAMMY, $A_2(E_n)$ data fitting together with spin separated and total fission cross-sections, and the neutron capture and total cross-sections was carried out. Some of the results are shown in Fig.2.

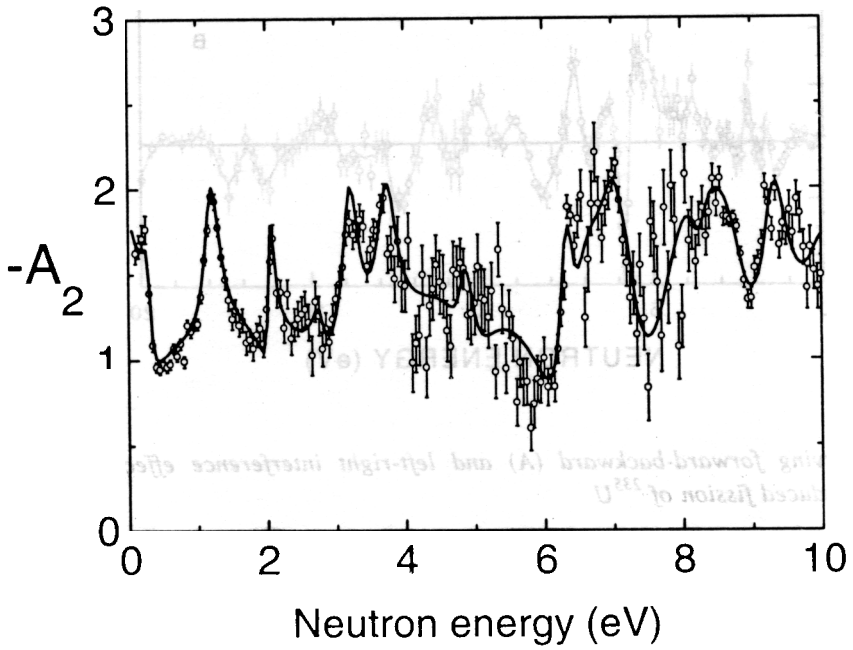

Fig.2

For the first time, three fission channels were taken into account: $J^{\pi}K$ = 3^-0, 3^-1 and 3^-2 for compound-states 3^- as well as the interference of the ^{236}U excited states with different spins. The presence of the $A_2(E_n)$ data influences the results of the analysis, namely, the signs and values of fission partial amplitudes. It is clear that the experimental accuracy over the inter-resonance regions has to be improved in order to have an unambiguous analysis.

Even at this stage of the investigation, the obtained partial fission amplitudes form a reliable basis for the quantitative analysis of other angular correlations of fission fragments measured recently by a FLNP-PINP collaboration and related with the interference of s- and p-wave neutron induced fission. As mentioned above, P-odd correlations were first measured in 1996. Also in 1996, the measurements of the left-right (with respect to the plane formed by the directions of the neutron spin and moment) correlations (see Fig.3) were completed. For

comparison, in the same Fig.3, the previously obtained data for the energy dependence of the forward-backward correlation (between k_n and k_f) are shown.

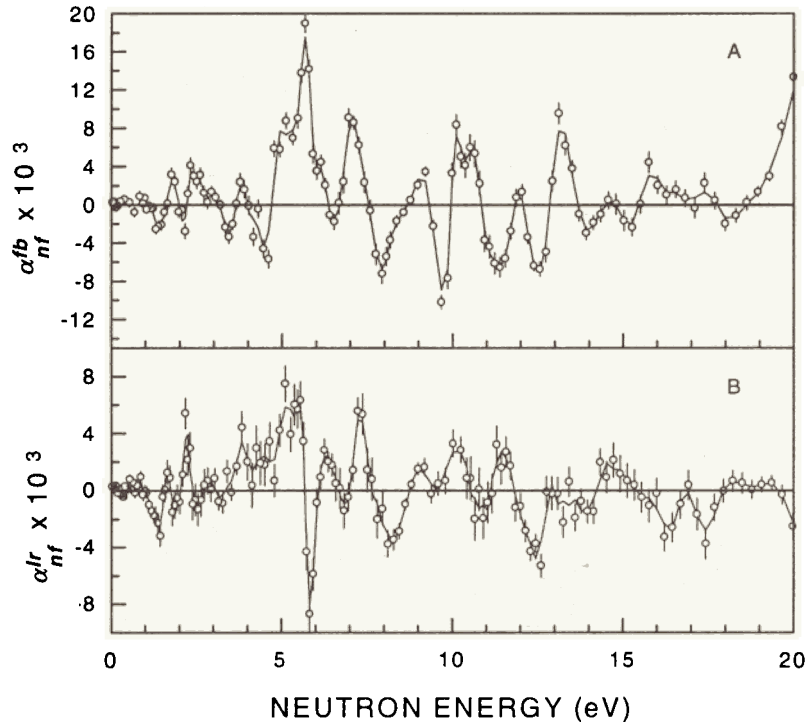

Fig.3. The parity conserving forward-backward (A) and left-right interference effects (B) of fission fragment emission in the neutron induced fission of ^{235}U

Irregularities in both dependences take place near unknown *p*-wave neutron resonances of ^{235}U. Fitting of these data is necessary to determine the full set of unknown *R*-matrix parameters for all *p*-wave resonances involved. This could be achieved, in principle, if all necessary parameters of the *s*-wave resonances are extracted from other experimental data. A comparison of the partial fission amplitudes of *s*-wave and *p*-wave neutron resonances allows one to study the parity structure of fission barriers.

Subthreshold fission and delayed neutron yields

On the basis of the experimental technique described in the previous annual review the measurements and analysis of the data on the cross-sections and relative yields of prompt gamma-quanta from the $^{234}U(n,f)$ reaction were completed. The energy dependence of the cross-section up to 1 keV was obtained and the neutron resonance parameters up to 300 eV were found. It was established that no correlations of gamma-quanta yields with reciprocal fission widths exists and an approximately constant ratio $R = N_{coin}/N_{fis}$ for all observed resonances

(within a limit of two standard deviations). This means that the (*n*,gamma *f*) process makes a negligibly small contribution to the subthreshold neutron induced fission of ^{234}U.

In the course of 1996, the study of delayed neutrons (DN) continued with the aid of a modernized ISOMER setup. The results for the DN yield from the thermal neutron induced fission of ^{239}Pu were essentially improved due to the use of new metallic plutonium samples (30 and 56 mg). The background connected with the (α,*n*)-reaction decreased by an order of magnitude. The measurements of the ratio β of delayed to prompt neutron fission yields for ^{237}Np at thermal energies were performed. Due to a very low cross-section (< 20 mb) even for a large (40 g) and highly purified (to 10^{-6} of $^{233, 235}U$ and ^{239}Pu) sample, these measurements were difficult to carry out. However, a high neutron flux of the IBR-2 reactor allowed the β value at a thermal point to be first obtained with an acceptable accuracy: β=(0.41± 0.06)%.

Also, the first direct measurements of the time dependence of the DN count rate have been made for ^{235}U and ^{239}Pu in time intervals of 350 ms. The results are shown in Fig.4.

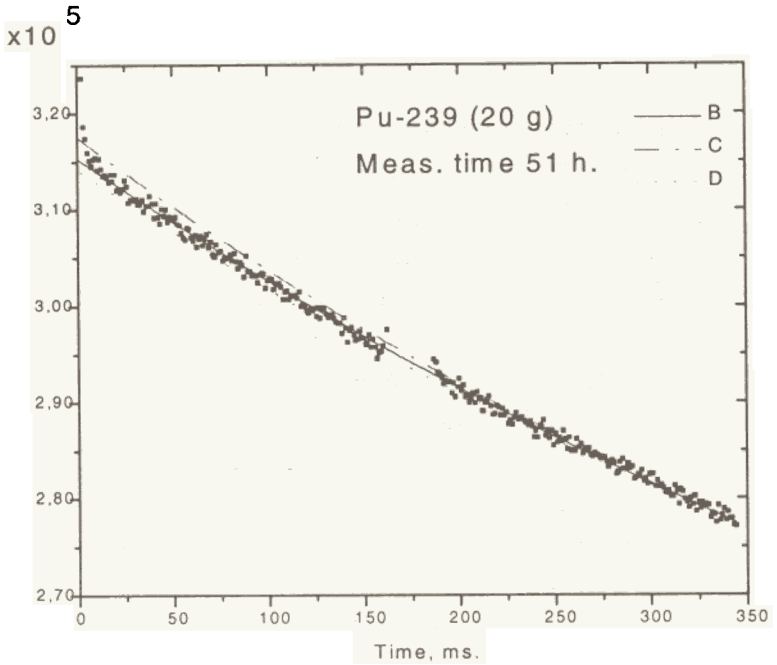

Fig.4. The experimental delayed neutron decay curve for ^{239}Pu and the calculated ones using different six-group sets of constants: B- R.J. Tuttle, C- A.C. Wahl, D- R.W. Waldo et al.

These data could be used to evaluate the contributions of shortest-life DN groups with the precursor lifetime less than 0.1 s.

Highly excited states of nuclei

Cascade gamma decay of compound states after thermal neutron capture

The coincidence gamma spectra of the $(n,2\gamma)$ for ^{128}I, ^{166}Ho, $^{176,177}Lu$ and ^{182}Ta target nuclei with excitation of intermediate levels below the neutron binding energy, were studied. The probabilities of primary gamma-transitions and transitions from intermediate to low-lying levels obtained from the experimental data for these isotopes, as well as for a broad set of previously investigated heavy nuclei, demonstrate the following general peculiarities of gamma decay: a) the dominant role of the vibration excitation modes in the excitation energy interval

1-3 MeV; and b) the failure of common nuclear models to reproduce the shape (and energy dependence) of the observed gamma spectra. These results could be interpreted as a strong evidence of the existence of the phase transition from mainly vibrational excitations to quasi-particle ones in heavy excited nuclei.

Radiative resonance neutron capture

On the basis of the modified ROMASHKA setup, spectra of gamma quanta multiplicities after the radiative capture of neutrons with energies from 20 eV to 2 keV on the ^{115}In, ^{117}Sn, ^{127}J, ^{175}Lu, and ^{239}Pu targets were measured on the sixth beam of IBR-30. The spins of the neutron resonances of the ^{118}Sn and ^{176}Lu compound nuclei were obtained. From the measurements of the multiplicities of gamma-quanta emitted after fission and radiative capture in the ^{235}U target, the ratios $\alpha = \sigma_\gamma / \sigma_f$ were extracted for 72 resolved resonances and energy groups below 1 keV. These data allows one to resolve the contradictions between the α values obtained for the resonance region and those from experiments with critical assemblies.

Neutron capture by ^{48}Ca at thermal and thermonuclear energies

The thermal cross-section of the $^{48}Ca(n,\gamma)^{49}Ca$ reaction was measured at the BR1 reactor in Mol, Belgium. It was obtained by the registration of γ-quanta from the reaction, as well as from the decay of ^{49}Ca using a set of Compton suppression HP Ge detectors. The result is 0.982+-0.046 b. This value is about 10% lower than the previously measured one. Our experimental error is also three times less.

The cross-sections of the same reaction were measured at the Van-de-Graaf accelerator, Karlsruhe, Germany, by the method of fast cyclic activation at the neutron energies 25, 151, 176, and 218 keV. The enrichment of the ^{48}Ca sample was 77.87%. The respective results were 751±68, 331±40, 306±31 and 304±31 μbarn.

The astrophysical reaction rate extracted from our data does not depend on temperature and is equal to $N\langle\sigma v\rangle = 1.2 \times 10^5$ cm^3 mol^{-1} s^{-1}.

Neutron induced reactions with charged particle emission

For the first time, the cross-section of the $^{35}Cl(n,p)^{35}S$ reaction was measured at thermal energies by the time-of-flight method using the neutron beam of the IBR-30 source. Different from previous measurements, which were done by the activation technique, the original ionization chamber was used to register the emitted protons. The obtained result 575±13 mb considerably exceeds the previously published ones.

Investigations with ultracold neutrons

The first stage of the test experiments has been completed with the high-density ultracold neutron (UCN) source at the BIGR pulsed reactor, VNIIEF, Sarov. The results show the opportunity for an essential increase in the obtained UCN density, which is now on the order of 50 n/cm^3. This value, even at the preliminary stage, appeared to be close to the UCN density achieved at the most powerful UCN source in ILL, Grenoble, France.

The first experiments studying UCN up-scattering in the velocity range of 10-200 m/s were carried out on the MANAGR experimental setup created in 1995 at the ILL reactor, Grenoble, in collaboration with PINP, Gatchina. The results stimulated the modernization of the

installation, which will be completed by the beginning of the next experimental run in the second quarter of 1997.

In the frame of the FLNP–Kurchatov Institute, Moscow–ILL–Melbourne University collaboration, the first experiments were carried out on a precision test of the neutron wave dispersion law using an original method based on the Fabri-Perrot interferometry. These measurements confirm the feasibility of the technique and allow the actual sensitivity of the method to be estimated. These experiments will be continued in 1997 at ILL.

1.2.2. THEORETICAL

The contradiction between the results of two experimental groups reporting different values of the n-e scattering amplitude extracted from transmission and diffraction measurements was analysed. It was shown that in the transmission experiments, important corrections due to the difference between the coherent scattering length and the scattering amplitude were not taken into account. In the diffraction experiment, it was pointed out that scattering by a crystallite is not necessarily proportional to the coherent cross section. For a sufficiently large crystallite, it is proportional to the coherent scattering amplitude. Thus, it is necessary to measure the distribution of the crystallites in the given sample, which had not been done. Therefore, for now, neither experimental value for the *n-e* scattering amplitude can be taken as reliable.

An analytic derivation of the extended (generalized) Hartry-Fock potential (EHFP) and the real part of the nucleon optical potential for finite spherical nuclei have been obtained, taking into account the structure of the free nucleon-nucleon interaction. It is shown that in finite nuclei, the real part of the nucleon optical potential constructed on the basis of the EHFP has more complicated radial, isotopic and energy dependences, and the form of the spin-orbit term in comparison with phenomenological optical potentials. In calculations based on the proposed approach the realistic scale of the spin-orbit potential was first obtained without the use of relativistic nuclear models. The essential role of the gradient terms of the EHFP in forming the optical potential was revealed.

1.2.3. METHODOLOGY

New method of neutron spectra generation at star temperatures

The method of Maxwellian neutron spectra generation (creation) is proposed with a variable temperature in the range of 10-50 keV. To obtain the necessary spectra, the reactions $^{7}Li(p,n)$ and $T(p,n)$ as neutron sources and a graphite or lead moderator of special configuration can be used. The calculation of the setup parameters and Monte-Carlo simulation of the neutron spectra have been carried out. The first experiments with the new neutron source are planned for the middle of 1997.

Test experiment on the UGRA setup

The first stage of testing of the UGRA setup has been completed and the test measurements at planned vacuum were performed. It was confirmed that the accuracy necessary to measure the electric polarizability of the neutron can be achieved. The problem of more stable and effective detectors has to be solved to start data taking.

1.3. APPLIED RESEARCH

In the reported year, analysis of methodological possibilities for analytical and radiation investigations on the IBR-2 channels continued. In particular, the directions of scientific research and the present state of the instruments and their equipment on channel 11 (BPC) were discussed. Earlier plans were to use the channel mainly for biophysical experiments and dynamic neutron radiography. Recently, the mirror neutron guide forming the thermal neutron spectrum on channel 11 (one of the first channels at IBR-2) has been successfully used for investigations in the physics of delayed neutrons by the group of Yu.S.Zamyatnin together with the NAA sector staff. This work has got financial support and is developing successfully. At the same time, experiments to investigate residual stresses in materials (A.M.Balagurov and J.Schreiber) have a claim (also financed) on channel 11 with a mirror neutron guide. These two directions form the scientific activity on channel 11. In this situation, a compromise has been made by proposing the creation of a split neutron guide system instead of the old system of collimators and one neutron guide.

In the reported year, experimental investigations were carried out in several directions.

On the IBR-2 radiation channels of the pneutransport facility REGATA, NAA investigations of the distributions of heavy metals and other elements in environmental objects and novel materials were conducted.

The NAA sector, in cooperation with Romanian scientists, completed the biomonitoring stage of heavy metals and other elements in industrial and adjacent areas in Romania under the auspices of the European project "Heavy Metal Atmospheric Deposition in Northern Europe". The data on the *Cu, Cd, Pb, V, Cr, Fe, Ni, Zn,* and *As* contents (the *Pb* and *Cd* contents were determined by the method of atomic adsorption (AAS) in Norway) were accepted by the Organizing Committee for publication in European Atlas for 1996. It is the first time the obtained experimental information on 37 elements, including rare-earth and toxic elements, in addition to the above enumerated elements, has allowed a complete picture of the technogenic effect on the environment of the heavy industry centers and gas- and oil-refining plants of Romania to be obtained.

Under the auspices of the bilateral agreement with the Polish Republic "Determination of Elemental Composition of Aerosols by INAA as a Tool for Evaluation of Environmental Pollution", an analysis of air filters taken from Warsaw and Krakow was conducted to determine the main pollutants and finishing off the method of analysis by different types of filters. The analysis has shown that Krakow experiences a strong influence of the most developed industrial region in Poland, the Katowice region.

Investigations of the moss, peat, and soil samples collected above the Pole circle in Norway and Finland were completed. The analysis of peat drills to the depth of 50 cm allows changes in the element composition of distant air transfers over a long historical period to be detected. Analysis of halogen contents over the Arctic Ocean - European continent transacts has allowed the role of marine components in atmospheric aerosols in Scandinavia to be determined.

The important directions of research connected with monitoring of different ecosystems in Russia, in particular, the Murmansk region and central Russia (ecosystems of the Volga and Oka rivers), and the atmosphere in West and East Siberia were conducted in cooperation with ecologists from the Kola Scientific Research Center of the Institute of Industrial Ecology of the North of RAS (the town of Apatity), The Institute of the Lithosphere of Earth (Moscow), and the Institute of Chemical Kinetics and Burning of the Siberian Branch of RAS (Novosibirsk).

On the basis of the analysis of 160 samples of soil and pine needle taken in the vicinity of the plant for production of phosphorus fertilizers in the town of Apatity and the adjacent areas in the Murmansk region, the source of environmental pollution with a number of elements, including rare-earth elements (REE), *La, Ce, Nd, Sm, Eu, Tb,* and *Yb,* was identified. The REE concentration is very high in Apatity. These results are extremely important because for the present, the role of REE and their influence on ecosystems and animal life is yet little studied.

For monitoring of ecosystems of central Russia (the basin of the Volga and Oka rivers) samples of soil, plants and sediments were analyzed. The data on the concentrations of 30 to 45 elements in 150 samples were submitted to the Institute of the Lithosphere of Earth of RAS (Moscow).

The element analysis of atmospheric aerosols (AA) with different dispersion compositions from West and East Siberia was conducted with the aim of a complex investigation of their properties and characteristics. The NAA analysis of 500 AA samples yielded the data on AA compositions in different areas of the Novosibirsk and Baikal regions (Novosibirsk, Kliuchi, Karasuk, Lake Chany, Lake Baikal, etc.) important for clarifying the similarities and peculiarities of AA compositions on the regional and local levels and studies of year's and seasonal changes in the dynamics of the AA element composition. The obtained data were submitted to the Institute of Chemical Kinetics and Burning and will be used for the formation of the data bank on AA in Siberia, determination of the sources of antropogenic pollution to estimate the AA effect on the environment, vegetation and animal world, as well as on the health of local population.

To investigate radiation-resistant materials for new detectors, the nature of radiation dying centers, and the structure of defects, the following work has been carried out.

Single crystals of *TlSe, $TlInSe_2$* and *InSe* superconducting compounds with a strongly anisotropic lattice structure were synthesized and grown by the method of orientational crystallization.

With the REGATA facility at IBR-2, crystals of *TlSe* ($\rho_{\parallel} \approx \rho_{\perp} \approx 1 \cdot 10^{1}$ ohm cm) and *$TlInSe_2$* ($\rho_{\parallel} \approx \rho_{\perp} \approx 2 \cdot 10^{4}$ ohm cm and $\rho_{\parallel} \approx \rho_{\perp} \approx 5 \cdot 10^{7}$ ohm cm) were irradiated with a fast neutron fluence $1.5 \cdot 10^{16}$ n cm^{-2} and $1.5 \cdot 10^{17}$ n cm^{-2} to investigate the influence of radiation defects on the anisotropy in electric conductivity and the parameter "a" of the tetragonal crystal lattice.

The heterotransitions *TlSe - $TlInSe_2$* (110) were obtained by the method of liquid epitaxy. Some of their physical properties were investigated. It is shown that the volume charge region is displaced relative to the metallic boundary of the transition towards the *$TlInSe_2$* substrate. It has also been shown that heterotransitions are sensitive to γ-n-radiation.

The new method for intercalation of anisotropic crystals has been developed. We applied for the RF patent and it was granted.

Distributions of different admixtures in a number of minerals (topaz, beryl, olivine) were studied and their correlation with dying centers before and after neutron irradiation at IBR-2 was found.

A cycle of neutron diffraction experiments was conducted at the reactors in BENSC (Berlin, Germany), FNIFKhI (Obninsk, Russia), and FLNP JINR. *X*-ray experiments were carried out in the University of Kiel and Munich (Germany) and the data on Bragg diffraction and diffusion scattering on single crystals of the *ZrO_2 - Y_2O_3* system (3, 12, 30 mol%) were obtained. On the basis of calculations, models of defect structures accounting for short-range and long-range orders have been suggested.

2.1. CONDENSED MATTER PHYSICS

CONTENTS

2.2. Neutron Nuclear Physics

CONTENTS

NEUTRON DIFFRACTION STUDY OF STRUCTURAL CHANGES IN AMMONIUM HALIDES ND_4Br AND ND_4Cl UNDER HIGH PRESSURE

A.M.BALAGUROV, D.P.KOZLENKO, B.N.SAVENKO
FLNP, JINR, 141980, Dubna, Russia.

V.P.GLAZKOV, V.A.SOMENKOV
RRC "Kurchatov Institute", 123182, Moscow, Russia

The ammonium halides NH_4Br, NH_4Cl, NH_4I and their deuterated analogs have attracted a great deal of attention in the scientific literature. They show a number of phases[1] and the order-disorder phase transition (λ-transition) was proved to be of great interest[2].

Structural changes in ammonium halides ND_4Br at pressures up to 45 кbar and ND_4Cl up to 35 kbar have been studied with the DN-12 diffractometer[3]. The samples were placed between sapphire anvils[4], which were used to create the pressure. The sample volumes were 2.5 mm^3. Two ring-shaped detectors (16 independent ^3He-counters in each ring) 800 and 700 mm in diameter were used to gather the scattered neutrons. The scattering angles were 45° and 90°; the diameter of the incident beam was 2 mm. All the experiments were performed at room temperature. The pressure was measured by a ruby fluorescence technique.

A orientational phase transition from the phase in which the ammonium tetrahedra are randomly oriented (CsCl-type cubic structure, space group Pm3m) into the phase in which the ammonium tetrahedra are oriented in parallel (CsCl-type cubic structure, space group P-43m), for ND_4Br at the pressure 26<P<31 kbar and ND_4Cl at the pressure P<13 kbar was observed, in agreement with the previous investigations by other methods.

The obtained equations of state with the ones for nondeuterated systems NH_4Br and NH_4Cl obtained by piston-displacement technique[5] are shown in fig.1.

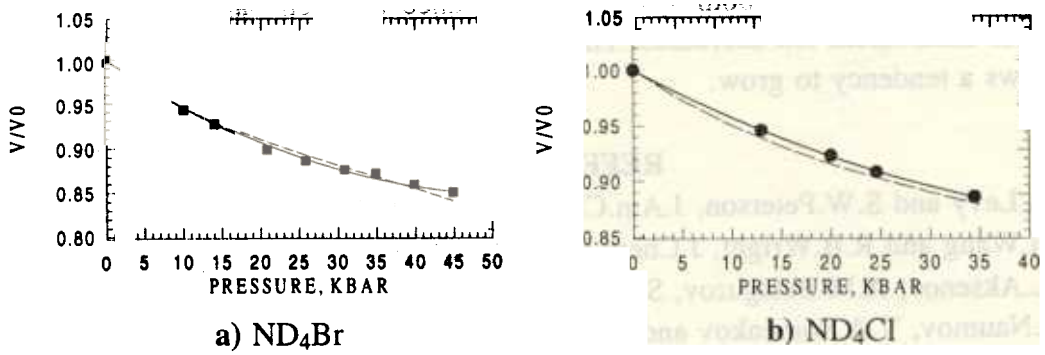

***Fig.1** Equations of state for ND_4Br (■) and ND_4Cl (●) with the data for NH_4Br and NH_4Cl (------) taken from ref.[5].*

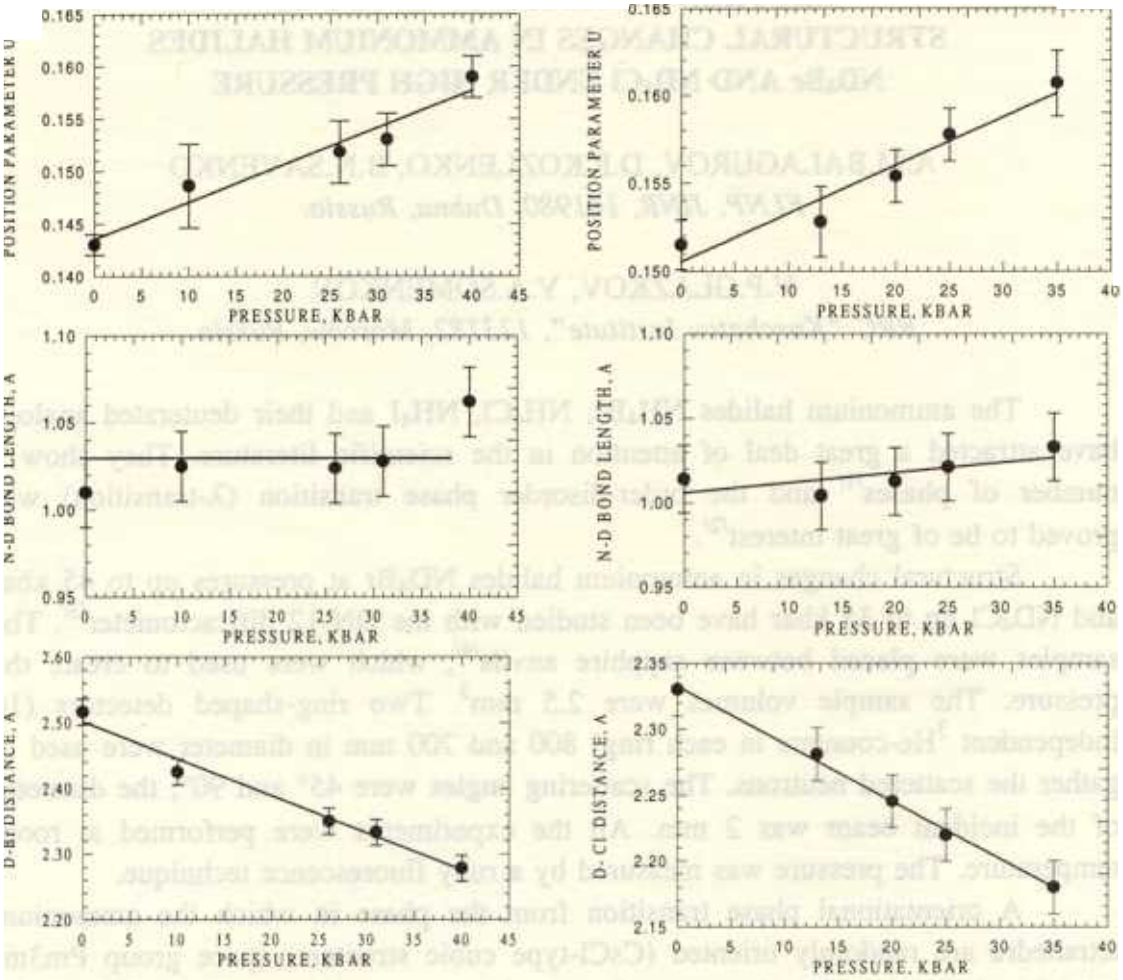

Fig.2 Position parameter, N-D bond length and D-Br (D-Cl) interatomic distance as functions of pressure.

Position parameter, N-D bond length and D-Br (D-Cl) interatomic distance as functions of pressure are shown in fig.2.

Under pressure, in both systems the distance between halide ions and the molecular ammonium ion decreases. The N-D bond length remains nearly the same but shows a tendency to grow.

REFERENCES

1 H.A.Levy and S.W.Peterson, J.Am.Chem.Soc. 75, 1536 (1953)

2 C.H.Wang and R.B.Wright, J.Chem.Phys. 57, 4401 (1972)

3 V.L.Aksenov, A.M.Balagurov, S.L.Platonov, B.N.Savenko, V.P.Glazkov, I.V.Naumov, V.A.Somenkov and G.F.Syrykh, High Pressure Research 14, 181 (1995)

4 V.P. Glazkov and I.N.Goncharenko, Fizika i tehnika vysokih davlenij (in russian), 1, 56, (1991)

5 S.N.Vaidya and G.C.Kennedy, J.Phys.Chem.Solids, 32, 951, (1971)

RESIDUAL STRESS STUDIES AT THE NEUTRON HIGH RESOLUTION FOURIER DIFFRACTOMETER

V.L.Aksenov[1], A.M.Balagurov[1], G.D.Bokuchava[2], M.Kröning[3], J.Schreiber[3], N.R.Shamsutdinov[1], Yu.V.Taran[1]

[1] Frank Laboratory of Neutron Physics, JINR, 141980 Dubna, Russia
[2] Institute for Nuclear Research of RAS, 117312 Moscow, Russia
[3] Fraunhofer Institute for Nondestructive Testing, W-6600 Saarbrücken, Germany

Introduction

Putting into operation in 1992 of high resolution Fourier diffractometer (HRFD) [1] at the IBR-2 pulsed reactor has allowed to begin realization of the residual stress investigation program in bulk samples for industrial applications [2]. HRFD includes the following equipment: four detectors at the scattering angles of ±90°(the solid angles of 28 and 7 msr) and ±152° (the solid angle of 80 msr each), 4-axis (x,y,z,ω) neutron scanner for simple experiments, two multi-slit radial collimators with gauge volume resolution of 2 mm for both ±90°-detectors, load testing machine and nitride boron slit systems. In nearest future 5-axis (x,y,z,ω,Ω) "HUBER" goniometer will be used for full strain tensor measurements. High neutron flux at the sample position (~10^7 n/cm^2/s) and high d-spacing resolution ($\Delta d/d=1\cdot10^{-3}$ at $2\theta=\pm152°$ and $4\cdot10^{-3}$ at $2\theta=\pm90°$ for d=2 Å) of HRFD gives a possibility for precise strain measurements within reasonable beam time. A combination of the time-of-flight technique and two-detector system at the scattering angles ±90° allows one to measure a large number of reflections simultaneously in two mutually perpendicular directions. With the help of these detectors measurements of residual stresses were performed in some samples for the industrial application.

Research program is realized in the frame of the agreement between FLNP, Dubna and FINT, Saarbrücken. This report describes some experiments for residual stress investigation performed at HRFD during last 2 years.

Austenitic steel tube with a welded ferritic cover

Shape welding is an interesting alternative method for manufacturing, but the existence of uncontrollable residual stress distributions in welded materials prevents its wide application. On the other hand, shape welded ferritic layers on austenitic tubes can help suppress stress corrosion because these layers produce compressive stress states on the austenitic tube. The analysis of residual stresses through the ferritic weld into the austenitic material can be helpful for the optimization of the corresponding welding technique.

Seven layers of the ferritic steel with 135 welding traces and a total cover length of 1100 mm were welded on a 15 mm thick austenitic steel tube with an outer radius of 148 mm. The outer radius of the whole manufactured two-layer tube was 168 mm. The sample with the size of 10×30×35 mm^3 was cut from this tube (fig. 1).

Two orthogonal strain components can be measured simultaneously by two detectors at the scattering angles of ±90°. Since the aim of the study was to compare the data obtained by neutron diffraction method with those by the destructive turning out method and the theoretical predictions by the finite element method, it had sufficed to measure strains only in two orthogonal directions of the scattering vector **Q**. In our case, these were the radial (ε_{rad}) and tangential (ε_{tan}) strain components. Strain scanning in a radial direction (x-axis) across the weld to a depth of 2 mm from the surface of the sample was conducted with the neutron scanner. To form the direct beam, a boron nitride diaphragm with a slit of 2 mm wide by 20 mm high was installed at the exit of a mirror neutron-guide. To set the scattered beams at ±90°, diaphragms with a slit width of 2 mm were

installed at a distance of 42 mm from the center of the diffractometer. The gauge volumes formed by these diaphragms were 2.1×4.5×19.4 and 2.1×2.6×19.4 mm^3 for the +90° and the -90° detectors, respectively.

From experimental data it is easy to calculate the difference between the tangential and radial components of the stress tensor $\sigma_{tan}-\sigma_{rad}=E(1+\nu)^{-1}(\varepsilon_{tan}-\varepsilon_{rad})$ (under the elastic model assumption). For the ferritic part (α-phase), good agreement of the neutron data with the results of other methods was found (fig.2). For the austenitic part (γ-phase), disagreement is obviously due to uncontrollable influence of II.kind microstresses on the neutron results.

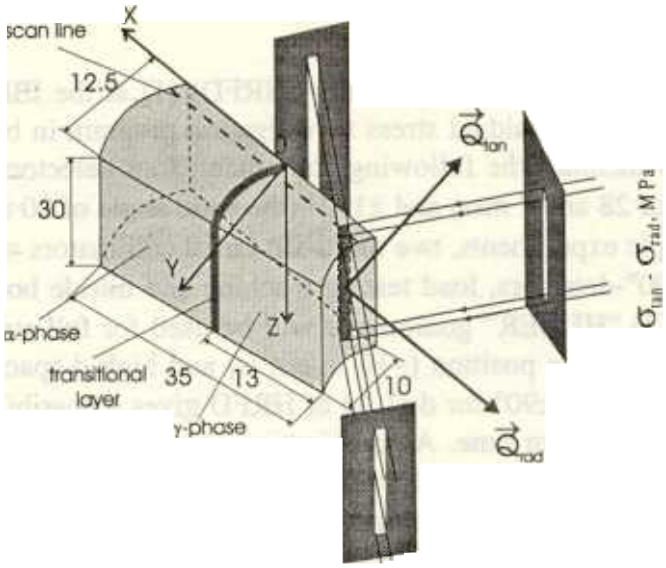

Fig. 1. The investigated sample and the (x,y,z) sample-related coordinate system.

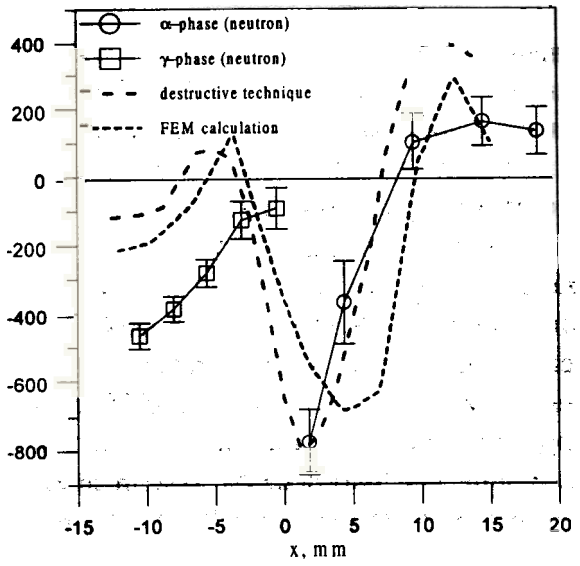

Fig. 2. The dependence of $\sigma_{tan}-\sigma_{rad}$ on the coordinate x, where x=0 corresponds to the transition layer.

In summary it should be noted that the first neutron diffraction investigations of residual stresses in shape welded tubes yielded satisfactory results. Qualitative and even quantitative agreement with the destructive turning out method results, as well as the FEM calculations can be acknowledged. However, in subsequent investigations a more complete analysis of the residual stress state can be expected. It is planned to measure all three stress components with a larger tube segment. For this purpose, the so called $\sin^2\psi$-method will be applied using X-ray and neutron diffraction techniques. In addition, it would be useful to determine the elastic constants for the both phases by carrying out a tensile test experiment.

Neutron elastic constants

Austenitic stainless steels are widely used because of their high corrosion resistance and toughness. High resolution neutron diffraction was applied to estimate the mechanical properties of austenitic stainless steel and to determine neutron elastic constants of the given material. The examined material was an austenitic stainless steel X6CrNiTi1810 of the following content (wt %): C - 0.04, Si - 0.44, Mn - 1.14, P - 0.033, S - 0.004, Cr - 17.74, Ni - 19.3, Ti - 0.35. The investigated sample of austenitic steel was subjected to a load in situ in the neutron beam, using a special purpose testing machine. The elastic strain was measured for different crystal planes (hkl), parallel and perpendicular to the applied load direction (fig. 3). From the slopes of the strain-stress linear dependencies the elastic modules $E_{||}$ and $E_{\perp}$ as a function of the anisotropy factor $\Gamma_{hkl}=(h^2k^2+h^2l^2+k^2l^2)/(h^2+k^2+l^2)^2$ were obtained (fig. 4). The strains determined from the lattice parameter changes by the Rietveld profile refinement technique and corresponding to the anisotropy

factor Γ_{hkl}=0.2 are also included. The elastic constants S_{11}, S_{12} and S_{44} were calculated in the frame of the Hill model which assumes taking of an arithmetic average of the Reuss and Voigt model values and gives the results very close to the Kröner model values. Thus, the following values were obtained: $S_{11}=6.70\times10^{-6}$ MPa^{-1}, $S_{12}=-2.24\times10^{-6}$ MPa^{-1}, and $S_{44}=12.43\times10^{-6}$ MPa^{-1}.

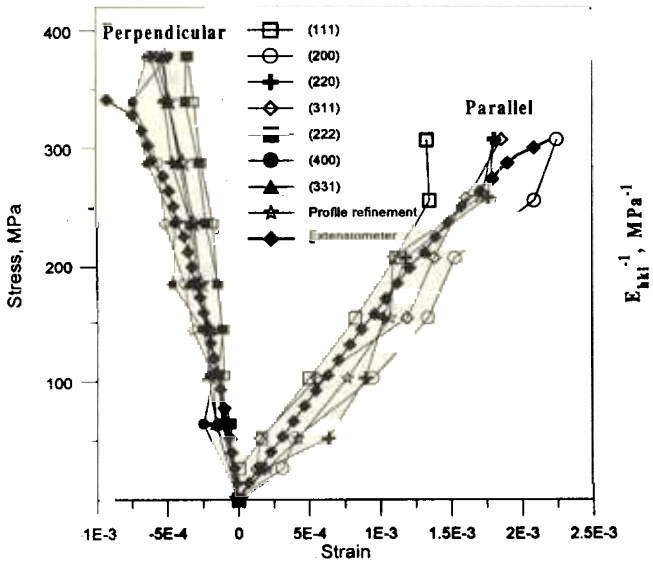

Fig. 3. Stress-strain relationships for different reflections (hkl) measured in direction parallel and perpendicular to the applied load.

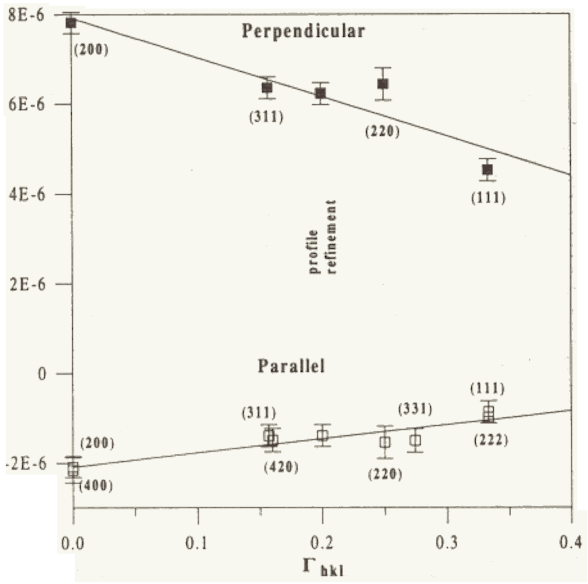

Fig. 4. Dependence of the elastic modules $E_{||}$ and $E_{\perp}$ parallel and perpendicular to the applied load versus the anisotropy factor Γ_{hkl}.

Austenitic steel samples with different degree of low cycle fatigue

The influence of applied cyclic load on the materials mechanical properties is of great current interest. In order to investigate residual stress evolution a series of the austenitic steel samples with different degree of low cycle fatigue was studied. The cylindrical samples produced from austenitic stainless steel X6CrNiTi1810 (see above) were subjected to a number of tensile-compressive loading cycles with a maximum plastic deformation of ± 0.6% at the frequency of 0.1 Hz. The number of cycles corresponding to the sample failure was $N_{max}\approx1020$. As is well known, as a result of thermal treatment or plastic deformation, austenitic stainless steel undergoes a phase transition to the tetragonal martensitic phase. The tetragonal distortion value for the martensitic structure strongly depends on the carbon content. In our experiment due to a low carbon content only the diffraction peaks characteristic for a martensitic cubic structure were registered. An increase in the martensite volume fraction was observed at an increase in the cycle fatigue degree N/N_{max} (fig. 5). The data were obtained from the Rietveld profile refinement. The residual strain for both phases was measured in the longitudinal and radial directions. It was assumed that the stress field distribution in the sample had the cylindrical symmetry. The stresses calculated from the (311) and (220) reflections for austenite and martensite, respectively, are shown in fig. 6. For an austenitic matrix, the elastic constants determined from the previous experiment were used and for martensite were taken from the literature. It is necessary to note that stresses in austenite are mainly compressive while stresses in the martensite phase are tensile.

The analysis of the diffraction peak broadening point to a partial relaxation of estimated microstresses as the fatigue degree increases. Most likely this phenomenon is connected with a growth of microcracks in the bulk of the material. For a more brittle martensitic phase, this effect is more pronounced in comparison with austenite. Usually after plastic deformation the martensite phase produces a structure of oriented plates or laths. Therefore martensite texture formation during

phase transition can be expected. Indeed the registered neutron diffraction spectra from austenitic fatigued samples shown texture presence and its variation in dependence of the fatigue degree. Consequently further detailed researches will be devoted to the quantitative analysis of the texture evolution in dependence of fatigue degree and its influence on the residual stress distribution.

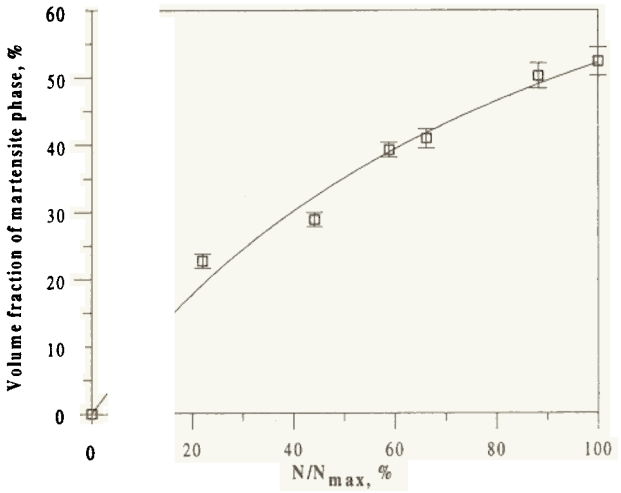

Fig. 5. Dependence of the martensitic volume fraction versus the fatigue degree. The line serves as a guide for the eye.

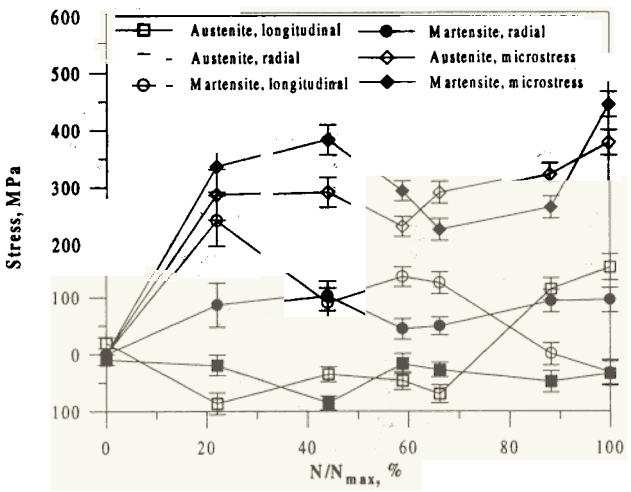

Fig. 6. Phase stresses and microstresses versus the fatigue degree

Other experiments

The functionally gradient materials (FGM) as well as composites are very promising type of advanced materials with enhanced properties. It is obvious that the mixture of materials with rather different parameters of thermal expansion is followed by the appearance of residual stresses, which have to be controlled. At the HRFD the structural changes and the variation of the residual stresses in different W-Cu and SiC-$MoSi_2$ gradient samples, prepared by an anode oxidation of porous electrodes and other methods, were studied. The samples were scanned by neutron beam with spatial resolution of ~1 mm in gradient direction. The tungsten and silicon carbide volume content and macrostress component changes were estimated from Rietveld profile refinement.

Another interesting type of material studied at HRFD are composites with Al infiltration in porous Al_2O_3 matrix (the matrix porosity degree was 15%, 25% and 35). The analysis of Al diffraction peak intensities revealed sharp texture presence for this phase while in the matrix phase the preferred orientation was absent. The total profile refinement results which corresponds to averaging on all (hkl) directions are compared with ones obtained from separate diffraction peak processing, which enables to estimate the intergranular stress fluctuations.

To obtain information on the stress state at the interface of a Si-chip on a Al_2O_3 substrate the neutron and X-ray diffraction results were combined. The residual stresses in Al_2O_3 plate are due to the housing of the Si-chip by an epoxidic layer. The results fit quite well with the FEM simulation.

References

[1] V.L.Aksenov, A.M.Balagurov, V.G.Simkin, Yu.V.Taran, V.A.Trounov, V.A.Kudrjashev, A.P.Bulkin, V.G.Muratov, P.Hiismaki, A.Tiitta, O.Antson. The new Fourier diffractometer at the IBR-2 reactor: design and first results. Proc. of ICANS-XII (Abingdon), 1993, vol.1, p.124.

[2] V.L.Aksenov, A.M.Balagurov, V.G.Simkin, Yu.V.Taran, V.A.Trounov, V.A.Kudrjashev, A.P.Bulkin, J.Schreiber. On determination of residual stresses with the high resolution Fourier diffractometer at the IBR-2 reactor. Applied Crystallography, Proc. of XVI Confer. (Cieszyn), World Scientific, 1995, p.120.

INVESTIGATION OF $Y_{0.7}PR_{0.3}BA_2CU_3O_{6+X}$ STRUCTURE UNDER PRESSURES UP TO >3 GPA

V.N.Narozhnyj[a], A.M.Balagurov[b], B.N.Savenko[b], D.V.Sheptyakov[b], V.P.Glazkov[c]

[a]*Institute for High Pressure Physics, Troitsk*
[b]*FLNP, Joint Institute for Nuclear Research, Dubna*
[c]*Russian Scientific Center "Kurchatov Institute", Moscow*

We have studied the powder sample of $Y_{0.7}Pr_{0.3}Ba_2Cu_3O_{6+x}$ (further, Y(Pr)-123), prepared in the Institute for high pressure physics (Troitsk). The content of an extra oxygen in it was close to 0.9. Later this value as well as the stoichiometry of the compound were proved to be realistic from the point of view of neutron diffraction at ambient pressure in different scattering regimes (forward, perpendicular and back scattering) and were fixed to the exact values at all the refinements at high pressure.

We used the sapphire-anvils high pressure cell (designed at the RRC "Kurchatov Institute") to create the desirable pressures at the sample. The pressure was measured by detecting the displacement of the ruby luminescence lines; the uncertainty of these determinations was 0.05 GPa (0.5 kbar).

The experiments with the sample were carried out at the DN-12 [1] time-of-flight diffractometer specialized for microsample investigations at the IBR-2 pulsed reactor in Dubna. For each pressure, the neutron diffraction patterns were collected at two different angles simultaneously (usually near 45° and 90°). Besides that the whole series of measurements at ambient pressure were made at different scattering angles from 45° to 138° (covering the range of d_{hkl} from 1.0 to 5.0 E) on a sample with a volume of approximately 20 mm^3 in order to purify the peculiarities of the original structure (stoichiometry of the compound, thermal parameters of different atoms). As all the refinements at ambient pressure gave practically identical results these values were fixed to the ideal values at all the refinements at high pressure. The experiments in the high pressure cell (sample volume $\leq$2 mm^3) were carried out at pressures of 1.5, 2.8 and 3.3 GPa in the regions of d_{hkl} from 1.8 to 5.0 E (at scattering angle 2Θ=45°) and from 0.95 to 2.56 E (at scattering angle 90°). The later regions of the diffraction patterns were processed with the Rietveld method as containing the greater number of the Bragg reflections.

Rietveld refinement treatments of the diffraction patterns obtained at zero pressure at the DN-12 diffractometer were used to estimate the values of the initial lattice parameters and the atoms coordinates in the structure. The treatment of data obtained at high pressures gave us the information about the structural changes caused by applying the high external pressure to the system. A view of parts of the Rietveld refinements for the Y(Pr)-123 structure at zero pressure and at pressure 3.3 GPa are shown in fig. 3. Detailed results of the diffraction pattern treatments at pressures 0, 1.5, 2.8 and 3.3 GPa are presented in the table 1.

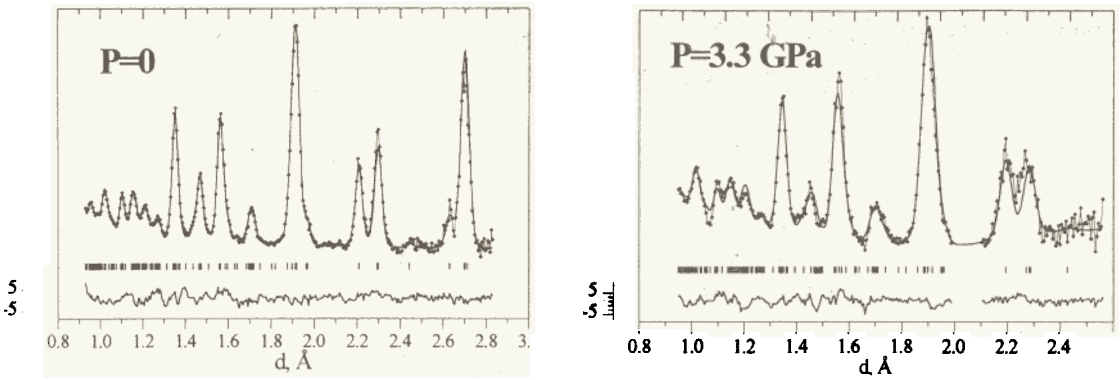

Fig. 1. The diffraction patterns of the Y(Pr)-123 measured at different pressures at the DN-12 diffractometer and processed with Rietveld method. The scattering angle 2θ≈90°. Experimental points, calculated and weighted difference profiles are shown. The ticks at the bottom of the graphs correspond to the positions of the calculated Bragg peaks.

Table

Refined structural parameters of Y(Pr)-123 ceramics at different pressures.
Instrument: DN-12. 2Θ=90 deg.

Parameter \ Press.	**0 kbar**	**15 kbar**	**28 kbar**	**33 kbar**
2Θ, deg	45°, 90°, 138°	90°	90°	90°
a, E	3.824(3)	3.787(3)	3.768(4)	3.769(3)
b, E	3.863(4)	3.844(5)	3.827(5)	3.827(3)
c, E	11.563(12)	11.462(18)	11.38(18)	11.380(15)
V, E^3	170.810	166.855	164.101	164.626
d_{hkl} – range, E	0.93 – 4.35	0.95 – 2.56	0.95 – 2.56	0.95 – 2.56
Y(0.5,0.5,0.5), n	0.7	0.7	0.7	0.7
Pr(0.5,0.5,0.5), n	0.3	0.3	0.3	0.3
Ba(0.5,0.5,z), z	0.181(2)	0.176(3)	0.168(3)	0.165(2)
Cu1(0,0,0), n	1	1	1	1
Cu2(0,0,z), n	2	2	2	2
z	0.359(2)	0.355(2)	0.358(2)	0.356(1)
O1(0,0,z), z	0.163(2)	0.158(3)	0.155(3)	0.155(2)
O2(0.5,0,z), z	0.374(5)	0.376(5)	0.379(4)	0.378(4)
O3(0,0.5,z), z	0.378 (4)	0.369(7)	0.369(7)	0.377(4)
O4(0,0.5,0), n	0.9	0.9	0.9	0.9

The obtained dependencies of the lattice constants on pressure are presented in the figs. 4 and 5. As it can be seen from the table 1, the only changes in the structure visible within the experimental and statistical errors are the displacements of the Ba atoms and of the oxygen O1 atoms in barium-containing planes. The dependencies of this coordinates on pressure are presented in the fig. 6. It is obvious that the compressing of the structure corresponds to the prior compressing of the crimped BaO plane. The absolute value of this splitting reduces by almost 45% under the pressure of 3.3 GPa.

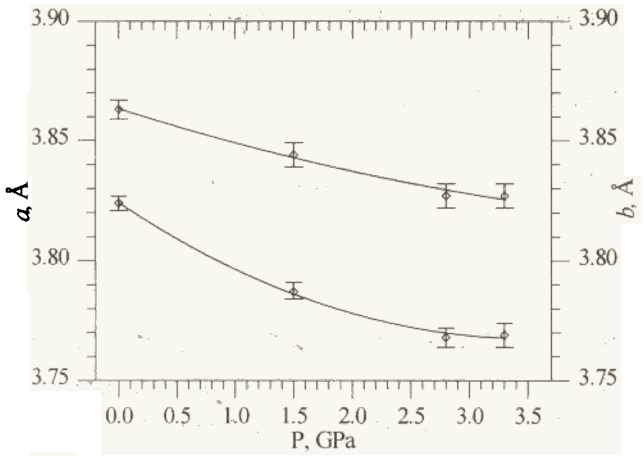

*Fig. 2. Dependencies of lattice constants **a** and **b** of Y(Pr)-123 structure versus pressure.*

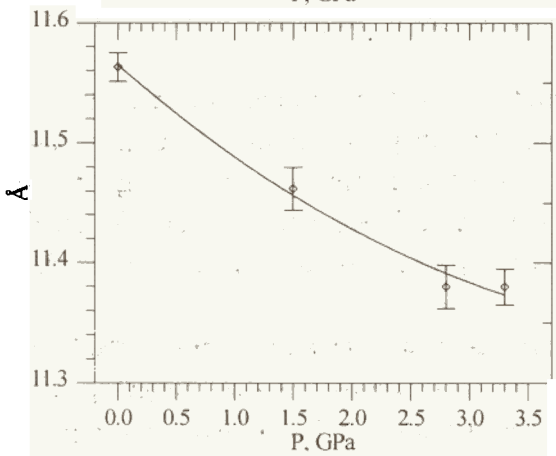

*Fig. 3. Dependence of lattice constant **c** of Y(Pr)-123 structure versus pressure.*

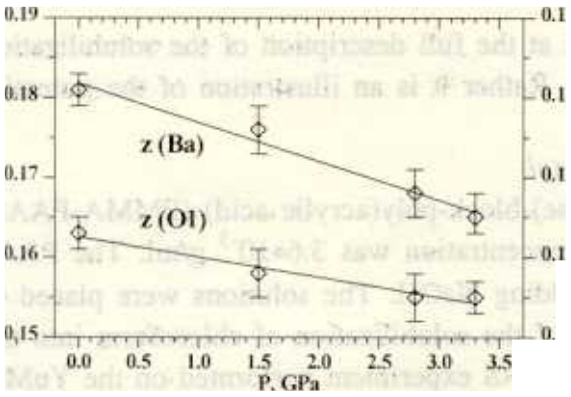

Fig. 4. Dependencies of the z-coordinates of Ba and O1 atoms in Y(Pr)-123 structure versus pressure.

V.L.Aksenov, A.M.Balagurov, S.L.Platonov, B.N.Savenko, V.P.Glazkov, I.V.Naumov, V.A.Somenkov, G.F.Syrykh, High Press. Res. 14 (1995) 181

Time-resolved SANS study of kinetics of solubilization

J. Plestil, H. Pospisil, M. Steinhart, M.A. Kiselev*

Institute of Macromolecular Chemistry, Academy of Sciences of the Czech Republic, Heyrovsky Sq.2, 162 06 Prague
**FLNP, JINR, 141980 Dubna Russia*

It has been known for some time that amphiphilic block copolymers consisting of one hydrophilic and one hydrophobic block form micelles with relatively narrow size in aqueous media. The ability of these micelles to solubilize various hydrophobic organic molecules, which has been studied by several techniques, is one of their important and interesting properties.

SANS has proven to be an extremely useful method for the structural studies on the micellar systems, including various aspects of the solubilization phenomenon. This technique provides not only the parameters characterizing micelle as a whole (mass, radius of gyration) but also an information about its internal structure (radius of micelle core and shell). These parameters are varying during solubilization can therefore be used for the description of this process.

Full understanding of the solubilization phenomenon is not possible without studying of its kinetics. The SANS technique can be employed to this purpose, if the scattering data can be taken rapidly enough. The YuMO TOF SANS spectrometer at the JINR, Dubna is an excellent instrument for such studies.

This short experimental report is not aimed at the full description of the solubilization of hydrophobic compound in the micellar solution. Rather it is an illustration of the potential of the YuMO spectrometer.

Experimental

Micelles formed by poly(methyl methacrylate)-block-poly(acrylic acid) (PMMA-PAAc) copolymer in D_2O were studied. The copolymer concentration was $3.6 \bullet 10^{-3}$ g/ml. The PAAc component was neutralized to various degree by adding NaOH. The solutions were placed in the optical cells with a path length 2mm. Kinetics of the solubilization of chloroform into the micellar solutions was followed in a time-resolved SANS experiment performed on the YuMO spectrometer.

Results

The copolymer forms micelles with PMMA core and PAAc corona in aqueous media. Solubilization into these micelles was studied for six samples with various degrees of neutralization simultaneously. The exposure time was 2 minutes per one spectrum. The resulting scattering curves provided the radii of the micellar cores for the intitial solutions and their variation with progressing solubilization of chloroform. The results for three degrees of neutralization are shown in Figure 1. In the absence of solubilizate the core radius decreases with increasing degree of neutralization α. However, preliminary NMR measurements suggest that PMMA cores are in frozen state. Thus it is likely, that the actual size of the cores is

independent of α. This discrepancy can be explained by a partial adhesion of the inner part of the corona chains (PAAc) to the PMMA core. To check this hypothesis we plan to perform similar measurements on the copolymer samples with one labelled block. Progressing solubilization of chloroform is reflected by increasing radius of the micelle core. For example, for α=0 the radius starts from the initial value of 78 Å and reaches the saturated value of 93 Å within two hours.

The described experiment shows that the YuMO spectrometer is a powerful instrument not only for the static studies but also for the time resolved experiments with the temporal resolution in the order of a minute. This is true even for not too strong scatterers like for example the dilute solutions investigated here.

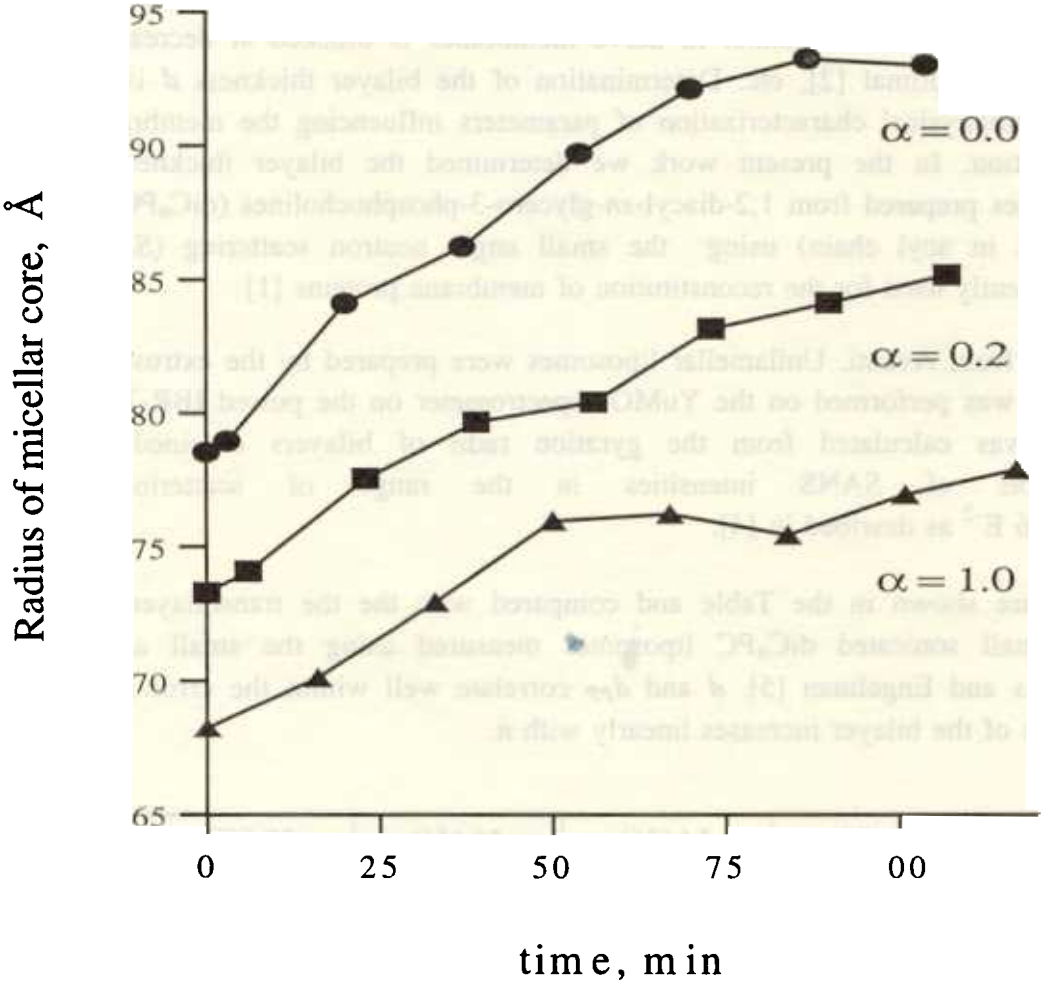

Fig.1 Variation the micellar radius during solubilization of chloroform into PMMA/PAAc micelles at chosen degrees of neutralization α. The mean radius was determined by the fitting of the experimental SANS data to the theoretical scattering curve of homogeneous spheres with a Schulz-Zimm distribution of radii.

BILAYER THICKNESS IN EXTRUDED UNILAMELLAR DIACYL-PHOSPHATIDYLCHOLINE LIPOSOMES: SANS STUDY

DUBNIKOV B.M., KISELEV M.[1], BALGAV P.

Faculty of Pharmacy, Comenius University, 83232 Bratislava (Slovakia)

[1]*Frank Laboratory of Neutron Physics, Joint Institute of Nuclear Reseach, Dubna (Russia*

Thickness of the lipid bilayer in biological membranes profoundly affects properties of transmembrane proteins. For example, the (Ca-Mg)ATPase from muscle sarcoplasmic reticulum displays maximum activity at particular bilayer thickness; the activity decreases in thinner or thicker bilayers [1], the sodium channel in nerve membranes is blocked at decreased bilayer thickness smaller than optimal [2], etc. Determination of the bilayer thickness ***d*** is thus very important for the biophysical characterization of parameters influencing the membrane protein structure and function. In the present work we determined the bilayer thickness in large unilamellar liposomes prepared from 1,2-diacyl-*sn*-glycero-3-phosphocholines (diC_nPC, ***n*** is the number of carbons in acyl chain) using the small angle neutron scattering (SANS). The liposomes are frequently used for the reconstitution of membrane proteins [1].

Lipids were from Avanti. Unilamellar liposomes were prepared by the extrusion method in D_2O [3]. SANS was performed on the YuMO spectrometer on the pulsed IBR-2 reactor in JINR Dubna. ***d*** was calculated from the gyration radii of bilayers obtained from the Kratky-Porod plots of SANS intensities in the range of scattering vectors $0.001\ E^{-2} \leq Q^2 \leq 0.006\ E^{-2}$ as desribed in [4].

The values of ***d*** are shown in the Table and compared with the the transbilayer phosphate spacing d_{PP} in small sonicated diC_nPC liposomes measured using the small angle X-ray scattering by Lewis and Engelman [5]. ***d*** and d_{PP} correlate well within the error of methods used. The thickness of the bilayer increases linearly with ***n***.

n (°C)	***12*** (20)	***14*** (36)	***16*** (44)	***18*** (60)
d	32.4±0.2 Å	34.2±0.2 Å	37.3±0.2 Å	39.8±0.2 Å
d_{PP}	30.5±1.0 Å	34.0±1.0 Å	37.0±1.0 Å	40.5±1.0 Å

1. Lee A.G., East J.M., Balgav P., Pest. Sci. 32, 317-327, 1991
2. Hendry B.M., Elliott J.R., Haydon D.A., Biophys. J., 47, 841-845, 1985
3. Gordeliy V.I., Golubchikova L.V., Kuklin A., Syrykh A.G., Watts A. Progr. Colloid Polym. Sci. 93, 252-257, 1993
4. MacDonald R.C., MacDonald R.I., Menco B.Ph.M., Takeshita K., Subbarao N.K., Hu L.-R., Biochim. Biophys. Acta 1061, 297-303, 1991
5. Lewis B.A., Engelman D.M., J. Mol. Biol. 166, 211-217, 1983

Critical Fluctuations of Lipid Membranes

V.I.Gordeliy, V.G.Cherezov
FLNP, JINR, 141980, Dubnà, Russia

Fluctuations are vital in biological macromolecules such as proteins, DNA and RNA. Fluctuations of biological membranes also seems to be important for some processes in living cell. When immersed in water lipid membranes form closed bilayer vesicles, performing small thermal undulations, governed by bending modulus of the membrane. These fluctuations can be highly enlarged by increasing the temperature or by approaching to the temperature of main phase transition. Melting of hydrocarbon chains in lipid membranes is first kind phase transition, which temperature is closed to the critical point. Near to this point in-plane density fluctuations are enhanced giving rise to decreasing of bending modulus and consequently to increasing of undulations.

Recently an anomalous increase in repeat distance of fully hydrated multilayer membranes from DMPC near phase transition temperature was observed [1, 2]. Such behavior was explained by increasing of intermembrane distance due to enlarged undulation repulsion near the critical point. However this can be argued by alternative possibility of increase in lipid bilayer thickness in intermediate region [3, 4].

We performed simultaneous measurements of temperature dependencies of both multilayer repeat distance and lipid bilayer thickness by small-angle neutron scattering. Experiments were held on small angle instrument YuMO of pulsed reactor IBR-2. Single lipid vesicles were obtained by extrusion of multilayer vesicles through filter with 100 nm pore size. [5]. Temperature was raised by successive steps 0.2°C, temperature fluctuations do not exceed 0.05°C. Repeat distance was determined from diffraction peak and bilayer thickness was obtained from radius of gyration as described in [6]. Intermembrane distance was calculated as difference between repeat distance and bilayer thickness. Results are shown in Fig.1. It can be seen from this figure that it is the increase in intermembrane distance which is responsible for the anomalous increase in repeat distance near the chain-melting phase transition temperature. This supports the hypothesis on decreasing of membrane bending modulus due to the enhanced in-plane density fluctuations in the vicinity of critical point.

References

1. T.Honger, K.Mortensen, J.H.Ipsen, J.Lemmich, R.Bauer, O.G.Mouritsen, *Phys. Rev. Lett.*, (**1994**), 72(24), 3911-3914;

2.J.Lemmich, J.H.Ipsen, T.Honger, K.Jorgensen, O.G.Mouritsen, *Modern Phys. Lett. B*, (**1994**), 8(29), 1803-1814;

3.R.Zhang, W.Sun, S. Tristram-Nagle, R.L.Headrick, R.M.Suter, J.F.Nagle, *Phys. Rev. Lett.*, (**1995**), 74(14), 2832-2835;

4.J.Lemmich, K.Mortensen, J.H.Ipsen, T.Honger, R.Bauer, O.G.Mouritsen, *Phys. Rev. Lett.*, (**1995**), 75(21), 3958-3961;

5.R.C. MacDonald, et al, *BBA*, (**1991**), 1061, 297-303;

6.V.I.Gordeliy, L.V.Golubchikova, A.Kuklin, A.G.Syrykh, A.Watts, *Progr. Colloid Polym. Sci.*, (**1993**), 93, 252-256;

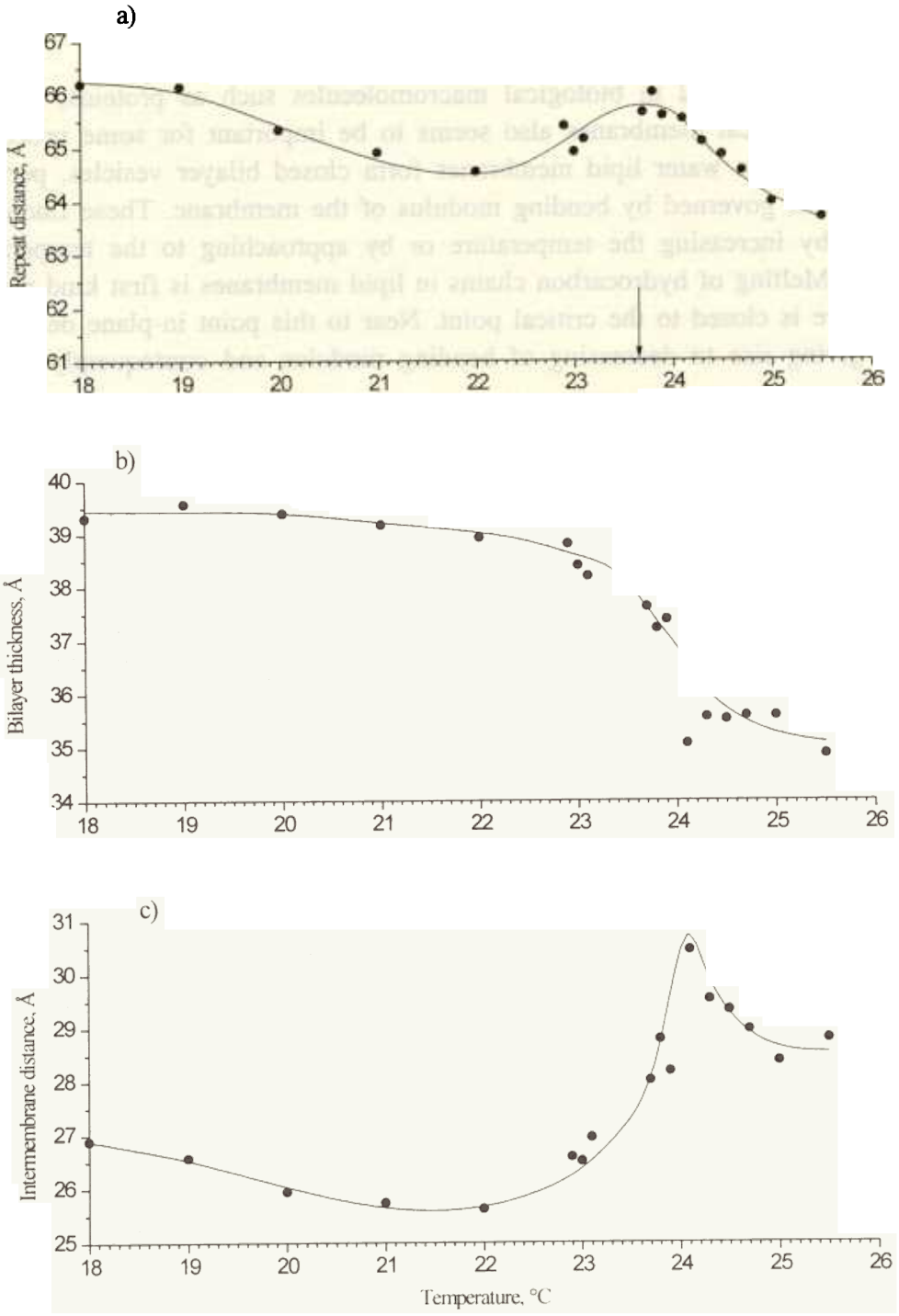

Fig.1. Temperature dependencies of a) multilayer repeat distance, b) lipid bilayer thickness and c) intermembrane distance for lipid membranes from dymiristoyl-phosphatidylcholine

Neutron Spectroscopy of C_{60} Fullerite Hydrogenated under High Pressure

A.I.Kolesnikov[1], V.E.Antonov[1], I.O.Bashkin[1], G.Grosse[3], A.P.Moravsky[2], E.G.Ponyatovsky[2] and F.E.Wagner[3]

[1] Institute of Solid State Physics, Russian Academy of Sciences, 142432 Chernogolovka, Moscow district, Russia

[2] Institute of Chemical Physics in Chernogolovka, Russian Academyof Sciences, 142432 Chernogolovka, Moscow district, Russia

[3] Physics Department, Technical University of Munich, D-85747 Garching, Germany

The inelastic neutron scattering spectra were measured at 85 K for the sample of hydrofullerite quenched after a synthesis at 620 K under a hydrogen pressure of 0.6 GPa, and then for the same sample with a hydrogen content decreased by 1.4 hydrogen molecules per C_{60} molecule after a 35 h annealing at 300 K.

Pure C_{60} fullerite has simple cubic lattice at ambient pressure and T≤255 K [1]. The lattice type changed on hydrogenation. According to the neutron and X-ray diffraction data [2], the $C_{60}H_x$ molecules of both quenched and annealed samples of hydrofullerites at T=85 K formed a *bcc* lattice with the lattice parameters of about 12.00 and 11.72 Å, respectively. The colour, crystal structure, and lattice parameter of the annealed sample agree with the earlier data for $C_{60}H_{36}$ [3]. The lattice contraction observed on annealing at 300~K indicates that hydrogen released from certain lattice sites rather than from bubbles in the crystal.

The sample measured by INS was collected of a few pellets and weighed 0.62 g. The quenched sample was measured first, then annealed at 300~K for 35~h and measured again. The background was determined in a separate empty can measurement and subtracted from the experimental data. The data were transformed to the G(ω) spectra of generalized vibrational density of states versus energy transfer.

Fig.1 shows the G(ω) spectra both of quenched and anneled sample states together with the spectrum of a 3.2 g sample of pure C_{60} measured at 77K.

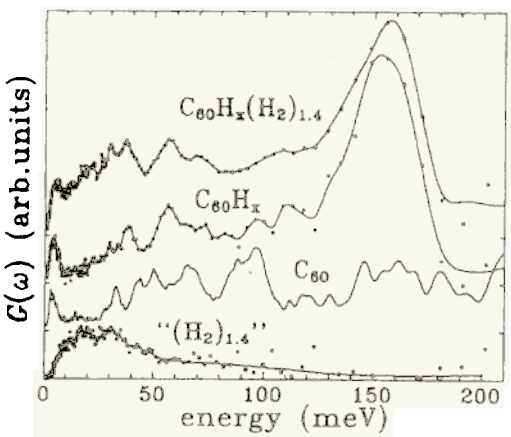

Fig.1 *The generalized vibrational density of states of 'quenched' $C_{60}H_x(H_2)_{1.4}$ and 'annealed' $C_{60}H_x$ samples measured at 85 K, the difference "$(H_2)_{1.4}$" between these two spectra which represents vibrations of interstitial molecular hydrogen in the quenched hydrofullerite, and the spectrum of pure C_{60}, measured at 77 K*

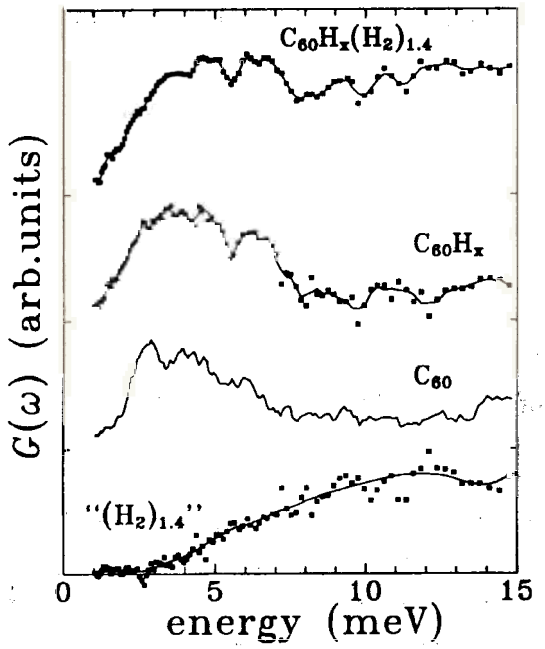

Fig.2 *The same as in figure 1, in the neutron energy transfer range 0-15 meV*

The sprectra of the annealed sample and pure C_{60} are much similar in the range 0-8 meV of intermolecular vibrations. Fig.2 provides the better evidence of it. This indicates that H atoms in the annealed $C_{60}H_x$ sample are chemically bound to C_{60} cages. An astimation from the areas under the G(ω) curves for the anneled $C_{60}H_x$ and pure C_{60} in the region below 8meV gave a correct value of x≅24.

In the range 25-110 meV of radial intramolecular modes in pure C_{60}, the spectra of the hydrofullerites exhibit peaks at 30, 38,56 and 70 meV. Compared to pure C_{60}, the peaks are drastically shifted in energy and have different relative intensities. This means that hydrogen strongly affects the intramolecular C-C interaction. At ω > 110 meV, one largebroad peak centered at ω≈155 meV is observed in the spectra of both $C_{60}H_x$ samples. Folloving the spectrum interpretation for hydrogenated amorphous carbon [4] we attribute this peak to C-H bending modes.

The difference between the spectra of quenched and annealed hydrofulleriets (Fig.1,2, bottom and fig 3) is quite anlike tree other spectra. The difference spectrum is evidentently due to "excess" 2.8 H atoms per C_{60} in the quenched sample. The observed dissimilarity together with the lattice contraction on annealing suggest that these H atoms are not chemically bound to the C_{60} cages and occupy interstitial in the *bcc* $C_{60}H_{24}$ lattice.

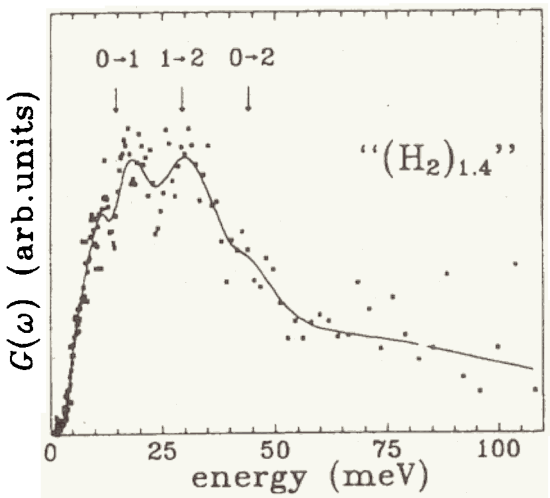

Fig.3 *The difference spectrum from Fig.1 represented on a larger scale. The arrows shows transition energies between rotation states of a free hydrogen molecule with the given rotation quantum numbers.*

As seen from Fig.3, the peaks in the difference spectrum at 12,18.30 and 45 meV can be reasonably well explained whithin the rotator model of molecular hydrogen [5]. The model energy states are given by $E(J)=B\cdot J(J+1)$, where B=7.35

meV and J is the rotational quantum number. The peaks at 30 and 45 meV agree with the (1→2) and (0→2) transitions. The latter has low intensity because it corresponds to the transition between two rotational states in parahydrogen molecules which are coherent neutron scatterers [5]. Two peaks at 12 and 18 meV are assumed to result from splitting of the (0→1) at 14.7 meV due to interaction between H_2 and nearby $C_{60}H_{24}$ molecules. Similar splitting of the (0→1) peak to a pair of peaks at 12.5 and 16 meV was observed ealier in the INS spectrum ofmolecular H_2 trapped in amorphous carbon [4]

1. Heiney P.A. et al 1992, Phys. Rev.B **45**, pp 4544-7
2. Kolesnikov A.I., Antonov V.E., Bashkin I.O., Cornell K., Moravsky A.P., Ponyatovsky E.G., and Wipf H., to be published
3. Hall L.E. et al, 1993 J.Phys.Chem., **97**, pp.5741-4
4. P.J.R.Honebone et al Chem.Phys.Lett. **180**, p.145 (1991)
5. L.D.Landau and E.M.Lifshitz, Quantum Mechanics (Oxford: Pergamon Press, 1965), p.616.

NEUTRON SCATTERING INVESTIGATION OF ICE UNDER HYDROSTATIC HELIUM PRESSURE

I. Natkaniec*[&], G.G. Malenkov[@], L.S. Smirnov*, L. Bobrowicz[#], S.I. Bragin*

*-Frank Laboratory of Neutron Physics, JINR, 141980 Dubna, Russia.
&-H. Niewodniczanski Institute of Nuclear Physics, 31-342 Krakow, Poland.
@-Institute of Physical Chemistry of Russian Ac. Sciences, 117915 Moscow, Russia.
#-Institute of Physics, A. Mickiewicz University, 60-780 Poznan, Poland.

Hydrogen bounded networks formed by water molecules in clathrate hydrates are stabilised by guest molecules and a direct comparison of filled and empty structures is not possible [1]. A remarkable exception is the clathrate-like phase of (H_2O+He), whose p-T phase diagram and crystal structure were recently studied [2,3]. Atoms of He can be enclosed in cavities of the ice II water molecule network without considerable change in its geometry. The He content - x, where x is the fraction of occupied cavities, varies with pressure and the phase is stable when P>2.8 kbar (x=0.62) [3]. The crystal structure of helium clathrate is close to that of ice II and is also orientationally ordered.

Our investigation of the water dynamics in the (H_2O+He) system were performed with the help of the GCA-10 gas compressor used for neutron scattering studies of condensed matter under high pressure [4]. Inelastic incoherent neutron scattering (IINS) spectra of (H_2O+He) system were measured on the NERA-PR spectrometer [5] at a helium pressure of ca. 1 and 3 kbar for different temperatures. The IINS spectra obtained at 1 kbar of helium pressure at 270 K and 236 K correspond to liquid water and ice Ih, respectively. Then the pressure of the helium gas was increased at 270 K up to 3.28 kbar. The subsequent IINS spectra obtained at the following temperatures: 271-270 K, 256-253 K, 253-249 K, 249-239 K, 239-236 K, 236-235 K and 115-114 K, indicate the freezing temperature of the (H_2O+He) system at ca. 239 K. At cooling, the helium pressure was stabilised at ca. 3 kbar. The IINS spectra of H_2O and (H_2O+He) at P=3 kbar close to freezing temperatures are presented in Fig. 1. One can see that the water compressed by helium gas at ca. 3 kbar does not freeze to ice III at ca. 255 K but remains in a liquid state down to ca. 239 K.

The phonon density of states G(E) obtained from the IINS spectra of (H_2O+He) in the solid phases at P=1 kbar and T=236 K and at P=3 kbar and temperatures of 236 and 115 K, respectively, are presented in Fig. 2. One may conclude that the G(E) spectrum of (H_2O+He) at 1 kbar and T=236 K corresponds to ice Ih. The G(E) spectrum of (H_2O+He) at 3 kbar and T=236 K is similar to the G(E) of ice II and this similarity enhances with decreasing temperature, as one may see in Fig. 3. The G(E) spectra obtained at the same pressure for ice III at 250 K and (H_2O+He) at 236 K are also presented in Fig. 3.

References:

1. G.G. Malenkov, Zh. Struct.Khimii, **3** (1962) 220.
2. D. Londono, W.F. Kuhs, J.L. Finney, Nature, **332** (1988) 141.
3. D. Londono, J.L. Finney, W.F. Kuhs, J. Chem. Phys., **97** (1990) 547.
4. S. Habrylo, S.I. Bragin, J. Brankowski, K. Zawalski, W. Iwanski, J. Mayer, W. Nawrocik, I. Natkaniec, PTE, **5** (1989) 63.
5. I. Natkaniec, S.I. Bragin, J. Brankowski, J. Mayer, Proc. ICANS-XII, Abingdon 1993, RAL Report 94-025, Vol. I. p.89-96.

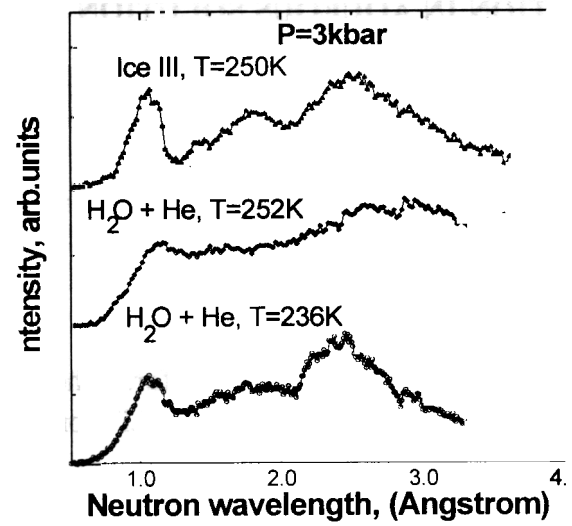

Fig. 1
Comparison of IINS spectra at a hydrostatic pressure of P=3 kbar for ice III at 250 K with a liquid and solid (H_2O+He) mixture close to the freezing temperature at 239 K.

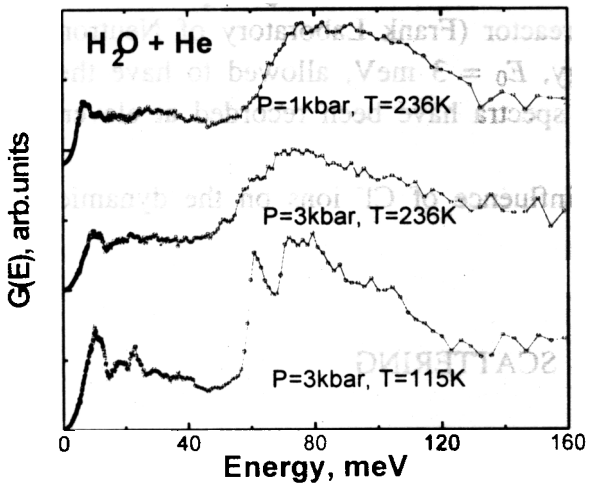

Fig. 2.
Pressure and temperature dependence of the G(E) weighted density of vibrational spectra of (H_2O+He) ices.
At 1 kbar, the G(E) spectrum of (H_2O+He) ice corresponds to the G(E) spectrum of ice Ih, while at 3 kbar these spectra are similar to the corresponding spectra of ice II.

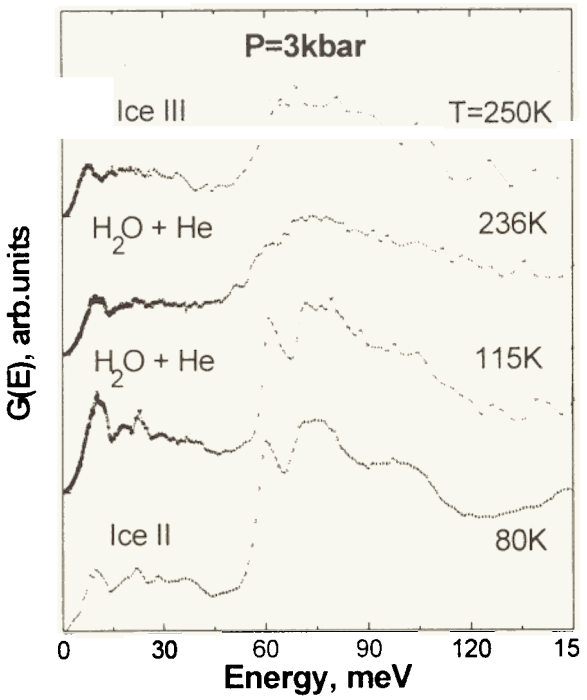

Fig. 3.
Comparison of the G(E) spectra for (H_2O+He) ice under hydrostatic helium pressure of 3 kbar with the corresponding spectra of ice III and ice II compressed in the cylinder-piston high pressure cell at similar temperatures

THE INVESTIGATION OF IONIC HYDRATION IN AQUEOUS SOLUTION OF LICL BY INELASTIC NEUTRON SCATTERING

A.G.Novikov[a], M.N.Rodnikova[b], V.V.Savostin[a] and O.V.Sobolev[a]
[a]State Scientific Centre - Institute of Physics and Power Engineering, 249020, Obninsk, Kaluga Region, Russia
[b]Kurnakov Institute of General and Inorganic Chemistry, Russian Academy of Science, 117907, Moscow, Russia

The aim of this work: using inelastic neutron scattering method, to perform the analysis of diffusion and vibration-rotation motions of water molecules hydrating Li^+ ion in comparison with pure water molecules.

The experiment has been performed on 2M lithium chloride solution and on pure water. It has been carried out with the use of DIN-2PI double time-of-flight spectrometer operating on a neutron beam of the IBR-2 pulsed reactor (Frank Laboratory of Neutron Physics, JINR, Dubna)[1]. The initial neutron energy, E_0 = 3 meV, allowed to have the resolution, ΔE_0 = 0.14 meV. The neutron scattered spectra have been recorded at eleven angles in the range from 11° to 134°.

In the course of data processing we supposed the influence of Cl^- ions on the dynamic properties of water molecules could be neglected [2].

RESULTS: QUASI-ELASTIC SCATTERING

To get the results, concerning with quasi-elastic scattering, the following steps have been done:

– from the total $S(Q,\varepsilon)$ the effects of multiple and inelastic scattering have been removed.

– the experimental quasi-elastic scattering law, $S_{q.el}(Q,\varepsilon)$, obtained for Θ = const. by interpolation procedure has been transformed into the form for Q = const;

- $S_{q.el}(Q,\varepsilon)$ for solution studied was approximated by superposition of two lorentzians [3]:

$$S_{q.el}(Q,\varepsilon) = \frac{1}{\pi}\left[\frac{\alpha\Delta E_1/2}{(\Delta E_1/2)^2+\varepsilon^2}+\frac{(1-\alpha)\Delta E_2/2}{(\Delta E_2/2)^2+\varepsilon^2}\right]\otimes R(Q,\varepsilon) \quad (1$$

where: ΔE_i are the FWHWs of the Lorentzians corresponding to the scattering on the molecules of hydration and bulk water, α - the share of hydration molecules in solution; $R(Q,\varepsilon)$ is the spectrometer resolution function. Sign $\otimes$ means the convolution operation.

For the analysis of the FWHM of the $S_{q.el}(Q,\varepsilon)$ natural line the model of mixed diffusion [4] has been used:

$$\Delta E(Q^2) = \frac{2\hbar}{\tau_0}\,\frac{1+D_0Q^2\tau_0}{1+(D-D_0)Q^2\tau_0}\,\frac{\exp(-2W)}{} \quad (2)$$

Here,τ_0 - residence time, D_0 is the coefficient of continuous (collective) diffusion, D is the total coefficient of self-diffusion, exp(-2W) is Debye-Waller factor $2W = \overline{u^2}Q^2$ where $\overline{u^2}$ is the mean-square amplitude of molecular vibrations.

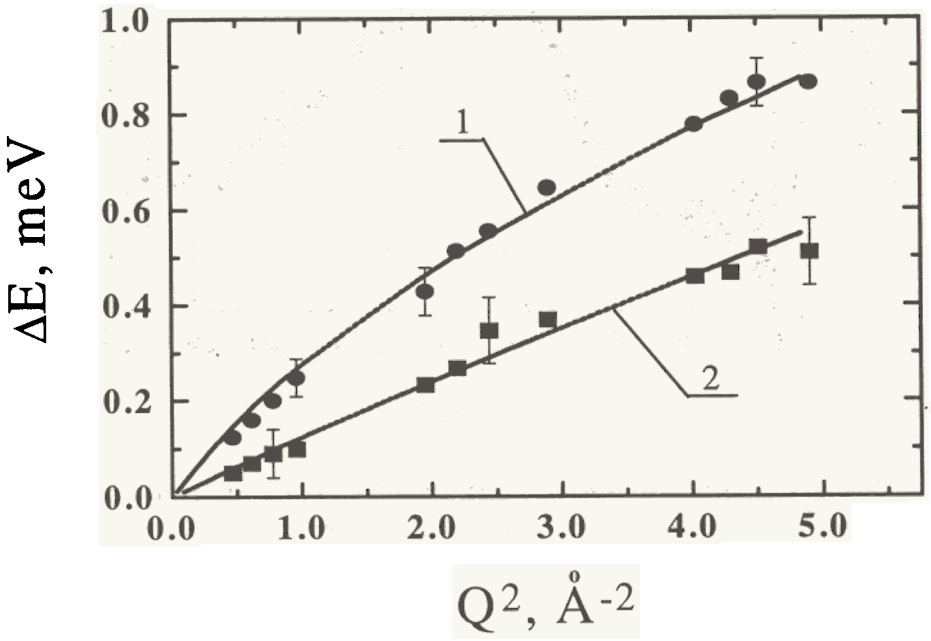

Fig.1. The FWHM of quasi-elastic scattering law natural line for pure water (one lorentzian approximation)and LiCl solution (two-lorentzian approximation).1 - the experimental FWHM for pure water (description by model (3)); ● - the experimental FWHM for bulk water; ■ - and 2 - the experimental FWHM for hydration water and its description by model (3).

The experimental FWHMS for pure water (one lorentzian approximation) and for solution (two lorentzian approximation) are shown on Fig. 1.

For FWHM of pure water model (2) gives following parameters: D = (2.2 ± 0.1)×10^{-5} cm^2/s, D_0 = (0.8 ± 0.05)×10^{-5} cm^2/s, τ_0 = 3.1 ± 0.5 ps.

For FWHM of hydrated water these parameters are: D^{hyd}= (0.95 ± 0.05)×10^{-5} cm^2/s, D_0^{hyd}= (0.79 ± 0.05)×10^{-5} cm^2/s, τ_0^{hyd}=25 ± 10ps.

The D_0^{hyd} obtained is equal to $D_{ion} \approx 0.8\times10^{-5} cm^2/s$ achieved in [5]. τ_0^{hyd} is in agreement with the results of Hertz ($\tau^R \geq 20$ps [5]).

The share of hydration lorentzian in the common square under quasi-elastic peak $\alpha \approx 0.15 \pm 0.05$ corresponds to four molecules in hydration shell of Li^+ ion.

RESULTS: INELASTIC SCATTERING

The analysis of the inelastic component of $S(Q,\omega)$ has been aimed to get the generalized frequency distribution (GFD) of proton for water molecules in pure water and solution studied.

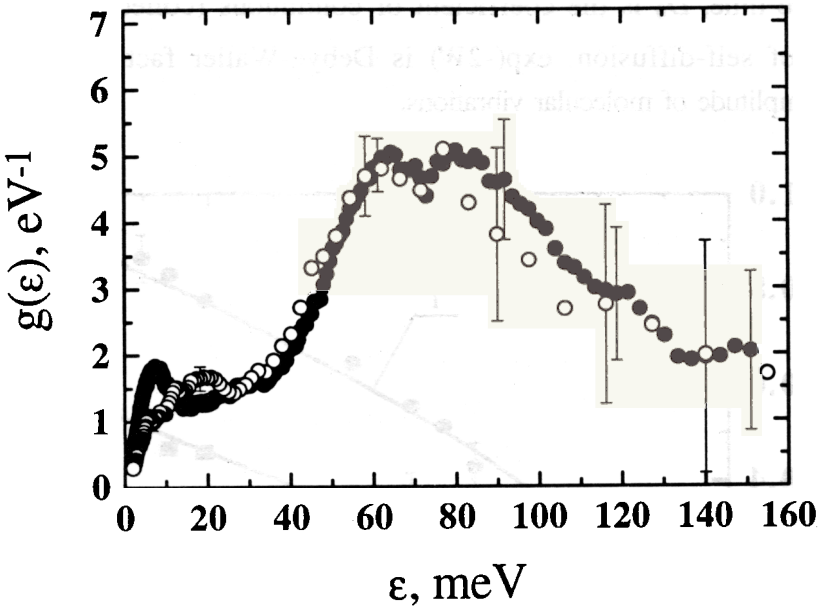

Fig. 2. Generalized frequency distribution of water molecules.
●- pure water; ○- hydration water of Li^+ ion

The procedure of GFD extraction for hydration molecules from inelastic neutron scattering experiment data involved following steps:

- the double-differential scattering cross-section (DDSCS) of pure water has been subtracted from DDSCS of solution. The first has been taken with the weight equal to the relative fraction of bulk water molecules in 2M solution, determined during the analysis of quasi-elastic component of solution studied ($\eta \approx 0.85$). So we get the DDSCS of hydration water.
- the GFD for hydration water has been extracted from its DDSCS obtained above. The method we used for this purpose has been developed and tested on pure water (details and corresponding formulas see in [6]).

Fig. 2 presents the final GFD's we got for pure water and hydration water. GFD extracted corresponds to the region of intermolecular interactions for water molecules ($2meV<\varepsilon<175meV$), and it does not include diffusion and intramolecular degrees of freedom.

As follows from Fig. 2:

- the intensity of the firs translation mode (with the location about $\varepsilon_0 \approx 6$ - 7 meV) corresponding to bending of the O-O-O angle is decreased more than twice;
- the intensity of the second translation mode ($\varepsilon_0 \approx 20meV$) assumed to be connected with H-bonds stretching is increased.
- the libration region of GFD (with maximum at $\varepsilon_0 \approx 60meV$) within the limits of experimental errors we consider as un-changed one.

REFERENCES

1. User Guide. Neutron Experimental Facilities at JINR, ed. Yu.V. Taran. Dubna:JINR Press, 1992.

2. J.Enderby and G.Neilson, Rep. Prog. Phys. 44 (1981) 593.

3. P.S. Salmon, J. Phys. C. 20 (1987) 1573.

4. V.S. Oskotskii, Fiz. Tverd. Tela. 5 (1963) 1082.

5.H.G Hertz, R. Tutsch and H Versmold, Ber.Bunsen.Phys.Chem. 75 (1971).1177.

6. A.G.Novikov, Yu.V.Lisichkin, and N.K.Fomichev, Russian J. Phys. Chem. 60 (1986) 1337.

LATTICE AND METHYL GROUPS DYNAMICS IN SOLID *p*-XYLENE WITH DIFFERENT DEUTERATED MOLECULES

I. Natkaniec[a#], J. Kalus[b], W. Griessl[b], K. Holderna-Natkaniec[c].

[a] - *Frank Laboratory of Neutron Physics, JINR, 141980 Dubna, Russia,*
#- on leave from: H. Niewodniczanski Institute of Nuclear Physics, 31-342 Krakow, Poland.
[b] - *Institute of Physics, University of Bayreuth, 95440 Bayreuth, Germany.*
[c] - *Institute of Physics, A. Mickiewicz University, 61-614 Poznan, Poland.*

Solid *p*-xylene, $C_6H_4(CH_3)_2$, provides a relatively simple example of methyl group rotation within a weak potential caused mainly by intermolecular interaction. This kind of interaction also determines the lattice dynamics. The experimental and calculated phonon density of states G(E) for protonated *p*-xylene are presented in Fig. 1. The lattice dynamics model, based on the"6-exp" atom-atom potential set of parameters fitted to the lattice dynamics of solid benzene [1], can not satisfactorily explain the dynamics of the *p*-xylene crystal. The modified set of potential parameters reproduce the experimental amplitude weighted phonon density of state G(E), quite well, what allow one to study the coupling of the internal methyl rotation with the lattice modes [2].

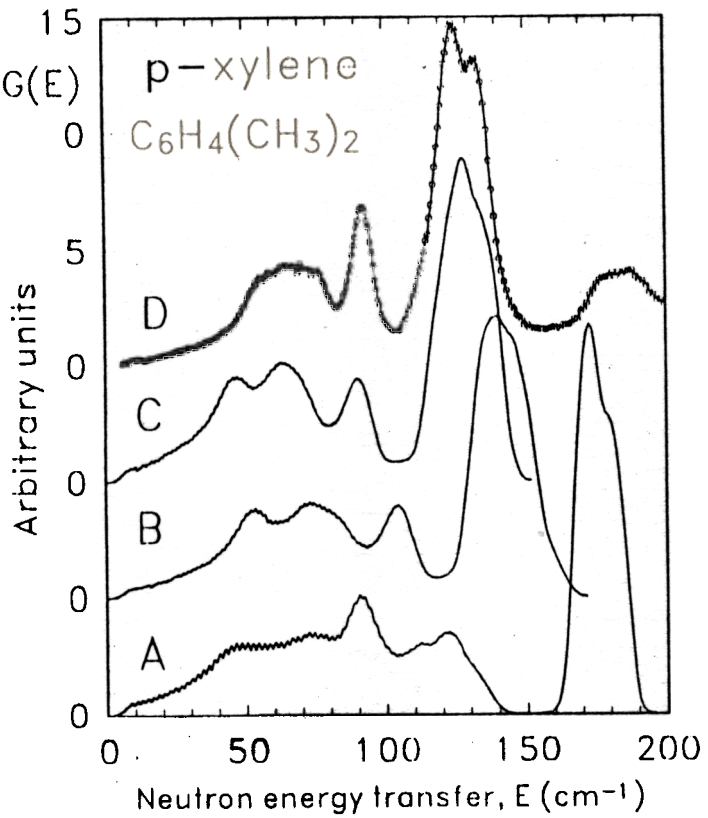

Fig. 1. The calculated amplitude weighted phonon density of states G(E) for protonated p-xylene, covoluted with the resolution of the NERA-PR spectrometer:
A - using the Williams IV(a) set of atom-atom potential parameters fitted to the lattice dynamics of solid benzene [1].
B - using the Williams IV(a) set of parameters, renormalized to the experimental structure [3] of the deuterated p-xylene at 10 K.
C - using a modified set of parameters for the hydrogen atoms of the methyl groups [2].
D - the experimental G(E), obtained from the IINS spectrum of p-xylene measured on the NERA-PR spectrometer at 10 K.

We recently investigated the IINS spectra of solid *p*-xylene with differently deuterated molecules: *p*-xylene-D4 = $C_6D_4(CH_3)_2$, -D6 = $C_6H_4(CD_3)_2$ and -D10 = $C_6D_4(CD_3)_2$. These deuterations change the frequencies of the methyl and lattice vibrations in different ways. This allowed us to test the model of atom-atom potentials in more detail for its usefulness in determining the rotational dynamics of methyl groups. The IINS measurements were performed at 10K in a

neutron energy-loss mode using the NERA-PR inverted geometry multicrystal spectrometer [4] at the IBR-2 high flux pulsed reactor. The IINS spectra measured for 14 scattering angles between 20 and 160 degrees were transformed into the amplitude weighted phonon density of state G(E) using a one phonon scattering approximation. The calculated and experimental G(E) spectra for differently deuterated *p*-xylene molecules are compared in Fig. 2.

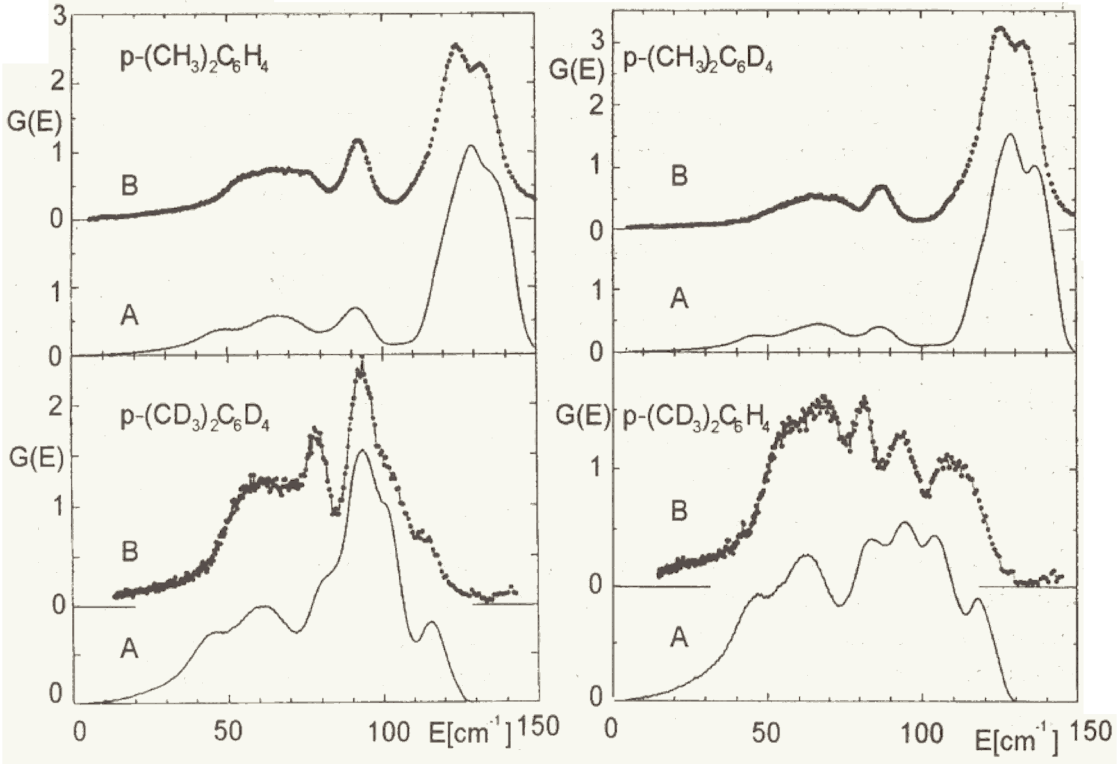

Fig.2. The calculated (A) and experimental (B) amplitude weighted phonon density of states G(E) of solid p-xylene at 10K for differently deuterated molecules.

From the results presented in Fig 2. one can conclude that atom-atom potentials satisfactorily reproduce the modifications in the lattice dynamics and internal rotation of the methyl groups caused by deuteration. By decreasing the potential depth for the H or D atoms of the methyl groups with their neighbouring atoms, we are able to obtain, for one set of potential parameters, the correct energies for the torsional vibrations and to show how they are coupled to the lattice modes. However, this procedure weakens the direct molecule-molecule interaction. The calculated cut-off frequencies of the acoustic translational phonons, at ca. 45cm^{-1}, are lower than their experimental value of ca. 60 cm^{-1}. Thus, the atom-atom potential model has rather limited applications in the study of low-frequency rotational dynamics of molecular groups in crystals.

[1]. G. Tadei, H. Bonadeo, M.P. Marzocchi, S. Califano, J. Chem. Phys., **58** (1973) 966.

[2]. J. Kalus, M. Monkenbush, I. Natkaniec, M. Prager, J. Wolfrum, F.Worlen, Mol. Cryst. Liq. Cryst., **268** (1995) 1-20.

[3]. M. Prager, W.I.F. David, R.M. Ibberson, J. Chem. Phys., **95** (1991) 2473.

[4]. I. Natkaniec, S.I. Bragin, J. Brankowski, J. Mayer, Proc. ICANS XII, Abingdon 1993, RAL Report 94-025, Vol. I. p.89-96.

Phonon dispersion curves in Fe-18Cr-10Mn-15Ni FCC steel

S.A.Danilkin [a], *E.L.Yadrowski*

[a] Institute of Physics and Power Engineering, Obninsk, Russia

Austenitic Fe-Cr-Mn(Ni) alloys are of interest because interstitial nitrogen stabilizes the FCC structure and improves the strength, toughness and corrosion resistance. The Nitrogen effect on the interatomic interactions in austenitic steel was studied earlier for polycrystalline samples by inelastic neutron scattering [1]. To obtain detailed information on the force constants, measurements with single crystals are necessary to be conducted. So far the difficulty was to producing large single crystals of nitrogen austenitic steel.

Phonon dispersion curve measurements were started with an austenitic Fe-18Cr-10Mn-15Ni steel single crystal containing no nitrogen additions. First, the lattice parameter was measured. For this purpose the chopper in the spectrometer DIN-2PI [2] was removed and the time-of-flight diffraction spectrum of an oriented crystal was measured. The lattice parameter equals a=0.359 nm for the (200) plane at the scattering angle 2Θ=128.87°. The mosaic spread of the crystal was estimated to be as large as 40'. This is commensurable with an angular divergence of the neutron beam.

Dispersion curve measurements were performed with the multidetector spectrometer DIN-2PI. In the measurements, we used the geometry with the wave vector of the scattered neutrons $\boldsymbol{k}$ coinciding with the selected symmetry direction which does not pass through the origin of the reciprocal space. With this method, we measure phonons with a wave vector in the desired symmetry direction for the selected scattering angle Θ. The value of $\boldsymbol{k}_0$ and the crystal orientation are defined by the crystal structure and Θ.

For the optimal choice of experimental conditions, we performed model calculations with dispersion curves for a invar alloy $Fe_{0.7}Ni_{0.3}$ of [3]. We performed 13 different scans. The number of phonons measured in one scan varied from 2 to 4, the measuring time was from 2 hours for low frequency phonons to 10 - 12 hours for phonons with $q/q_m \cong 0.5$. In the measurements we used simultaneously 15 - 30 detectors, but for the lattice dynamics analysis only phonons with the wave vectors in the [110] direction were selected.

Figure 1 shows the results obtained for a Fe-18Cr-10Mn-15Ni steel. Only two phonon branches, L and T_1, are shown because for the(100) reciprocal plane $S(\boldsymbol{K},\omega)$=0 for theT_2 branch. The maximum frequencies of the L and T_1 branches are in agreement with the peak positions in the vibrational frequency distribution of the polycrystalline alloy - 23 and 32 meV [1].

The experimental data were analyzed in the frame of the model of lattice dynamics with considering the central force interaction for the first two neighbours [3]. For two measured dispersion branches it is possible to determine the force constants for the first neighbours $a_1=V''(r_1)$ and $b_1=V'(r_1)/r_1$, and the sum of the force constants a_2+b_2 for the second neighbours. The fitting procedure gives the following values: a_1=3.899±0.012, b_1=-0.198±0.008 and a_2+b_2=0.109±0.016 ($\times 10^4$ dyn/cm). To determine a_2 and b_2, additional measurements of the [110] T_2 branch or phonon dispersion in other symmetry directions should be performed.

Figure1 shows that the calculated dispersion curves are in good agreement with the experimental data for the transversal branch T_1 and longitudinal phonons for $q/q_m < 0.4$. The difference for high-energy L-phonons ($\hbar\omega \cong 32$ meV) may be connected with a simplification

of the dynamic model used or the incoherent scattering background. For the alloys studied the incoherent cross section is significant due to the presence of Ni and Cr. Therefore, for this energy region it was difficult to distinguish the peaks due to coherent scattering.

References:

[1] V.G.Gavriliuk, S.A.Danilkin et al., Izvestija RAN, Metalli, 5 (1995) 51.

[2] Neutron experimental facilities at JINR, User Guide, Frank Laboratory of Neutron Physics, Joint Institute for Nuclear Research, Dubna, 1992, p.24.

[3] S.Garg, H.Gupta et al., J.Phys.F, Met. Phys., 15 (1985) 1895.

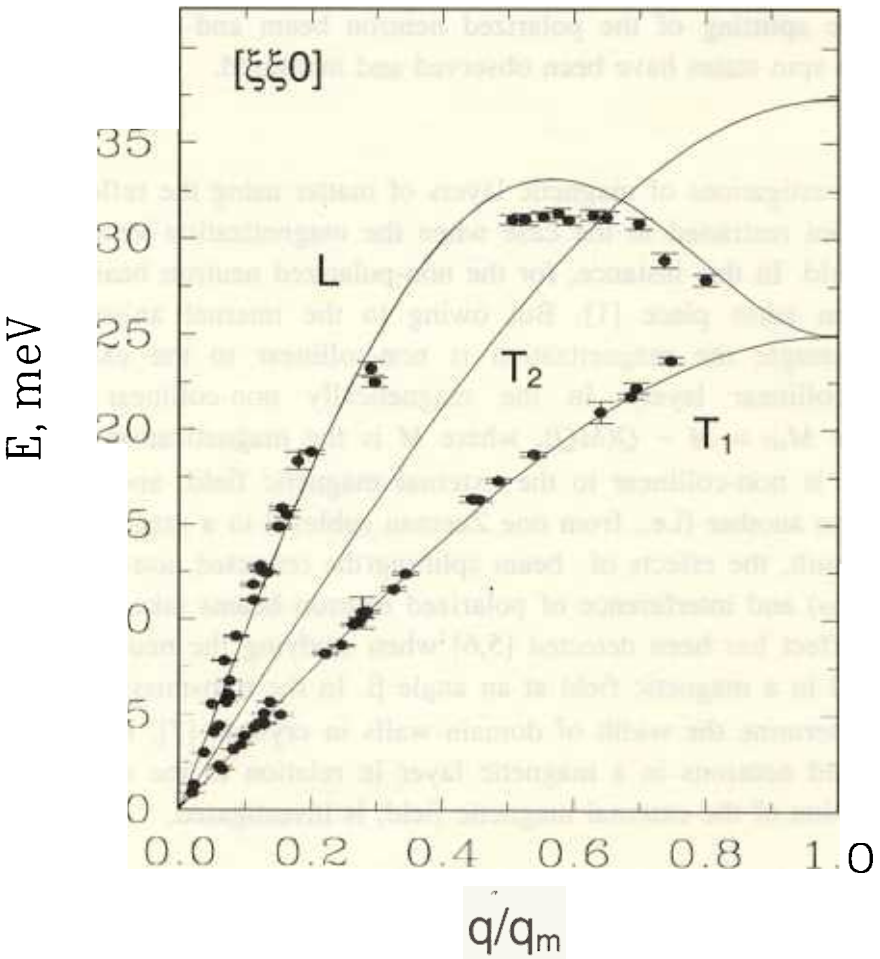

Fig.1. Phonon dispersion curves in a Fe-18Cr-10Mn-15Ni steel. • - experiment; — model.

REFRACTION OF POLARIZED NEUTRONS IN A MAGNETICALLY NON-COLLINEAR LAYER

V.L. Aksenov[a], E.B. Dokukin[a], S.V. Kozhevnikov[a],
Yu.V. Nikitenko[a], A.V. Petrenko[a] and J. Schreiber[b]

Frank Laboratory of Neutron Physics, JINR, 141980 Dubna, Moscow Region, Russia
[b] Fraunhofer Institute for Non-destructive Testing, D-01326 Dresden, Germany

The refraction of polarized neutrons in a magnetic layer in relation to the neutron wavelength, the magnitude and direction of an external magnetic field, has been investigated experimentally. The effects of space splitting of the polarized neutron beam and the interference of neutron beams with different spin states have been observed and measured.

1. Introduction

So far the investigations of magnetic layers of matter using the reflection or transmission of neutrons have been restricted to the case when the magnetization vector is collinear to the external magnetic field. In this instance, for the non-polarized neutron beam in a magnetic layer the double refraction takes place [1]. But owing to the internal anisotropy and the shape anisotropy of the sample the magnetization is non-collinear to the external magnetic field (magnetically non-collinear layer). In the magnetically non-collinear layer the effective magnetization vector $M_{eff} = M - Q(MQ)$, where M is the magnetization vector, and Q is the transfer momentum, is non-collinear to the external magnetic field, and the neutron transition from one spin state to another (i.e., from one Zeeman sublevel in a magnetic field to another) is realized [2]. As a result, the effects of beam splitting(the refracted non-polarized neutron beam splits into four beams) and interference of polarized neutron beams take place [3,4]. At present, the beam splitting effect has been detected [5,6] when studying the neutron reflection from the magnetic film placed in a magnetic field at an angle β. In the transmission geometry this effect has been used to determine the width of domain walls in crystals [7]. In the present paper the refraction of polarized neutrons in a magnetic layer in relation to the neutron wavelength, the magnitude and direction of the external magnetic field, is investigated.

2. Experimental details

The investigations have been conducted at the polarized neutron spectrometer at the IBR-2 reactor. A scheme of a complete polarization analysis [2] has been realized. The angle β between the direction of the magnetic field and the sample plane was set within $0 \div 90°$. The divergence of the neutron beam in the horizontal plane was ± 0.1 mrad, and the grazing angle of the beam incident on the sample was $\theta = 3.17$ mrad. The investigated sample was a magnetic layer produced by evaporation sputtering of FeSiAl(Si-4.4at.%, Al-9.6at.%)on a ceramics substrate($10 \times 20 \times 1 mm^3$). The thickness of the layer was 5μm and the coercivity was 3.5Oe.

3. Results and discussion

Figure 1 presents the integral in wavelength ($1 \div 12$ E) count versus the grazing angle θ_{tr} of the transmitted beam. It is seen from the figure that for $\beta = 70°$ as compared with $\beta = 0°$ a

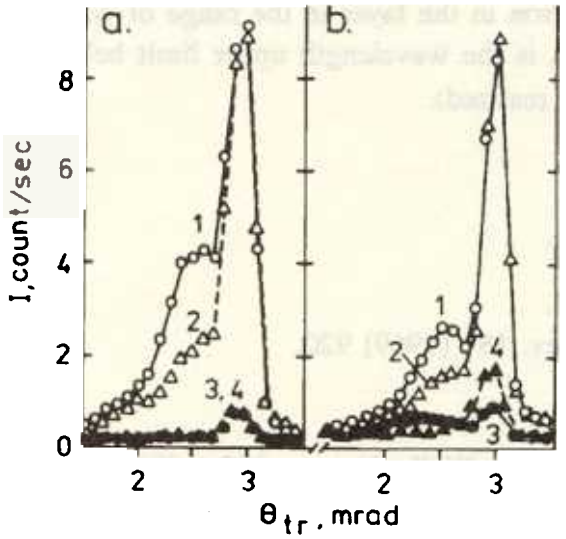

Fig. 1. The dependence of the integral neutron intensity I(count/sec) on the grazing angle θ_{tr} at β=0°(a) and 70°(b) for the "– –"(curve 1), "+ +"(curve 2), "– +"(curve 3), "+ –"(curve 4) beams.

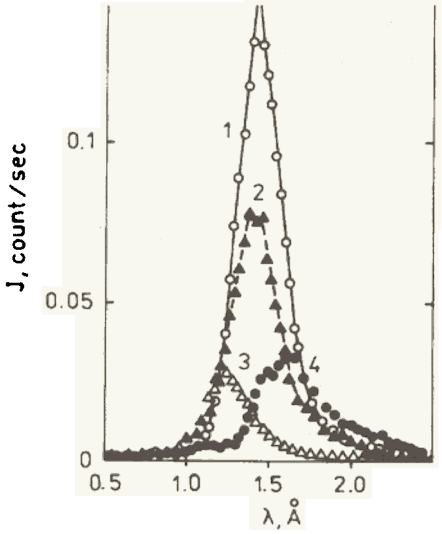

Fig. 2. The spectral dependence of the intensity J(λ) at θ_{tr}=2.8 mrad, β=70° and H=4.6kOe for the "– –"(curve 1), "+ +"(curve 2), "– +"(curve 3), "+ –"(curve 4) beams.

decrease in intensity of the "– –" and "+ +" refracted beams (peaks at the left) can be observed. At the same time, the "+ –" and "– +" beams appear; the first one is on the right of the "– –" beam, and the second is on the left of the "+ +" beam. The distance between the "–+" and "+ –" beams at the detector is 1.4 mm ($\Delta\theta_{tr}$ = 0.535 mrad). This result is interpreted as the observation of the generation of new beams at β≠0. The experimental data is represented as the difference of the squares of the grazing angles of the "+ –" and "– +" beams $\Delta\theta^2 = \theta_{tr,+-}^2 - \theta_{tr,-+}^2$. The observed dependence $\Delta\theta^2(\text{mrad}^2) = \alpha H(\text{kOe})\lambda^2(\text{E}^2)$ (λ is the neutron wavelength, α is the proportionality coefficient) is in agreement with the concept of beam generation associated with the existence of the transition between the Zeeman sublevels in the external magnetic field *H*. For *H*=4.6kOe and 6.8 kOe, however, the α coefficient is 0.23, which is 20% less than the theoretical value $\alpha = 8m\mu/h^2 = 0.294$ (*m* is the neutron mass, μ is the neutron magnetic moment, *h* is the Planck constant). The spectral dependence of the neutron intensity at θ_{tr}=2.8mrad is illustrated in Fig.2. It can be seen that the transmittance for all beams has a maximum at some wavelength values λ_{ij}, where i,j= +, –. $\Delta\lambda^{-2} = (\lambda_{+-}^{-2} - \lambda_{-+}^{-2}) \propto H$ in the range of values *H*=1÷6.8 kOe. The conducted measurements of the transmittance in relation to the angle β in the interval 0÷90° at *H*=4.6 kOe have shown that as β increases the transmittance of the "+ +" and "– –" beams decreases, and the transmittance of the "+ –" and "– +" beams increases. The spectral dependence of the transmittance of the "+ +" beam is presented in Fig.3.

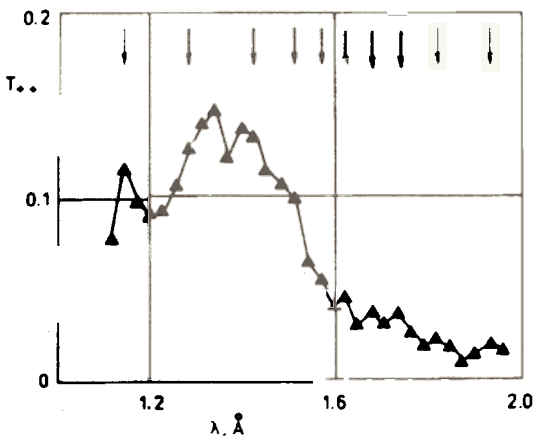

Fig. 3. The spectral dependence of the transmittance $T_{++}(\lambda)$ of the "+ +" beam at θ_{tr}=2.8 mrad, H=6.8kOe and β=70°. The arrows denote the wavelengths at which the transmittance has local maxima.

The transmittance oscillations whose period decreases as the neutron wavelength increases up to λ≈1.6 E can be easily seen. This behaviour is explained by the

interference of the "+" and "-" states of the neutron in the layer in the range of wavelengths from 0 to the boundary wavelength $\lambda_{lim} \approx 1.6$Å ($\lambda_{lim}$ is the wavelength upper limit below which the "+ +" neutron transition on the first interface is realized).

References

[1] D. Hughes, M. Burgy, Phys. Rev. 81 (1951) 498.
[2] R.M. Moon, T. Riste and W.C. Koehler, Phys.Rev. 181 (1969) 920.
[3] V.K. Ignatovich, Letters to JETP 28 (1978) 311.
[4] N.K. Pleshanov, Z.Phys. 94 (1994) 233.
[5] G.P. Felcher, S. Adenwalla, V.O. De Haan, A.A. Van Well, Nature 377 (1995) 409.
[6] D.A. Korneev, V.I. Bodnarchuk, V.K. Ignatovich, Letters to JETP 63 (1996) 900.
[7] O. Schaerpf, Physica Scripta 24 (1988) 58.

Element Depth Profiles of Porous Silicon

A.P.Kobzev, O.A.Nikonov
Frank Laboratory of Neutron Physics, Joint Institute for Nuclear Research, Dubna, Russia

M.Kulik, J. Żuk, H. Krzyżanowska, T.J. Ochalski
Institute of Physics, Maria Curie-Skłodowska University, Lublin, Poland

1. INTRODUCTION

Porous silicon has been a subject of intensive investigations since the initial demonstration of efficient visible photoluminescence in this material by L.T. Canham in 1990 [1].The progress in research on porous Si was reviewed recently [2,3]. Emission from porous Si is completely different from that observed in bulk crystalline Si, where the weak near-infrared luminescence associated with the indirect band gap of 1.1 eV has been known for a long time. For porous silicon, a large „blue" shift of the fundamental absorption edge has been reported. Spectacular optical properties of porous silicon are generally attributed to the spatial confinement of photo-excited carriers in nanometer-sized Si quantum wires or dots [1-3].

There are however, some other mechanisms of light emission in porous silicon. One of them has been linked to the E' centre in SiO_2 (an oxygen vacancy with unpaired electron) and proposed to explain strong blue emission observed in porous silicon, when excited with ultra violet light or protons [4]. It would be interesting therefore, to estimate oxygen content on a large (up to 1000 m^2/cm^3) surface of porous silicon.

2. EXPERIMENT

The samples used in a present experiment were prepared from p-type (111) silicon wafers of 10 Ωcm resistivity. The porous layers were formed by anodization in a 48 % HF-ethyl alcohol solution at a current density of about 20 $mAcm^{-2}$. The technology of preparing porous silicon was described in [4]. The thickness of the porous layer was about 5 μm, as determined by interferometric microscopy.

Both non-destructive nuclear methods ERD (Elastic Recoil Detection) and RBS (Rutherford Backscattering Spectroscopy) have been used in the investigation the depth element profiles in porous silicon. The measurements of RBS and ERD spectra have been carried out at EG-5 accelerator in the Frank Laboratory of Neutron Physics.

In the RBS experiment the detector was positioned at scattering angle 170° with respect incident beam. The surface of sample was tilted to the ion beam at the angle 60°. The detector resolution was 15 keV for 5.5 MeV α-particle. We have overcome the difficulties of the RBS method in the investigations of the concentration of light element (O) along with the heavier (Si) and used in this case the nuclear

reaction $^{16}O(\alpha,\alpha)^{16}O$ to profile oxygen directly [5]. The elastic nuclear resonance at 3.045 MeV is particularly suitable, because it has a large back scattering cross section (17 times greater than for Rutherford scattering) and a width of resonance is about 10 keV . The measurements have been performed in a such way, that the energy of incident beam of ions $^4He^+$ was changed in small increments in the range from 3.04 MeV to 3.20 MeV. The backscattering spectra were collected for everything energies. So the resonance shifted from surface into 5000 nm for highest energy and we had measured the oxygen profile in detail over the range of depth above.

The ERD spectra have been investigated for both porous and crystalline silicon. The 2.5 MeV ^4He ions were incident on a solid target at an angle of 15° with respect to surface of the sample. The scattered $^4He^+$ ions were absorbed in stopper aluminium foil of 9.5μm thickness. In contrary the recoiling nuclei (protons) lost only a part of the full energy and were collected by a detector positioned at an laboratory scattering angle of 30° away from the direction of incidence.

3. RESULTS AND DISCUSSION

The typical spectra of ^4He ions scattered from the sample of porous silicon are presented in Fig.1 for two initial energies. The peak of the resonantly scattered $^4He^+$ particles rides over the background non-resonant scattering from oxygen. This background, in turn, sits on a top of the continuum of the elastic scattering by silicon nuclei in the porous layer of the investigated sample.

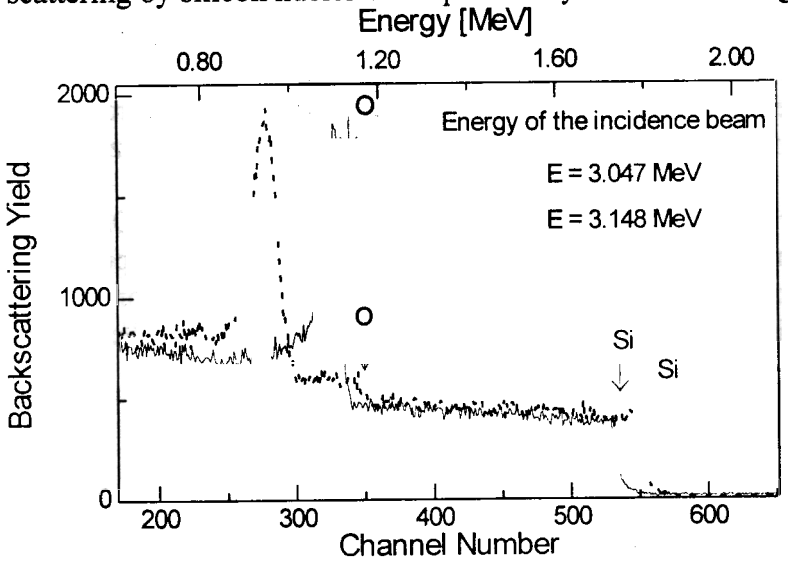

Fig. 1. Spectra of $^4He^+$ backscattered by porous silicon sample.

The peak for 3.047 MeV ^4He ions has more sharp right edge because the resonance entered to the target partially in this case. A shift to depth of the peak of oxygen resonance with increasing the initial energy of bombarding particles is observed since ^4He ions reaches of the resonance energy at the increasing depth . A square of the peak is proportional to an oxygen atom concentration for the given depth.

On the spectra one can see the yield ^4He ions scattered by Si atoms. The background for the spectral regions according to surface layers is absent in this case. The element concentrations are obtained with help a computer code [6] after modelling everything spectra using one joint model of the sample.

The ERD spectra obtained for the crystalline silicon and porous silicon sample are shown in Fig.2 At a spectrum for crystalline silicon one can see the peak near the channel number 460. The yield of this peak is very small, as compared to the one for the porous silicon layer. It means that the hydrogen

atoms present only at the surface of silicon. Since porous silicon has the vast specific surface the yield of the recoiling hydrogen atoms for the porous sample is substantially more than for crystalline and depth profile extends at a whole depth available for the measurement.

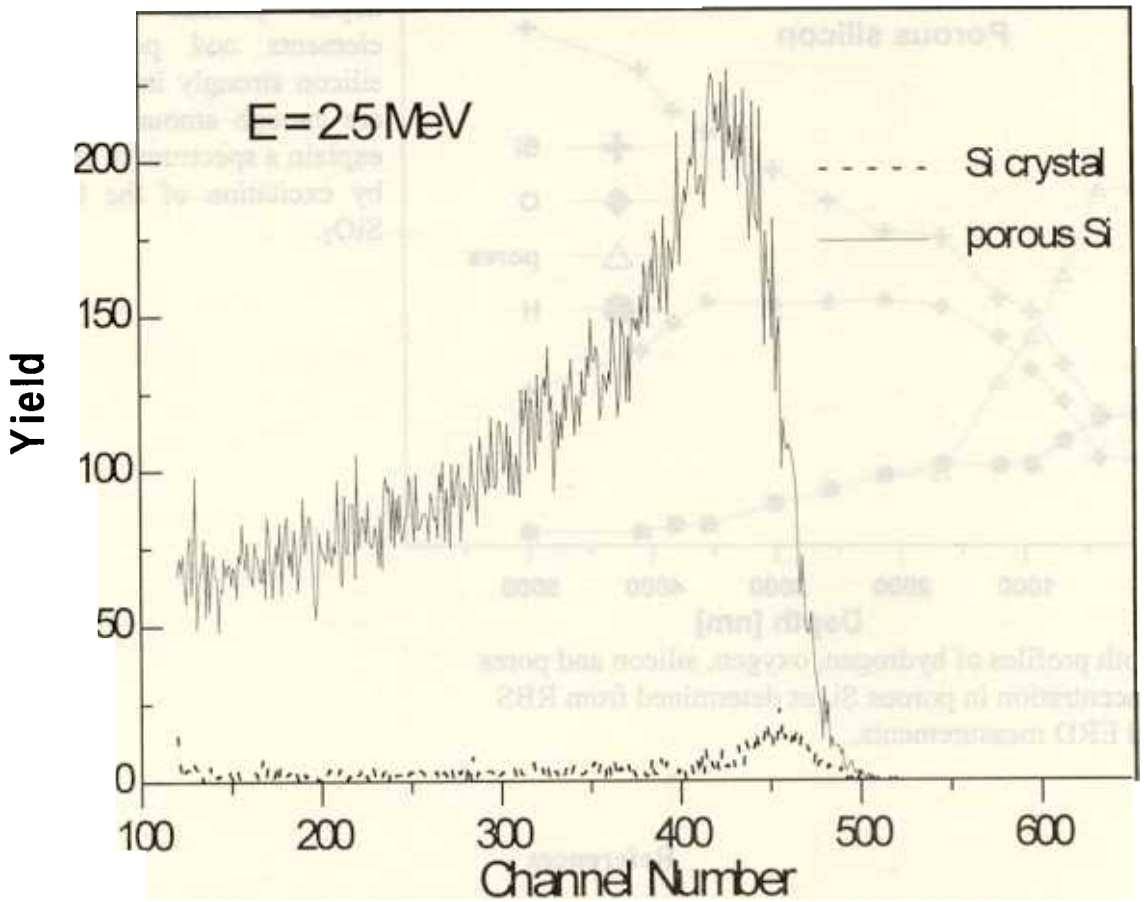

Fig. 2. ERD spectra of porous and crystalline Si

The depth profiles of the different elements and pores in the porous silicon layer were calculated in two steps.. In the first step, the depth profile of hydrogen in the porous silicon was determined on a basis of the ERD spectrum. Than these data were used in the calculations of the depth profiles of other elements (Si,O) and pores by modelling of twelve RBS spectra with the help of a computer code[6]. These results are shown in Fig. 3. A special element was included in the model of a sample what we attributed with the pores. It did not scatter He ions and had very small stopping cross sections. This procedure gives possibility to account the presence the pores in solid with first approximation only.

The concentration of Si atoms is the smallest (~20 %) in the subsurface region and gradually increases with a depth up to 75% (Fig. 3). The porous Si layer is non-homogeneous, with a porosity (after anodization) ranging from about 50 % close to the surface to less than 10 % at a depth of 1600 nm and slowly decreases up to almost zero for the depth 4000 nm. A concentration of oxygen is less than 30% for whole thickness of porous silicon layer. A ratio C_{Si}/C_O increases from 1.2 at surface to 3.2 with

the growth a depth to 5000 nm. Therefore, it can be assumed, that the Si wires in porous silicon are covered with silicon oxide layers. Moreover the hydrogen atoms, which are present in porous silicon after anodization, probably, appear as H_2O.

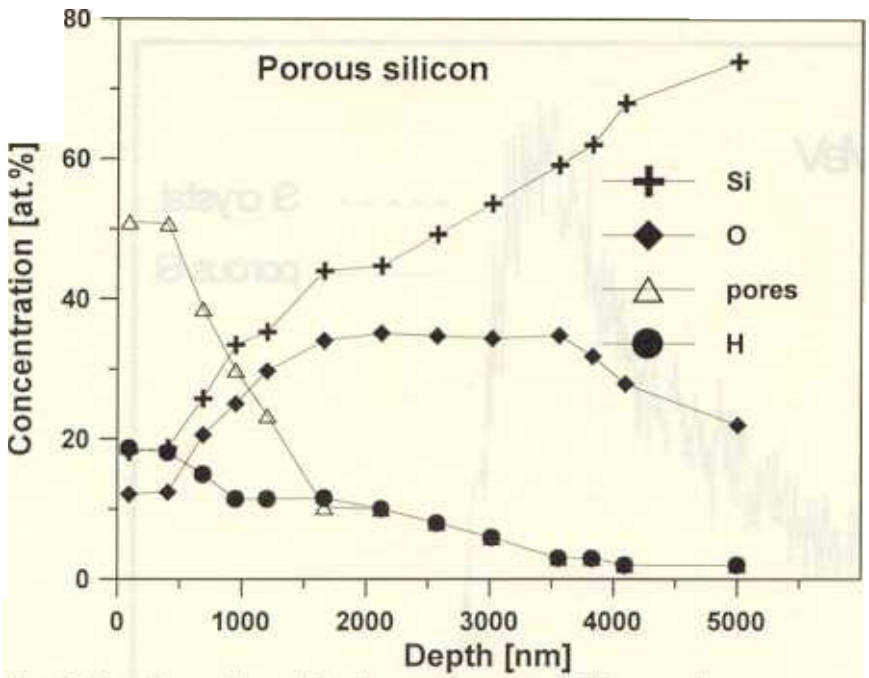

Fig. 3. Depth profiles of hydrogen, oxygen, silicon and pores concentration in porous Si, as determined from RBS and ERD measurements.

So, the performed investigation of depth profiles of everything elements and pores in porous silicon strongly indicate, that there are enough amounts of oxygen to explain a spectrum of luminescence by excitation of the E' centre in SiO_2.

References

1. L.T. Canham. Silicon quantum wire array fabrication by electrochemical and chemical dissolution of wafer. Appl. Phys. Lett. **57** (10),1046 - 1051 (1990).
2. Y. Kanemitsu. Light emission from porous silicon and related materials. Phys. Rep. **263** (1), 1-91 (1995).
3. G.C. John and V.A. Singh. Porous silicon: theoretical studies. Phys. Rep. **263** (2), 93-151 (1995).
4. J.Żuk, R. Kuduk, M. Kulik, J. Liśkiewicz, D. Mączka, P.V. Zhukovski, V.F. Stelmakh, V.P. Bondarenko and A.M. Dorofeev. Ionoluminescence of porous silicon. J. Lumin. **57**, 57-60 (1993).
5. L.P.Chernenko, A.P.Kobzev, D.A.Korneev and D.M.Shirokov. Backscattering methods possibilities for precise determination of oxygen profile in axide films by use of the elastic resonance in reaction $^{16}O(^4He, ^4He)^{16}O$ at 3.045 MeV of ^4He. Surface and Interface Analysis. vol.**18**, 585-588 (1992).
6. V.Bogac and D.M.Shirokov. New computer iterative fitting program DVBS for backscattering analysis. Nucl. Instrum. and Meth. in Phys. Res. **B85**, 264-267 (1994).

EPITHERMAL NAA FOR STUDYING THE ENVIRONMENT

M.V. FRONTASYEVA, E. STEINNES*

Joint Institute for Nuclear Research (JINR), Dubna, Russia
*Norwegian University of Science and Technology, Trondheim, Norway

The advent of analytical techniques for the simultaneous determination of a great number of elements has created an enormous interest for multi-element studies in environmental sciences. Instrumental neutron activation analysis (INAA) has shown to be useful for a number of sample types of interest in environmental studies, and should find more extensive use in this area. Epithermal neutron activation analysis (ENAA) has certain advantages over the conventional INAA for many trace elements in terms of improvement in precision and lowering of detection limits, reduction of high matrix activity and fission interferences if any.

Since Brunfelt and Steinnes [1] reported the first multi-element study on silicate rocks using ENAA, this technique soon became a routine tool in many earth science laboratories. ENAA was early shown to exhibit an excellent multi-element capability in the case of coal and coal fly ash [2].

Two areas of environmental analysis seems to deserve particular attention when the feasibility of ENAA relative to non-nuclear multi-element techniques is to be discussed: the analysis of airborne particulate matter, and the related subject on analysis of biomonitors of atmospheric deposition: Analyses of airborne particulate matter is a case where ENAA should be particularly useful. This is mainly due to the fact that the total mass of the aerosol collected on a filter sample is often rather small, and thus favours direct instrumental techniques rather than those depending on dissolution of the sample prior to analysis. Air filter analysis therefore seems to be an area where INAA hardly can be replaced by any non-nuclear analytical technique at the present state of the art. Comprehensive texts on INAA of airborne particulate matter have appeared in the literature [3, 4]. The elements that form the major activity upon neutron activation of aerosols are very much the same ones as in the case of. silicate rocks and fly ash. This means that the advantages of using epithermal activation should also be similar, provided that the induced activity is sufficient to yield satisfactory counting statistics. As shown by Landsberger [5] this is indeed the case for several trace elements of importance in studies of long range atmospheric transport. In the opinion of the authors this is an area where much remains to be done, and at JINR, Dubna, ENAA is now being used in several projects involving the analysis of aerosol filters. A similar case where ENAA has shown strong performance is in the analysis of mosses used as biomonitors of atmospheric deposition. Mosses have been used in Norway since 1977 on a regular basis to monitor atmospheric deposition of heavy metals in a nation-wide grid. The analytical approach used from the beginning was INAA, supplemented by atomic absorption spectrometry for the elements Pb, Cd, Cu, and Ni. Prior to the survey in 1990 it became evident that ICP-MS, which had then become available, was able to produce results of acceptable quality for all elements of first priority, and has therefore been used since then in the regular monitoring work.

During the same period, work has continued to test the feasibility of other analytical techniques for the trace element determination in moss. In particular the use of ENAA was

investigated employing the IBR-2 pulsed fast reactor in Dubna, which is characterised by a particularly high fraction of resonance and fast neutrons in the total spectrum. By this means the determination of 15 elements (Zr, Sn, Hf, Ta, W, Au, Th, and eight REE) previously not detected in such samples was demonstrated [6], and the relative merits of ENAA and ICP-MS in moss analysis were discussed on the basis of an intercomparison exercise [7]. ICP-MS laboratories are now capable of producing apparently satisfactory results for about 55 elements in mosses. The corresponding figure for ENAA is around 45. In 40 cases both techniques can be used, and for a majority of these elements it is difficult on the basis of present evidence to give preference to one technique or the other. In 7 cases (Sc, As, Sb, Hf, Ta, Au, Th) ENAA is judged to be the preferred technique, whereas ICP-MS seems preferable in 5 cases (Sr, Sn, Ba, Ce, Nd). Four elements (Cl, Br, I, Se) could only be determined well by ENAA, whereas the reverse situation applied for another 14 elements (Li, Cu, Ga,Ge, Y, Cd, Te, Pr, Dy, Ho, Er, Tl, Pb, Bi). The choice of either multi-element technique thus depends on the purpose of the investigation and the priority of elements. It should be added that the simultaneous determination of the halogens Cl, Br and I, which is rather straightforward by ENAA in mosses as well as in several other environmental sample types, is hardly possible at all by any existing non-nuclear technique at the levels concerned.

REFERENCES

1 BRUNFELT, A.O., STEINNES, E., Instrumental activation analysis of silicate rocks with epithermal neutrons, Anal. Chim. Acta **48** (1969) 13-24.

[2] ROWE, J.J.,STEINNES,E., Instrumental activation analysis of coal and fly ash with thermal and epithermal neutrons, J. Radioanal.Nucl. Chem. **37** (1977) 849-856.

[3] ALIAN, A., SANSONI, B., A review on activation analysis of particulate matter, J. Radioanal. Nucl. Chem., **89** (1985) 191-275.

[4] INTERNATIONAL ATOMIC ENERGY AGENCY, Sampling and Analytical Methodologies for INAA of Airborne Particulate Matter, Training Course Series No. 4,Vienna (1992), 56 pp.

[5] LANDSBERGER, S., Improved methodology for the determination of the seven elemental tracer long-distance pollution signatures using thermal and epithermal neutron activation analysis, Anal. Chem. **60** (1988) 1842-1845.

[6] FRONTASYEVA, M.V., NAZAROV, V.M., STEINNES, E., Moss as monitor of heavy metal deposition: Comparison of different multi-element analytical techniques, J. Radioanal. Nucl. Chem. **181** (1994) 363-371.

[7] FRONTASYEVA, M.V., GRASS, F., NAZAROV, V.M., STEINNES, E., Intercomparison of moss reference material by different multi-element techniques, J. Radioanal. Nucl. Chem. **192** (1995) 371-379.

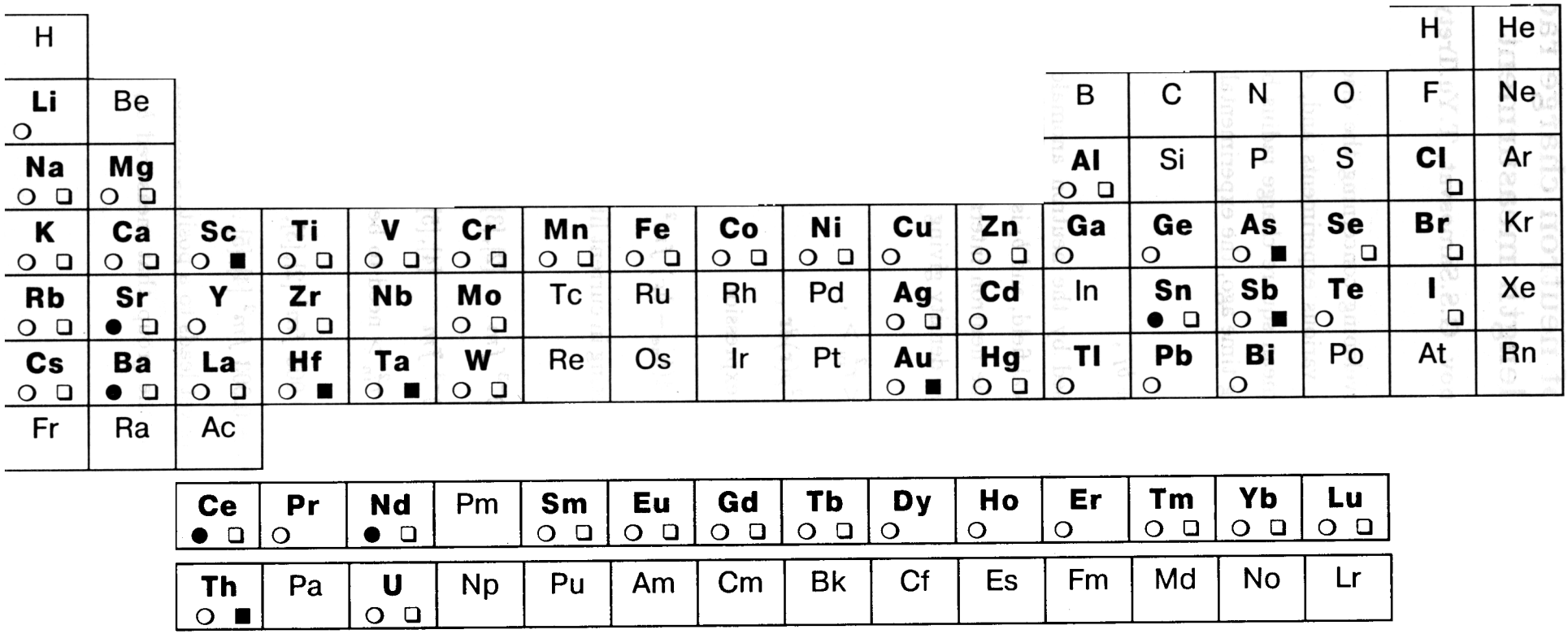

Fig. 1. Elements suitable for determination in moss by the present version of INAA (□) and by ICP-MS (❍). Closed symbols indicate the preferred method for the element in question.

On the estimate problem of neutron charge radius from (n,e)-scattering length measurment

G.G.Bunatian, V.G.Nokolenko, A.B.Popov, G.S.Samosvat, T.Yu.Tretyakova

Lately, an intense discussion has been developing concerning the discrepancies in the ne–scattering length data obtained from various experiments and, consequently, the controversial estimations of the neutron mean square charge radius based on b_{ne}–values. Having originated with Foldy [1] a long time ago, the experimental quantity b_{ne} is presumed to consist of two terms

$$b_{ne} \quad b_F + b_I \ ,$$

where b_F is the Foldy scattering length caused by the neutron anomalous magnetic moment μ interacting with the electron electrical field, and b_I is the scattering length — as though rendering an interaction between the neutron internal charge structure and an electrical field (strictly speaking, the charge density giving birth to this field). The following notations are used

$$b_I = \frac{1}{3}\frac{Me^2}{\hbar^2} < r_{in}^2 > \ ,$$

$$< r_{in}^2 >= \int r^2 \rho(\mathbf{r}) d\mathbf{r} \ ,$$

where M is the neutron mass. From this, the expression

$$< r_{in}^2 > \frac{3\hbar^2}{Me^2} b_I \quad 86.4(b_{ne} \quad b_F) \ fm^2$$

appears. The experimental b_{ne} estimations existing in current literature are concentrated in the proximity of the two following values:

$$b_{ne} \quad (-1.59 \pm 0.04)10^{-3} \ fm \qquad [2], [3],$$

$$b_{ne} \quad -1.31 \pm 0.03)10^{-3} \ fm \qquad [4], [5]$$

Eventually, two estimations of the quantity $< r_{in}^2 >$ need to be discussed:

$$< r_{in}^2 > \quad 0.010 \pm 0.003 \ fm^2 \ [2], [3],$$

$$< r_{in}^2 > \quad +0.014 \pm 0.003 \ fm^2 \ [4], [5]$$

While no model of the nucleon structure yet leads to a positive neutron mean square charge radius, the Garching group [5] and the group that measured b_{ne} by means of

liquid ^{208}Pb at Oak Ridge [6] have given up accounting for the Foldy-term (the first using vague arguments [7] and the latter without any explanations at all), thereby reducing the definition of the neutron mean square charge radius to the expression

$$< r^2 > \quad \frac{3\hbar^2}{me^2} b_{ne} \ .$$

Under such circumstances, we are forced to face the primary sources of the problem and glance over the history to find the gist of the question.

Here, from the very first, it is necessary to determine the genuine relation between the measured ne–scattering length and the nucleon structure. In our opinion, there is a certain misunderstanding of this question [8] and we believe it will be instructive to trace back how this relation is acquired in various approaches. As the ne–scattering length is obtained from slow neutron scattering in the field produced by atomic electrons, the neutron interaction with an electromagnetic field will be described first.

A free nucleon, as well as any free particle with spin 1/2, is described by the Dirac equation. Yet the "external field" concept is limited and, generally speaking, untenable. In fact, even for an electron itself, the Dirac equation in the face of an external electromagnetic field $A = (\Phi, \mathbf{A})$

$$i\hbar\frac{\partial\psi}{\partial t} = (c\boldsymbol{\alpha}(\mathbf{p} - \frac{e}{c}\mathbf{A}) + \beta mc^2 + e\Phi)\psi,$$

$$i\hbar\frac{\partial\phi}{\partial t} = \mathcal{H}\phi,$$

$$\mathcal{H} \approx \frac{1}{2m}(\mathbf{p} - \frac{e}{c}\mathbf{A})^2 + e\Phi - \frac{\mathbf{p}^4}{8m^3c^2}$$

$$\frac{e\hbar}{2mc}\boldsymbol{\sigma}\mathbf{H} - \frac{e\hbar}{4m^2c^2}\boldsymbol{\sigma}[\mathbf{E}\times\mathbf{p}] - \frac{e\hbar^2}{8m^2c^2}div\mathbf{E} \qquad (1$$

(where $\mathbf{E} = -(\nabla\Phi)$, $\mathbf{H} = [\nabla \times \mathbf{A}]$, $\frac{e\hbar}{2mc} = \mu_0$, $\boldsymbol{\alpha}, \beta$ are Dirac matrixes, $\boldsymbol{\sigma}$ is the Pauli matrix, and ϕ is the large component of the bispinor ψ) does not enable to describe properly the properties of this point-like particle, because self-coupling to its own electromagnetic quantum field (radiative corrections) [9] is known to result in the additional terms in the equation to describe the behaviour of the electron in an external field A. The last three terms in $\mathcal{H}$ in eq. (1) are thus replaced by

$$-(\frac{e\hbar}{2mc} + \mu_e')\boldsymbol{\sigma}\mathbf{H} - \frac{1}{2mc}(\frac{e\hbar}{2mc} + 2\mu_e')\boldsymbol{\sigma}[\mathbf{E}\times\mathbf{p}] - \frac{\hbar}{\quad}(\frac{e\hbar}{\quad} + 2\mu_e')div\mathbf{E}, \qquad (1a)$$

where $\mu_e' = \frac{1}{2\pi}(\frac{e^2}{\hbar c})\frac{e\hbar}{2mc} + \ldots$ is the electron anomalous magnetic moment.

It is to emphasize here that in accounting for the radiative corrections, the coefficients prefixed to $\boldsymbol{\sigma}\mathbf{H}$ and to $div\mathbf{E}$ and $\boldsymbol{\sigma}[\mathbf{E}\times\mathbf{p}]$ are modified in different ways: the anomalous

magnetic moment μ'_e has been added to the magnetic moment $\frac{e\hbar}{2mc}$ in the term containing $\mathbf{H}$, whereas a twofold quantity has been added to the coefficients in two latter terms. Thus, it is quite impossible for even an electron to obtain eq. (1a) from eq. (1), that is, to account for the electron interaction with quantum fields (the radiative corrections) merely by replacing the magnetic moment of the point-like particle in the Dirac equation by the total magnetic moment that incorporates the anomalous one as well.

In a general form, the behaviour of a particle with spin 1/2 can be described in a formal way by means of the relativistic and gauge invariant equation [1], [9]

$$[c(p_\mu\gamma^\mu - \frac{e}{c}A_\mu\gamma^\mu) + i\mu\frac{1}{2}\gamma_\mu\gamma_\nu F^{\mu\nu} + Mc^2 + \epsilon\Box(\gamma_\mu A^\mu)]\psi \quad 0$$

$$i\hbar\frac{\partial\psi}{\partial t} = \mathcal{H}\psi \quad [c\boldsymbol{\alpha}(\mathbf{p} - \frac{e}{c}\mathbf{A}) \quad \mu\beta(\boldsymbol{\Sigma}\mathbf{H} - i\boldsymbol{\alpha}\mathbf{E}) + \beta Mc^2 + e\Phi - \epsilon\Box\Phi + \epsilon\boldsymbol{\alpha}\Box\mathbf{A}]\psi, \quad (2)$$

where we restrict ourselves to accounting for the first order terms in field A and the D'Alamber operator $\Box$ only; here $\boldsymbol{\Sigma}$ is the spin operator and $F^{\mu\nu}$ is the electromagnetic field tensor. The lowest approximation in $1/c$ runs as follows

$$i\hbar\frac{\partial\phi}{\partial t} = \mathcal{H}\phi,$$

$$\mathcal{H} \approx \frac{1}{2M}(\mathbf{p} - \frac{e}{c}\mathbf{A} + \frac{\epsilon}{c}\Box\mathbf{A})^2 + e\Phi \quad (\frac{e\hbar}{2Mc} + \mu)\boldsymbol{\sigma}\mathbf{H} -$$

$$\frac{1}{2Mc}(\frac{e\hbar}{2Mc} + 2\mu)\boldsymbol{\sigma}[\mathbf{E}\times\mathbf{p}] - [\epsilon + \frac{\hbar}{4Mc}(\frac{e\hbar}{2Mc} + 2\mu)]div\mathbf{E}. \qquad (2a)$$

In such a purely phenomenological approach, the empirically introduced parameters μ, ϵ render both the internal structure of a particle and its interaction with a vacuum of the electromagnetic and other quantum fields, which are not taken into account in the Dirac equation (1). The physical meaning of the quantity μ emerges unambiguously as the coefficient prefixed to $\boldsymbol{\sigma}\mathbf{H}$ in eq. (2a). Consequently, it is understood to be the "nucleon anomalous magnetic moment", completing the magnetic moment $\frac{e\hbar}{2Mc}$ of a point-like particle with spin 1/2, mass M and charge e. Yet, according (2a), this empirically introduced quantity μ shows up to determine not only the interaction of the particle with a magnetic field, but with an electrical field $\mathbf{E}$, as well: the "Schwinger interaction" (next to last term in eq. (2a)) and the "Foldy interaction" [1] (last term in (2a)). Certainly, expression (1a) for an electron ($\mu = \mu'_e$) corresponds completely with the general phenomenological equations (2), (2a).

As far as the parameter ϵ is concerned, no unambiguous conclusion about its physical contents can be drawn immediately from eqs. (2), (2a). The fact that ϵ is incorporated side by side with the terms containing μ in the coefficient prefixed to $div\mathbf{E}(\mathbf{R}) = -\triangle_R$

$\Phi(\mathbf{R}) = -4\pi\rho_e(\mathbf{R})$ in eq. (2a) ($\rho_e(\mathbf{R})$ is the charge density inducing the electric field) does not constrain the equation

$$\epsilon = \frac{1}{6}\int d\mathbf{r}\mathbf{r}^2\rho_n(\mathbf{r}),$$

(here ρ_n- is the density of the charge distribution inside the nucleon), contrary to what was presumed in [1], [8], and [10], as well as in some other publications. In such a phenomenological approach, this quantity ϵ is, as a matter of fact, a fitted-parameter that is allowed to take any value, including zero.

The interaction represented by the last term in eq. (2a) results in the Born amplitude of neutron scattering ($e = 0$)

$$f_{ne}(\mathbf{q}) \qquad \frac{2M}{\hbar^2}[\epsilon + \mu\frac{\hbar}{2Mc}]\int d\mathbf{R}e^{-i\mathbf{qR}}\rho_e(\mathbf{R}$$

in the field, induced by the charge density $\rho_e(\mathbf{R})$, and in particular by the charge distribution of the atomic electrons, the atom being nailed down (bound). With the quantity μ being equal to the experimental value of the neutron anomalous magnetic moment, and the quantity ϵ is assumed to be equal to zero, the ne–scattering length $b_{ne} = -f_{ne}(0)/Z$ proves to be equal to the value $b_{ne} = -1.468\,10^{-16}cm$, coinciding within a small error with up to date experimental results [2] - [7]. This is evidence that the ϵ value is small. However, pursuing this phenomenological approach, no rigorous conclusion about the nucleon structure can be acquired through this result. Certainly, as it was already emphasized long before [1], an approach can not been asserted as expedient if the coefficients assigned to describe the nucleon structure are introduced purely empirically and are never gained through any more-or-less general and profound physical theory or, at least, a model.

As pointed out above, accounting for radiative corrections for the electron itself modifies the coefficients by $\mathbf{H}$ and by $div\mathbf{E}$ in different ways. All the more, when the nucleon, being a much more complicated composite system, interacts with an external electromagnetic field, its structure can not be taken into account merely through modification of the Dirac equation, in particular, through replacement of the point-like-particle magnetic moment by the total one, including the anomalous one as well. At this time, because of the lack of a rigorous, thorough theory, the nucleon structure is investigated in the framework of various approaches and models.

The consideration of the magnitude of the ne-scattering amplitude in the framework of the Cloudy Bag Model **CBM** [11],[12] does nothing proportional to the μ $div\mathbf{E}$ (like (4)) contribution to the ne–scattering amplitude. By the way, it might be instructive

here to point out that the question about the "Foldy term" in the electron–nucleon interaction has never arisen, while the Lamb shift is investigated in either the ordinary or in the mesonic atoms (see, for example, [13]). On the other hand, in the framework of the phenomenological Foldy approach [1], the ne–scattering amplitude is expressed through the quantity μ according to eq. (4), yet nothing can be concluded immediately about the hidden physical sense of the quantity ϵ, namely that this approach is only phenomenological. Foldy himself, suggesting eq. (3) as being the plausible physical representation for the quantity ϵ, had, as a matter of fact, only designated such an interpretation, but never made any concise statements. Instead he referred to experiments to disentangle the physical meaning of the quantity ϵ. For years, in successive works, the quantity ϵ has been assumed to be exactly equal to the value of the second momentum of the nucleon charge distribution (3), no new or additional argument having been managed at all.

Obtaining $< r_n^2 >$ with high precision experimentally will promote, in our opinion, the development and improvement of the various models now suggested for describing the nucleon, ignoring for the moment that these approaches are apparently not yet in position to provide an accuracy better than $\sim$ 10%. Beyond question, any theoretical approach must be able to successfully describe not only one characteristic of the nucleon, but the majority of the following, simultaneously: $< r^2 >$, μ , m_N , g_A, and so on. Therefore, it is desirable to obtain the values of all of these quantities from experimental data with equal precision. Specifically, the $< r^2 >$ value needs to be known to the same accuracy as the values of μ, g_A and so forth.

On the other hand, exact determination of the ϵ value will enable us to judge to what degree the anomalous magnetic moment incorporates all the main features and peculiarities of the neutron structure while describing, according to aforecited phenomenological approach, the behavior of a neutron in an external electromagnetic field. If the ϵ value proves to be very small, almost negligible, an amazing and intriguing conclusion will be inescapable: that the spectacular phenomenological approach really does exist in which the anomalous magnetic moment thoroughly renders the structure of the neutron as it interacts with an external electromagnetic field. The goals of further experimental investigations are to obtain the b_{ne} value with better accuracy than before and that these measurements will not require significant corrections in the processing their results.

The research described in this publication was made possible in part by Grant RFS000 from the International Science Foundation and by Grants 94-02-03118 and 96-02-16538 RFFI.

References

[1] Foldy L., Phys.Rev. **87**, 688 (1952); Phys.Rev. **87**, 693 (1952); Rev.Mod.Phys. **30**, 471 (1958)

[2] Melkonian E., Rustad B.M., Havens W.W., Phys.Rev. **114**, 1571 (1959)

[3] Alexandrov Yu. A., Machekhina T. A., Sedlakova L. N., Fykin L. N., Yadernaya Fisika, **20**, 1190 (1974); Sov. J. Nucl. Phys. **60**, 623 (1975)

[4] Krohn V.E., Ringo G.R., Phys.Rev. **D8**, 1305 (1973)

[5] Koester L., Waschkowski W., Kluver A., Physica, **137B**, 282 (1986)

[6] Kopecky S., Riehs P., Harvey J., Hill N., Phys.Rev.Lett. **74**, 2424 (1995)

[7] Koester L., Waschkowski W., Mitsyna L.V., Samosvat G.S., Prokofjevs P., Tambergs J., Phys.Rev. **C51**, 3363 (1995)

[8] De Benedetti S., "Nuclear Interections", John Wiley & Sons, New York, 1968;
Frauenfelder U., Henley E., "Subatomic Physics", Ch.VI, Prentice-Hall, Inc., New Jersey, 1974;
Alexandrov Yu. A., "Fundamental Properties of the Neutron", Energoizdat, Moscow, 1982; Clarendon Press, Oxford, 1992;
Gurevich I.I., Tarasov L.V., "Neutron Physics", Nauka, Moscow, 1965;
Alexandrov Yu.A., Neutron News, **5**, iss. 1, 20 (1994), **5**, iss.4, 17 (1994);
Byrne J., Neutron News, **5**, iss. 4, 15 (1994)

[9] Achieser A.I., Berestezky V.B., "Quantum Electrodynamics", "Nauka", Moscow, 1969.
Berestezky V. B., Lifshiz E. M., Pitaevsky L. P., "Relativistic Quantum Theory", "Nauka", Moscow, 1968.

[10] Sears V.F., Phys.Reports, **141**, 281 (1986)

[11] Thomas A. W., Adv. Nucl. Phys. **13**, 1 (1984)

[12] Bunatian G.G., Sov. J. Nucl. Phys., **46**, 188 (1987); **48**, 820 (1988); **51**, 637 (1990); Nucl. Phys., **A509**, 736, (1990)

[13] Borie E., Phys. Rev. Lett., **47**, 568 (1981)

ENERGY DEPENDENCE OF FISSION FRAGMENT ANGULAR ANISOTROPY IN RESONANCE NEUTRON INDUCED FISSION OF ^{235}U

W.I.Furman[1)], N.N.Gonin[2)], J.Kliman[3)], Yu.N.Kopach[1)], L.K.Kozlovsky[2)], A.B.Popov[1)], H.Postma[4)], D.I.Tambovtsev[2)].

1) FLNP JINR ,Dubna, Russia
2) RRC IPPE, Obninsk, Russia
3) IP SAS, Bratislava, Slovakia
4) TU Delft, Netherlands

The investigation [1] of energy dependence of fission fragment angular anisotropy in slow neutron induced fission of the ^{235}U aligned target was continued at the pulsed neutron source IBR-30 of the FLNP. The measurements were performed using a new dilution refrigerator with improved target consisting of two mosaics of monocrystals of uranyl rubidium nitrate mounted onto a copper backing, cooled down to a temperature of ~0.1 K to ensure an alignment of uranium nuclei. The processing of both new and earlier obtained [1,2] data was realized by a new algorithm, when the relative angular anisotropy A_2 was obtained as function of the neutron energy for each experimental run separately and thereafter averaged over all runs. The absolute scale of the A_2 values was chosen from a comparison of our average value with the one from [3]. The statistical accuracy was about 3-10 % for the energy bins of 0.05 eV in the region 0.04-10 eV.

The results [3] interpreted by the authors under the assumption that the angular anisotropy coefficient A_2 could be defined for a given resonance λ by the formula

$$A_{2\lambda}^{JK} = \sum_K A_2^{JK} \Gamma_{f\lambda}^{JK} / \Gamma_{f\lambda}^{J} \qquad 1)$$

where the factor A_2^{JK} is determined by the Racah and Clebsch-Gordan coefficients, which depend only on spin J and its projection K on the fission axis of the compound state under consideration. The contribution of the specific state λ is defined only by the ratio of the partial $\Gamma_{f\lambda}^{JK}$ to total $\Gamma_{f\lambda}^{J}$ fission widths. As a result of the analyses [3,4] it was concluded in [4] that in the s-wave resonance neutron induced fission of ^{235}U only fission channels with K=1 and K=2 are open for both compound state spins J=3 and 4. At the same time for states with J=3 an admixture of the channel K=0 is possible.

The new approach to the theoretical description of fission process using the microscopic representation of fission fragment channels and their convolution to the observed JK-channels led to the modified formulae for differential fission cross-sections induced by slow neutrons [5] :

$$\frac{\partial \sigma_{nf}(E)}{\partial \Omega} = \frac{1}{4\pi}\left[\sigma_{f0}(E) + f_2 \sigma_{f2}(E) P_2(\cos\theta)\right], \qquad (2)$$

where

$$\sigma_{f0} = \frac{\pi}{k^2} \sum_J g_J \sum_K \left| S^J(0\tfrac{1}{2} \rightarrow Kf) \right|^2 \qquad (3)$$

is the total fission cross-section and

$$\sigma_{f2} = G\frac{\pi}{k^2}\sum_{JJ'}\sqrt{g_J g_{J'}}U(\frac{1}{2}IJ'2;JI)\sum_{K}C^{J'K}_{JK20}S^{*J'}(0\frac{1}{2}\rightarrow Kf)S^{J}(0\frac{1}{2}\rightarrow Kf) \quad (4)$$

takes place due to an alignment of the target nucleus spin I. Here symbols f_2 and $P_2(\cos\theta)$ denote the alignment coefficient [3] and the Legendre polynomial respectively. In (2) - (4) the g_J and G are the statistical and geometric normalization factors defined by

$$g_J = (2J+1)/2(2I+1) \quad \text{and} \qquad G = \frac{15I^2}{\sqrt{(2I+1)I(I+1)(2I+3)}},$$

and $k = (2mE/h^2)^{1/2}$ is the wave number of incident neutrons. Symbols $U(1/2IJ'2;JI)$ and C^{JK}_{JK20} are the Racah and Clebsch-Gordan coefficients . The dynamics of the reaction is included via the S-matrix elements $S^J(lj \rightarrow Kf)$ which define the probability of a transition from the entrance neutron channel characterized by the orbital l and total j angular momenta of the neutron to the fission channel JK (for more detail, see [5]) .

With the aid of formulae (2)-(4) it is possible to define the angular anisotropy of fission fragments in a consistent way as

$$A_\gamma(E) = \frac{\sigma_{f2}(E)}{\sigma_{f0}(E)}$$

This formula allows one to assume that due to the interference of different resonances the $A_2(E)$ value is determined not only by the partial and total fission widths of the nearest resonance, as in formula (1), but depends essentially on the partial amplitudes $\sqrt{\Gamma^{J\pi K}_{\lambda f}}$ of all neighboring resonances. Besides, one should expect an influence of the effects from the interference of s-wave neutron resonances with different spins on the behavior of the $A_2(E)$.

For the analysis of the experimental data on the A_2 (E) values a special code was developed with the S-matrix parametrization proposed for the ENDF/B-VI library:

$$S^J_{cc'} = e^{-(\phi_c-\phi_{c'})}\left\{2\left((I-\tilde{K})^{-1}\right)_{cc'} - \delta_{cc'}\right\} \quad (6)$$

For neutron induced fission we have:

$$S^J_{nf} = 2e^{-i\phi_n}W^J_{nf} \quad (7)$$

(ϕ_f=0 for the fission channel, as shown in [5] and

$$W^J_{nf} = \left((I-\tilde{K})^{-1}\right)_{nf}$$

where

$$(I-\tilde{K})_{cc'}=\delta_{cc'}-\frac{i}{2}\sum_{\lambda}\frac{\sqrt{\Gamma^{J}_{\lambda c}}\sqrt{\Gamma^{J}_{\lambda c'}}}{E_{\lambda}-E-i\Gamma_{\lambda\gamma}/2} \qquad (9)$$

The function $A_2(E)$ was calculated by formulae (2) - (9). The fission channels with JK = 30, 31, 32, 41 and 42 were included in the calculations. Doppler broadening and the resolution function of the spectrometer were taken into account, as well. With the aid of the described procedure our data on the $A_2(E)$ in the neutron energy range from 0.1 up to 10 eV were analyzed together with the data [6] for 0.04 - 1.5 eV . In the calculation, 22 resonances were taken into account : 16 resonances in the energy interval under investigation plus 2 "negative" resonances and 1 resonance above 10 eV for each spin, respectively.

We have made an attempt to fit simultaneously as the $\sigma_{f0}(E)$ and the $A_2(E)$ values in energy interval 0.1-10 eV as well as the spin-separated fission cross sections $\sigma^{3^-}_{f0}(E)$ and $\sigma^{4^-}_{f0}(E)$ for neutron energy 0.1-1.9 eV with the fixed positions , neutron and total radiative and fission widths of the resonances under investigation taken from [7]. The ENDF/B-VI data file for $\sigma_{f0}(E)$ and data from [8,9] for spin-separated cross sections $\sigma^{J\pi}_{f0}(E)$ were used. We varied firstly only signs and relative weights of a partial fission amplitudes for all resonances mentioned above. It turned out to be impossible to fit the $A_2(E)$ dependence in the framework of this procedure. Thus all parameters of negative resonances and total neutron and fission widths of some positive resonances were „released" and new fit has be done taking care of the consistent description of the integral and spin-separated fission cross sections.

Fig. 1 shows the results of the $A_2(E)$ fitting where the points and curves represent, respectively, the experimental data and two variants of the fit. The calculations show significant sensitivity of the $A_2(E)$ to small variations of as neutron and as well as fission amplitudes and their signs. One of the main conclusions which has to be made is that the effects of interference between resonances have really strong influence on the structure of the $A_2(E)$. The effect of interference of resonances with different spins is also essential. The calculations demonstrate 10-20% variations in the $A_2(E)$ behavior after including of the JJ' terms in the σ_{f2} (compare the solid and dotted lines in Fig. 1). It is worth to note that hi-square values per point (including the σ_{f0} and $\sigma^{J\pi}_{f0}$ data) are 0.96 and 2.08 with and without accounting for the JJ' terms, respectively.

The "K-anatomy" of the A_2 fitted values is represented in Fig. 2 where contributions of different K projections (summed over J) to the total $A_2(E)$ dependence are apparently shown. It is clear that very peculiar energy dependence of the $A_2(E)$ function is the result of a rather irregular behaviour of its K-components. So it is obvious that the previous idea [3], that one can attribute a $A_{2\lambda}$ value (1) to each resonance λ connected only with its fission widths, is hardly correct since for any given energy the $A_2(E)$ is „formed" by a group of neighboring levels.

After this analysis very important problems still remain. They are the question of uniqueness of the fitted parameter set and the consistence of these calculations with the description of the neutron capture and transmission data. It is necessary also to include in the fitted data the spin-separated fission cross sections for neutron energy up to 10 eV. In any case, the analysis outlined above permits, in principle, to extract unambiguously the partial fission amplitudes of s-wave neutron resonances and gives

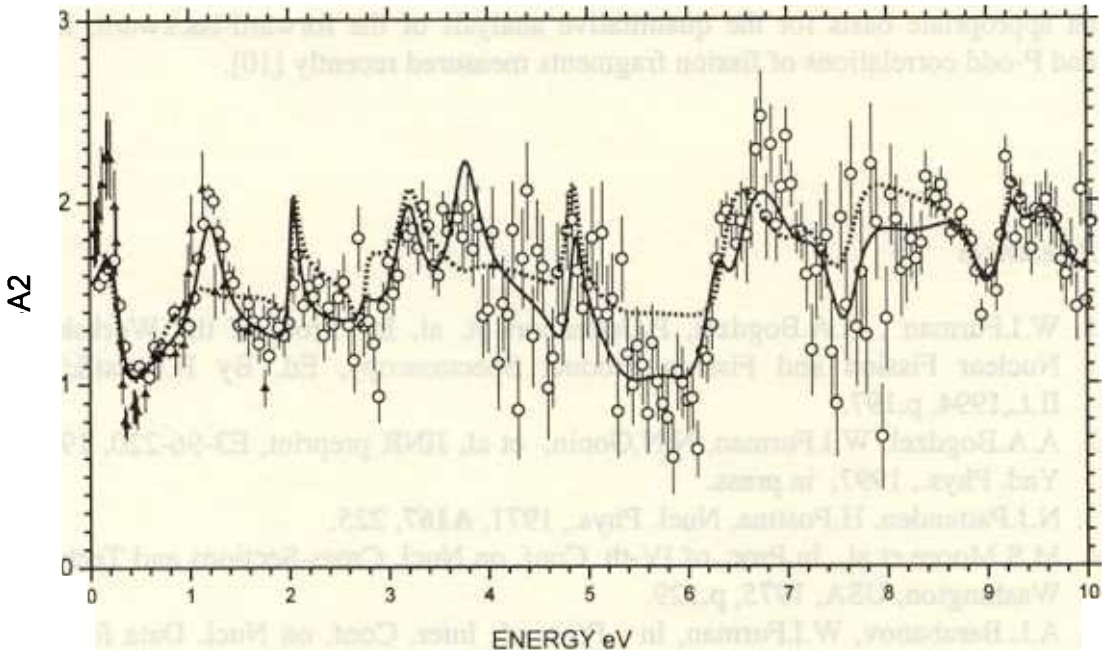

The dependence of the angular correlation between spin orientation of target 235U nucleus and fission fragment momentum on neutron energy. Experimental data: circles - present work, the fit: solid line - with JJ'-interference, dottted one - without it.

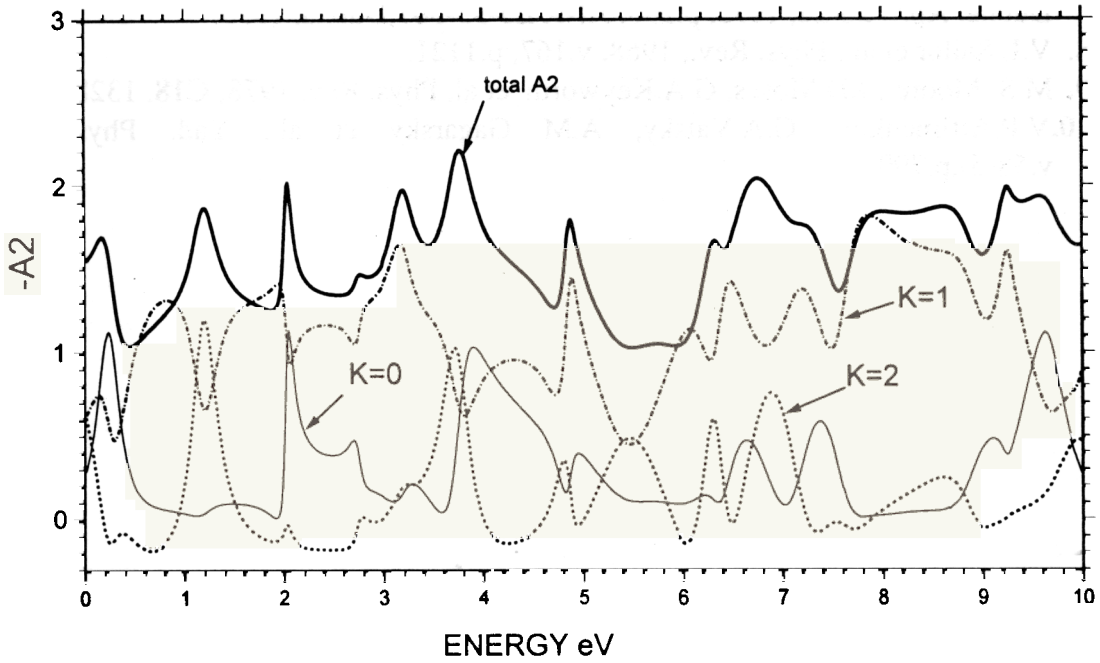

The contributions of diffrent K-projections in the A2(E).

an appropriate basis for the quantitative analysis of the forward-backward, left-right and P-odd correlations of fission fragments measured recently [10].

References

1. W.I.Furman , A.A.Bogdzel, P.Geltenbort et. al, In Proc. of the Workshop on Nuclear Fission and Fission Product Spectroscopy, Ed. By H.Faust&G.Fioni, ILL,1994, p.197.
2. A.A.Bogdzel, W.I.Furman, N.N.Gonin, et al, JINR preprint, E3-96-220, 1996, and Yad. Phys., 1997, in press.
3. N.J.Pattenden, H.Postma, Nucl. Phys., 1971, **A167**, 225.
4. M.S.Moore et al., In Proc. of IV-th. Conf. on Nucl. Cross-Sections and Technology, Washington, USA, 1975, p.129.
5. A.L.Barabanov, W.I.Furman, In Proc. of Inter. Conf. on Nucl. Data for Science and Technology, Gatlinburg, Tennessee, Ed. by J.K. Dickens, 1994, v.1, p.448.
6. H.Postma, In Proc. Int. Symp. on Neutron Capture, Gamma Ray Spectroscopy and Related Topics, Petten, 1974, p.619.
7. M.S. Moore, In Proc. of III-th Inter. Seminar on Interaction of Neutrons with Nuclei, Dubna, April 26-28, 1995, p.290, JINR E3-95-307,Dubna, 1995.
8. V.L.Sailor et al., Phys. Rev., 1968, v.167, p.1121.
9. M.S. Moore , J.D.Moses, G.A.Keyworth et al, Phys. Rev. 1978, **C18**, 1328.
10. V.P.Alfimenkov, G.A.Valsky, A.M Gagarsky et al., Yad. Phys., 1995, v.58(5),p.799.

3. PUBLICATIONS

CONDENSED MATTER PHYSICS

Reviews

V.L.Aksenov. The Pulsing Nuclear Reactor (40th Anniversary of Joint Institute for Nuclear Rsearch). Priroda, № 2, 1996, p.3-17 (in Russian).

2. V.L.Aksenov. Neutron Investigations of Surfaces and Thin Films. Preprint of JINR, P14-96-350, Dubna, 1996, -16p. Lecture at The Ninth International School on Condensed Matter Physics, Varna, Bulgaria, September 9-13, 1996 (in Russian).
3. V.L.Aksenov, A.M.Balagurov. Time-of-Flight Neutron Diffractometry. Uspekhi Fiz. Nauk, 1996, v.166(9), pp.955-986.
4. V.L.Aksenov. Scientific Program of the Frank Laboratory of Neutron Physics: Report for 1996 and Prospects for 1997. JINR 96-471, Dubna, 1996.

Diffraction

V.L.Aksenov, E.V.Antipov, A.M.Balagurov et al. Precision Neutron Diffraction Study of the High-T_c Superconductor $HgBa_2CuO_{4+\delta}$ JINR Communications, P13-96-266, Dubna, 1996 (in Russian); Phys.Rev. B, 1997, v.55, pp.3966-73.

2. V.L.Aksenov, A.M.Balagurov, B.N.Savenko, D.V.Sheptyakov, V.P.Glazkov, V.A.Somenkov, S.Sh.Shilshtein, E.V.Antipov, S.N.Putilin. Investigation of the Hg-1201 Structure under External Pressures up to 5 GPa by Neutron Powder Diffraction. JINR Communications, P14-96-385, Dubna, 1996 (in Russian); Physica C, 1997, 275, pp.87-92.
   V.L.Aksenov, A.M.Balagurov, V.G.Simkin, A.P.Bulkin, V.A.Kudrjashev, V.A.Trounov, O.Antson, A.Tiitta. Performance of the High Resolution Fourier Diffractometer at the IBR-2 Pulsed Reactor. JINR Communications, P13-96-164, Dubna, 1996 (in Russian); J. of Neutron Research, 1997.
   V.L.Aksenov, A.M.Balagurov, V.A.Trounov. High-Resolution Fourier Diffractometry for Long Pulse Neutron Source. J. of Neutron Research, 1997.
5. I.K.Arkhipov, A.N.Nikitin, T.I.Ivankina. A Method for Prediction of Induced Anisotropy of Powder Composites. Industrial Laboratory, 1996, v.47, pp.31-35 (in Russian).
6. A.M.Balagurov, G.D.Bokuchva, J.Schreiber, Yu.V.Taran. Neutron Diffraction Investigations of Stresses in Austenitic Steel. ECNS'96, Interlaken, 8-11 October, 1996.
7. A.M.Balagurov, V.Yu.Pomjakushin, V.G.Simkin, A.A.Zakharov. Neutron Diffraction Study of Phase Separation in La_2CuO_{4+y} Single Crystals. JINR Communications, P13-96-222, Dubna, 1996 (in Russian); Physica C, 1996, v.272, pp.277-284.
8. A.M.Balagurov, V.Yu.Pomjakushin, V.G.Simkin, A.A.Zakharov. Single Crystal Diffraction Study of Phase Separation Phenomenon in La_2CuO_{4+y}. Pisma v ZhETF, 1996, v.64 (4), p.254 (in Russian).
9. A.M.Balagurov, V.V.Sikolenko, I.S.Lyubutin, F.Bouree. Neutron Diffraction Study of Magnetic Structure of $U(Pd_{1-x}Fe_x)_2Ge_2$. ECNS'96, Interlaken, 8-11 October, 1996.
10. A.M.Balagurov, V.V.Sikolenko, V.G.Simkin, O.E.Parfionov, S.Sh.Shilshtein. Neutron Diffraction Study of $Yba_2Cu_{2.7}Zn_{0.3}O_{6+y}$ Isotope Enriched Samples. Physica C, 1996, v.259, pp.173-180.
    E.V.Colla, E.Yu.Koroleva, Yu.A.Kumzerov, B.N.Savenko, S.B.Vakhrushev. Ferroelectric Phase Transition in Materials Embedded in Porous Media. Ferroelectrics Letters, 1996, v.20, p.143.
12. V.T.Em, M.Yu.Tashmetov. Phase Transformations of Ordered Phases in Titanium Carbides and Carbonitrides with FCC Metal Matrix. Proceedings of the 5th Asian Symposium on Research Reactors, May 29-31, 1996, Taejon, Korea, v.2, pp.525-529.
13. V.T.Em, M.Yu.Tashmetov. The Structure of the Ordered Phase in Rocksalt Type Titanium Carbide, Carbidenitride and Carbidehydride. phys.stat.sol. b, 1996, v.198, p.571.
14. K.Helming, D.Schmidt, K.Ullemeyer. Preferred Orientations of Mica Bearing Rocks Described by Texture Components. Texture and Microstructures, 1996, v.25, pp.221-229.
15. V.V.Luzin, D.I.Nikolaev. On the Errors of the Experimental Pole Figures. Texture and Microstructures, 1996, v.25, pp.121-128.

16. V.V.Luzin, D.I.Nikolaev. "The Errors of Pole Figures Measured by Neutrons", in: Textures of Materials. Proceedings of the ICOTOM-11, Xian, China, September 1996, pp.140-145.
17. G.M.Mironova. From New Experimental Method to New Physical Concepts. International Seminar on Relaxor Ferroelectrics, 21-23 May 1996, Dubna, JINR Communications, E13-96-147, p.40, Dubna, 1996.
18. G.M.Mironova, A.M.Balagurov. Nonlinear Effects in Quartz, Iron and HTSC. International Seminar on Relaxor Ferroelectrics, 21-23 May 1996, Dubna, JINR Communications, E13-96-147, p.101, Dubna, 1996.
19. A.N.Nikitin. The Formation of Piezoelectric Textures in Quartzbearing Rocks. Physics of the Earth, 1996, v.10, pp.15-21 (in Russian).
20. A.N.Nikitin, T.I.Ivankina, I.K.Arkhipov. On the Formation of Preferred Inclusion Shape Orientations in Copper Based Composites. Textures and Microstructures, 1996, v.26, pp.1-8.
21 A.N.Nikitin, T.I.Savyolova. Normal Distribution on the Quartz Crystal Orientation on the Distribution of Local Stresses within a Texturized Polysrystallite. Scientific Report TGU, Tula, 1996, pp.51-59 (in Russian).
22. D.I.Nikolaev, K.Ullemeyer. The Effect of Smoothing on ODF Reproduction. Textures and Microstructures, 1996, v.25, pp.149-157.
23 V.Yu.Pomjakushin et al. Spin-Glass Ordering in Non-Phase Separated $La_2CuO_{4.03}$ Studied by μSR. Physica C, 1996, v.272, pp.250-256.
24 V.Yu.Pomjakushin, A.A.Zakharov et al. Study of Microscopic Phase Separation in La_2CuO_{4+y}. JINR Communications, E14-96-16, Dubna, 1996.
25 F.Prokert, B.N.Savenko, A.M.Balagurov. Neutron Diffraction Study of Phase Transitions in the Mixed Crystal $Sr_{0.7}Ba_{0.3}Nd_2O_6$ between 20 and 300 K. Ferroelectrics, 1996, v.188, pp.187-199.
26. R.A.Sadykov, A.I.Beskrovnyi. "Double-Level" High Pressure Cell for Neutron Diffraction Analysis. 1st European Conference on Neutron Scattering, Abstracts, 8-11 October, 1996, p.221.
27 V.A.Sarin, E.E.Rider, D.Hohlwein, W.Depmeier, H.Bessert, F.Frey, K.Hroudil, A.M.Balagurov, A.I.Beskrovny, T.E.Galinskaya, V.L.Levashvili. Neutron and *X*-Ray Bragg and Diffuse Scattering Investigation of Defect Structure of ZrO_2-Y_2O_3 (Y_2O_3 - 3,12,30 mol%) Single Crystals. ECNS'96, 8-11 October 1996, Interlaken, Switzerland, F63.
28. Yu.V.Taran, J.Schreiber, P.Mikula, P.Lukas, M.Vrana, G.D.Bokuchava, H.Kockelmann. Neutron Diffraction Measurements of Residual Stresses in an Austenitic Steel Tube with a Welded Ferritic Cover. Proc. of 4th European Conf. on Residual Stresses, July 4-6, 1996, Cluny, France.
29 M.Yu.Tashmetov, V.T.Em, N.N.Mukhtarova. The Trigonal Ordering Structure in Titanium Carbonitrides. Nonorganic Materials, 1996, v.32, pp.171-172 (in Russian).
30. K.Ullemeyer. Error Estimation of Multiphase Pole Density Measurements by TOF Neutron Diffraction: Application to a Granulite. Z. geol. Wiss., 1996, v.24, pp.671-678.
31 K.Ullemeyer, K.Weber. "Quantitative Texture Analysis of Polyphase Rocks: Estimation of Experimental Errors by Means of Reference Textures", in Textures of Materials. Proceedings of the ICOTOM-11, Xian, China, September 1996, pp.140-145.

Small-Angle Scattering

L.A.Bulavin, V.M.Garamus, T.V.Karmazina, M.V.Avdeev. Structure of Micellar Aggregates of Non-Ionic Surfactans in Salt-Water Solutions by SANS. Colloid J.Russ.Acad.Sci.-Engl., 1997, v.59, pp.30-35.
2. L.A.Bulavin, V.M.Garamus, T.V.Karmazina, E.N.Pivnenko. Measurements of the Structural, Electrostatic Parameters and Surface Tension of Micelles of an Ionic Surfactant Versus Concentration, Ionic Strength of Solution and Temperature by SANS. Colloids and Surfaces, 1997.
3. Lixin Fan, E.I.Zgurskaya, I.Shcherbakova, I.N.Serdyuk. Determination of Deuterium Incorporation into RNA and Protein Components of the *Escherichia Coli* Ribosome at Biosynthetic Deuteration by Small-Angle Neutron Scattering. J. Appl. Cryst., 1997, v.30, pp.59-64.
4. V.I.Gordeliy, V.G.Cherezov, A.V.Anikin, A.M.Anikin, V.V.Chupin, J.Teixeira. Evidence of Entropic Contribution to "Hydration" Forces Between Membranes. 1. The Forces between Polymeric Lipid Membranes. Progr. Colloid Polym. Sci., 1996, v.100, pp.338-344.
5. V.I.Gordeliy, V.G.Cherezov, A.D.Tugan-Baranovskaya, L.S.Yagujinskiy. Investigation of the Structure of Thylakoid Membranes (Spinach) by Means of Small-Angle Neutron Scattering. Biochemistry and Molecular Biology International, 1996, v.38 (3), pp.485-491. Biol. Membrany, 1996, v.13, pp.307-312 (in Russian).
6. N.Gorski, M.Gradzielski, H.Hoffmann. The Influence of Ionic Charges on the Structural and Dynamical Behavior of O/W Microemulsion Droplets. Ber. Bunsenges. Phys. Chem., 1996, v.100, pp.1109-1117.

7. M.Kiselev, P.Lesieur, V.Gordeliy, J.Teixeira, C.Grabiel-Madelmond, M.Ollivon. Influence of DMSO on the Main Phase Transition of the Lipid Membranes. Proc. of SOLEIL Conference, April 2-5, 1996, Orsay, France.
8. G.Klose, A.Islamov, B.Koning, V.Cherezov. Structure of Mixed Multilayers of Palmitoyloleylphosphatidylcholine and Oligo(Oxyethelene-Glycol) Monodo-decyl Ether Determined by *X*-Ray and Neutron Diffraction. Langmuir, 1996, v.12, pp.409-415.
9. J.Kriz, M.Masar, H.Pospisil, J.Plestil, Z.Tuzar, M.A.Kiselev. NMR and SANS Study of Poly (Methyl Methacrylate) - Block -Poly (Acrylic Acid) Mixelles and Their Solubilization Interactions with Organic Solubilizates in D_2O. Macromolecules, 1996, v.29, pp.7853-7858.
10. P.Lesieur, M.Kiselev, V.Gordeliy, G.Keller, M.Ollivon. Study of the Cryoprotection Property of Dimethylsulfoxed on the Lipid Membranes. Proc. of SOLEIL Conference, April 2-5, 1996, Orsay, France.
11 G.M.Mironova. New Conception of Magnetic Phase Transition Via Observation of Q-Independent Forward Neutron Scattering in Iron. Intern. Workshop Polarized Neutrons for Condensed Matter Investigations, Dubna, 18-20 June 1996, p.25.
12. G.M.Mironova. Second Order Phase Transitions as Studied by Real Time Transmission, Diffraction and SANS. XVII Congress and General Assembly IUCr, Seattle, Washington, USA, 8-17 August, 1996, C-434.

Inelastic Neutron Scattering

P.A.Alekseev, E.S.Klement'ev, B.N.Lazukov, I.P.Sadikov, M.N.Khlopkin, M.Adams, A.Yu.Muzychka, I.L.Sashin, N.B.Kolchugina, O.D.Chistyakov. The Crystalline Field in *CeNi*-Based Nonstable Valence Compounds. Pisma v ZhETF, 1996, v.63, pp.947-952 (in Russian).
2. A.V.Belushkin, I.Natkaniec, L.S.Smirnov, A.I.Solov'ev. Study of Ammonium Dynamics in Rhomboedric Phase of $K_{1-x}(NH_4)_xSCN$ (x<0.15). Izv. Ac. of Science, Seria Phys., 1996, pp. 30-41 (in Russian).
3. L.Bobrowicz, A.Kartusiak, W.Nawrocik, J.Wasicki, I.Natkaniec. Neutron Scattering Study of the Phase Transitions in 1,3-Cyclohexanedione Crystals at Ambient and High Pressure. phys. stat. sol. (b), 1996, v.196, pp.39-47.
4 S.Borbely, Yu.M.Ostanevich, Yu.K.Kovneristii, O.B.Tarasova, L.S.Smirnov. Small Angle Neutron Scattering Intensity Evolution in the Crystallization Process of Titanium-Based Metallic Glasses. Titanium'95: Science and Technology (Proceedings of the Eighth World Conference on Titanium). The Institute of Materials, London, 1996, v.3, pp.2531-2538.
5. A.V.Chumachenko, M.G.Zemlyanov, A.Yu.Muzychka, O.E.Parfenov, P.P.Parshin, A.A.Shikov. Experimental Investigations of the Influence of the Concentration of Free Carriers on the Vibrational Spectrum of a $Yba_2Cu_3O_{7-y}$ Compound. Pisma v ZhETF, 1996, v.109, pp.204-211 (in Russian).
6. B.E.Clements, H.Godfrin, E.Krotscheck, H.J.Lauter, P.Leiderer, V.Passiouk, C.J.Tymczak. Excitations in a Thin Liquid ^{4}He Film from Inelastic Neutron Scattering. Physical Review B, v.53, (1996) No.18, p.12242.
S.A.Danilkin, E.L.Yadrovsky. Measurements of Phonon Dispersion in a X18H15AГ10 Alloy. Preprint PEI-2505, Obninsk, 1996, p.14 (in Russian).
M.Dlouga, S.Vratislav, I.Natkaniec, L.S.Smirnov. Study of Structural Peculiarities of Phase Transition on $N(H/D)_4SCN$ by Neutron Scattering. JINR Comm., P14-96-157, Dubna, 1996 (in Russian).
9. V.V.Dolbilina, B.N.Savenko, L.S.Smirnov, A.I.Solov'ev, S.N.Sul'yanov, D.M.Kheiker, L.A.Shuvalov. Investigations of the NH_4SCN-NH_4Cl and $NaSCN$-NH_4SCN Systems by the Method of *X*-Ray Powder Diffraction. Izvestia Akad. Nauk., ser. phys,, 1996, No.10, pp.202-204 (in Russian).
10. M.Dorr, J.Kalus, M.Monkenbusch, I.Natkaniec, U.Schmelzer. The Lattice Dynamics of a Dipolar Disordered Crystal of 2,3-Dimethylantyracene. Physica B, 1996, v.219-220, pp.368-370.
Yu.Yu.Glazkov, S.A.Danilkin, Yu.V.Lisichkin, S.I.Morozov, V.M.Morozov, A.G.Novikov, A.F.Pavlov, A.V.Puchkov, V.A.Semenov, A.A.Tumanov, E.L.Yadrovsky. Investigations of Condensed Matter by Slow Neutron Scattering. Atomnaia Energiia, 1996, v.80 (5), pp.391-399 (in Russian).
12. E.A.Goremychkin, A.IO.Muzychka, R.Osborn. Crystalline Field Effects in RCu_2Si_2 *(R=Ce, Pr, Nd, Ho, Er):* Compounds: Inelastic Neutron Scattering Investigations. Pisma v ZhETF, 1996, v.110 (10), pp.1339-1354 (in Russian).
3. K.Holderna-Natkaniec, I.Natkaniec, J.Wasicki. Structural Phase Transition and Molecular Structure in Bornyl Chloride, Journal of Molecular Structure, 1996, v.374, pp.155-160.
14. S.N.Ishmaev, E.Shvab, O.B.Tarasova, L.S.Smirnov. Short-Range Order in Amorphous Alloys of the *Ti-Zr-Si* System. Titanium'95: Science and Technology (Proceedings of the Eighth World Conference on Titanium). The Institute of Materials, London, 1996, v.3, pp.2228-2235.

15. A.I.Kolesnikov, M.Adams, V.E.Antonov, N.A.Chirin, E.A.Goremychkin, G.G.Inikhova, Yu.E.Markushkin, M.Prager, I.L.Sashin. Neutron Spectroscopy of Aluminium Trihydride. J. Phys. Condens. Matter, 1996, v.8, pp.2529-2538.
16. A.Yu.Muzychka, E.A.Goremychkin, R.Osborn. The Crystalline Field in *RE-TR_2Si_2 (RE=Pr, Nd; TR=Cu, Ni, Fe)* Compounds. JINR Communications, P14-96-205, Dubna, 1996 (in Russian).
17 I.Natkaniec, L.S.Smirnov, A.I.Kolesnikov, A.N.Ivanov. Neutron Spectroscopy of Ice III. High Pressure Science and Technology. Ed. By A.Trzeciakowski. World Scientific, 1996, pp.369-371.
18. I.Natkaniec, L.S.Smirnov, S.I.Bragin, A.I.Solov'ev. Neutron Spectroscopy of *$K_{1-x}(NH_4)_xI$* Solid Solution. Izv.Ac. of Sciences, Seria Phys., 1996, No.10 (in Russian).
19. A.G.Novikov, A.V.Puchkov, V.A.Semenov, A.A.Tumanov. The DIN Spectrometers at the Pulsed Reactor. Submitted to the Book of Anniversary Selected Works of PEI, Obninsk, 1996 (in Russian).
20. A.G.Novikov, M.N.Rodnikova, V.V.Savostin, O.V.Sobolev. The Diffusion Spectra of the *$(CH_3)_4NCl$* Salt 2M Solution from Slow Neutron Inelastic Scattering Experiments. Zh. Fiz. Chim., 1996, v.70, No.6, pp.1056-1060 (in Russian).
21 A.G.Novikov, M.N.Rodnikova, V.V.Savostin, O.V.Sobolev. The Rotation-Vibration Motions of Water Molecules in 2M aqueous CsCl Solution. Chem.Phys.Letters, 1996, v.259, No.3-4, pp.391-396.
A.Pawlukojc, J.Leciejewicz, I.Natkaniec. The INS Spectroscopy of Amino Acids: *l*-Leucine. Spectrochimica Acta, 1996, v.A52, pp.29-32.
23. V.A.Semenov, V.S.Shakhmatov. Slow Neutron Inelastic Scattering by Hematite. Fiz. Tverd. Tela, 1996, v.38, No.6, pp.1844-1846 (in Russian).
24. E.F.Sheka, I.V.Markichev, I.Natkaniec, V.D.Khavryuchenko. Inelastic Neutron Scattering Studies and Computer Modeling of Structure and Dynamics of Highly Dispersed Amorphous Silicas. Particles and Nucleus, 1996, v.27, part 2, pp.493-560.
25. L.S.Smirnov, I.Natkaniec, S.I.Bragin, L.A.Shuvalov, S.N.Sulyanov. Ammonium Dynamics in $Rb_{1-x}(NH_4)_xSCN$ Mixed Crystals at 10K. XVII Congress IUCr., Seattle, 8-17 August, 1996, PS11.05.29. ECNS'96, Intelaken, 8-11 October, 1996, Physica B, 1997.
26. V.V.Sumin. Local Modes of Interstitial Atoms in Transition Metals. JINR Communications, E14-96-193, Dubna, 1996, p.11. Materials Science & Engineering, 1997.
27. G.F.Syrykh, V.P.Glazkov, A.V.Suetin, M.N.Khlopkin, E.A.Goremychkin, I.L.Sashin. Neutron and Calorimetric Investigations of the Excitation Spectrum of a *La_2CuO_{4+y}* (y=0.08, 0.00) Compound. Fiz. Tverd. Tela, 1995, v.37, pp.3661-3668 (in Russian).
28. O.B.Tarasova, L.S.Smirnov, L.E.Fykin. Some Peculiarities of Titanium-Based Amorphous Alloy Crystallization *(Ti-Zr-Si, Ti-Zr-Hf-Si).* Titanium'95: Science and Technology (Proceedings of the Eighth World Conference on Titanium). The Institute of Materials, London, 1996, v.3, pp.2523-2530.
29. V.Voronin, A.Mirmelstein, A.Teplykh, B.Goshchitskii, A.Ivanov, L.Smirnov. Neutron Diffraction Study of Anisotropy of Crystal Lattice Expansion in High-T_c Superconductors. Fizika Nizkikh Temp., 1996, v.22 (5), p.451 (in Russian).
30. M.V.Zaezzhev, M.N.Ivanovskii, A.G.Novikov, V.V.Savostin, A.L.Shimkevich. Selfdiffusion in Liquid Potassium. J.Phys.Cond.Matter, 1996, v.8, No.20, pp.325-336.

Reflectometry, Polarized Neutrons

V.L.Aksenov, E.B.Dokukin, S.V.Kozhevnikov, Yu.V.Nikitenko, A.V.Petrenko, J.Schreibier. Refraction of Polarized Neutrons in a Magnetically Non-Collinear Layer. Proceedings of the International Workshop "Polarized Neutrons for Condensed Matter Investigations", 18-20 June 1996, Dubna, E3-96-507. Physica B, 1997, v.179.
2. V.I.Bodnarchuk, L.S.Datyan, D.A.Korneev. The Geometrical Phase Effects in Neutron Optics. Uspekhi Fiz. Nauk, 1996, v.166, No.2, pp.185-194 in Russian).
3. B.Chesca. Of a UFN Pumped Double Squid. Physica C, 1996, v.270, pp.1-20.
4. L.S.Davtyan. Geometry of Adiabatic Changes. General Analysis, JINR Communications, E5-96-181, Dubna, 1996.
5. D.A.Korneev, V.I.Bodnarchuk, V.I.Ignatovich. Off-Specular Neutron Reflection from Magnetic Media with
6. F.Rieutord, A.Braslau, R.Simon, H.J.Lauter, V.Pasyuk. Moments Analysis of X-Ray Reflection Profile. Physica B, 1996, v.221, p.538.

Accelerated Ions

A.S.Borovik, A.P.Kobzev, E.A.Kovaleva, S.N.Potapov. Static Displacements of Oxygen Atoms in the Crystalline Lattice of $YBa_2Cu_3O_7$. Book of Abstracts. International Conference on the Interaction of Charged Particles with Crystals. 27-29 May, 1996, Moscow, p.31 (in Russian).

2. T.Czyzewski, L.Glowacka, M.Jaskola, J.Braziewicz, M.Pajek, J.Semaniak, M.Haller, R.Karschnick, W.Kretschmer, A.P.Kobzev, D.Trautmann. M-Shell *X*-Ray Production by *C, N,* and *O* Ions. Nuclear Instruments and Methods in Physics Research B, 1996, v.109/110, pp.52-58.
3. S.M.Duvanov, A.P.Kobzev. The Differential Cross Sections of the $^{12}C(p,p)^{12}C$ Reaction in the Resonance Energy Range at the Energy 1.726 MeV. JINR Communications, P15-96-69, Dubna, 1996 (in Russian).
4. V.Podgurski, A.P.Kobzev, T.Seudzinski, A.Latuszinski, T.Maewski, D.Mochka. An Element Analysis of Biological Samples by Nuclear Physics Methods, RBS and PIXE. JINR Communications, P19-96-309, Dubna, 1996 (in Russian).
5. V.M.Zavodchikov, A.P.Kobzev, Yu.Yu.Kryuchkov, V.F.Pichugin, V.V.Sokhoreva, T.S.Frangul'yan. Determination of the Composition of the Ion-Implanted Surface Layers of *MgO* by the Methods of Rutherford and Resonance Backward Scattering of Ions.. Pisma ZhETF, 1996, v.22 (1), pp.7-11 (in Russian).

Theory

V.L.Aksenov, Yu.A.Ossypian, V.S.Shakhmatov. Structure Peculiarities of the Polymer-Like Phase of a Fulleride AC_{60}. Pisma ZhETF, 1996, 64, v.2 (in Russian).

2. A.S.Alexandrov, V.V.Kabanov. Theory of Superconductivity T_c of Dopped Fullerenes. Phys.Rev.B, 1996, v.54, pp.3655-3661.
3. A.S.Alexandrov, V.V.Kabanov. Theory of the Charged Bose Gas: Bose-Einstein Condensation in Ultra-High Magnetic Field. Phys.Rev.B, 1996, v.54, pp.15363-15370; Czech.J.Phys., 1996, v.46, pp.959-960.
4. A.S.Alexandrov, V.V.Kabanov, N.F.Mott. Coherent 'ab' and 'c' Transport Theory of High-T_c Cuprates. Phys.Rev.Lett., 1996, v.77, pp.4796-4799.

NEUTRON NUCLEAR PHYSICS

Experiment

1. Yu.A.Alexandrov. On the Neutron Mean Square Intrinsic Charge Radius. Report to III Intern. Seminar on Interaction of Neutrons with Nuclei (ISSINN-3). Neutr. Spectroscopy, Nucl.Structure, Related Topics, Dubna, Apr. 26-28, 1995, E3-95-307, p.243.
2. Yu.A.Alexandrov. On the Problem of the Neutron Mean Square Intrinsic Charge Radius. Revista Mexicana de Fisica 42 (1996) 263.
3. Yu.A.Alexandrov. Polarizability of the Neutron. JINR, E3-95-61, Dubna, 1995; (ibid.)
4. Yu.A.Alexandrov. Polarizability of the Neutron. Revista Mexicana de Fisica, 42 (1996) 283.
5. Yu.A.Alexandrov. Problem of the Neutron Intrinsic Charge Radius. Report to "Baryons' 95", 7th Intern. Conf.on the Structure of Baryons, Oct.3-7, 1995, Santa Fe, USA, Abstracts, p.11.
6. Yu.A.Alexandrov. Problem of the Neutron Mean Square Intrinsic Charge Radius. JINR, E3-95-60, Dubna,1995 (Submited to the XVIII Nuclear Physics Symposium at Oaxtepec, Jan. 4-7, 1995, Mexico).
7. Yu.A.Alexandrov. Some Fundamental Properties of the Neutron. Report to VII School on Neutron Physics, Rattmino, 3-22 Sept. 1995, Lectures, v.I, p.9, Dubna, 1995, E3,14-95-323.
8. Yu.A.Alexandrov. Investigation of Electromagnetic Properties of the Neutron and the Charge Neutron Radius. Report to ISINN-4, Dubna, 27-30 April, 1996, E3-96-114, p.77.
9. A.Aleksejevs, S.Barkanova, T.Krasta, J.Tambergs, P.Prokofjevs, W.Waschkowski, G.S.Samosvat. Evaluation of Neutron Fundamental Parameters from the Nuclear Total Cross Section Data and in Quark Potential Model Approach. 9th International Symposium on Capture Gamma-Ray Spectroscopy and Related Topics. Abstract Booklet. Budapest, Hungary, 8--12 October 1996. Budapest, 1996, p.256.
10. V.I.Alfimenkov, L.B.Pikelner. Experiments with Polarized Neutrons and Nuclei. Particles and Nuclei, 26, issue 6, 1524 (1995).

11. V.P.Alfimenkov, A.N.Chernikov, A.M.Gagarski, S.P.Golosovskaya, I.A.Krasnoschokova, L.Lason, Yu.D.Mareev, A.M.Morozov, V.V.Novitski, G.A.Petrov, V.I.Petrova, A.K.Petukhov, Yu.S.Pleva, L.B.Pikelner, V.R.Skoy, V.E.Sokolov, S.M.Soloviev, M.I.Tsulaya. Experimental Method and Preliminary Results of Measurements of the Left-Right Asymmetry Effeet in Fragment Angular Distributions of the ^{235}U Fission Induced by Resonans Neutrons. Preprint PNPI, 2117, Gatchina, 1996.
12. V.P.Alfimenkov, I.S.Guseva, A.M.Gagarski, S.P.Golosovskaya, I.A.Krasnoschokova, A.M.Morozov, G.A.Petrov, V.I.Petrova, A.K.Petukhov, L.B.Pikelner, Yu.S.Pleva, V.E.Sokolov, S.M.Soloviev, G.V.Valiski. P-Odd, Left-Right and Forward-Backward Asymmetries of Fragment Angular Distributions in ^{233}U Fission Induced by the Low Energy Neutrons and Forward-Backward Asymmetry in ^{239}Pu Fission. ISINN-3, JINR, E3-95-307, Dubna, 1995, p.276.
13. B.V.Bagryanov, D.G.Kartashov, M.I.Kuvshinov, G.V.Nekhaev, I.G.Smirnov, A.D.Stoica, A.V.Strelkov, V.N.Shvetsov. A Dynamic UCN Converter at a Pulsed Reactor. Yad.Fiz., v.59 (1996) №11, p.1983 (in Russian).
14. B.V.Bagryanov, D.G.Kartashov, M.I.Kuvshinov, G.V.Nekhaev, I.G.Smirnov, A.D.Stoica, A.V.Strelkov, V.N.Shvetsov. Proposal for an Experiment to Measure the Neutron Lifetime at a Pulsed Source of Ultracold Neutrons (UCN). Report at the XI Seminar on Precise Measurements in Nuclear Spectrometry. Sarov, September 2-5, 1996 (in Russian).
15. H.Beer, C.Coceva, P.Mohr, H.Herndl, R.Hofinger, H.Oberhummer, P.V.Sedyshev, Yu.P.Popov. Measurement of Direct Neutron Capture and Stellar Reaction Rates of Light Isotopes at the Neutron-Rich Border of Stability. Int. Symp. on Nucl. Astrophys. "Nuclei in the Cosmos IV", University of Notre Dame, USA, 1996 (abstracts).
16. H.Beer, C.Coceva, P.V.Sedyshev, Yu.P.Popov, H.Hendl, R.Hofinger, P.Mohr, H.Oberhummer, Measurement of Neutron Capture on ^{48}Ca at Thermal and Thermonuclear Energies. Phys. Rev. C. 54 (1996) 2014 -2022.
17. H.Beer, C.Coceva, R.Hofinger, P.Mohr, H.Oberhummer, P.V.Sedyshev, Yu.P.Popov. Measurement of Direct Neutron Capture by Neuton-Rich Sulfur Isotopes. 9th International Symposium on Capture Gamma-Ray Spectroscopy and Related Topics. Abstract Booklet. Budapest, Hungary, 8--12 October 1996. Budapest, 1996
18. H.Beer, P.V.Sedyshev, Yu.P.Popov, W.Balogh, H.Herndl and H.Oberhummer. Cross Section of $^{36}S(n,\gamma)^{37}S$. Phys.Rev.C 52 (1995) 3442.
19. A.A.Bogdzel, W.I.Furman, N.N.Gonin, M.A.Guseinov, J.Kliman, Yu.N.Kopach, L.K.Kozlovsky, A.B.Popov, H.Postma, N.S.Rabotnov, D.I.Tambovtsev. Measurement of Energy Dependence of Fission Fragment Angular Anisotropy for Resonance Neutron Induced Fission of ^{235}U Aligned Target, E3-96-220, Dubna, 1996.
20. A.A.Bogdzel, W.I.Furman, Yu.N.Kopach, A.B.Popov, N.N.Gonin, M.A.Guseinov, L.K.Kozlovsky, D.I.Tambovtsev, J.Kliman, H.Postma. Status of Fission Experiment with ^{235}U Aligned Target. IV Intern. Seminar on Interaction of Neutron with Nuclei., Dubna, April 27-30, 1996, JINR E3-96-336, p.211, Dubna, 1996.
21. I.V.Bondarenko, A.I.Frank, S.N.Balashov, S.V.Masalovich and V.G.Nosov. Proposed Fundamental Investigations Using Interference Filter and Gravity Spectrometry. International Symposiom on Advance in Neutron Optics. (Kumatory, Osaka, Japan 19-21 March 1996). To be published in Jorn.Phys.Soc.Jap., 65A, 1996.
22. S.T.Boneva, V.A.Khitrov, Yu.P.Popov, A.M.Sukhovoj. Nuclear Phase Transition - the Discovery and Experimental Study Possibilities. Ninth International Symposium on Capture Gamma-Ray Spectroscopy and Related Topics, Abstract Booklet, Budapest, 996, Institute of Isotopes, p.204.
23. S.T.Boneva, V.A.Khitrov, Yu.P.Popov, A.M.Sukhovoj Phase Transition - the Discovery and Experimental Study Possibilities in the (n,γ)-Rreaction. Nuclear Physics: Chaotic Phenomena in Nuclear Physics, Crete, Greece, 28 September - 3 October 1996, Contributions, European Reseach Conferences, p.10.
24. S.T.Boneva, V.A.Khitrov, Yu.P.Popov., A.M.Sukhovoj Nuclear Phase Transition - Discovery and Experimental Study Possibilities in the (n,γ)-Reaction Proc. of IV International Seminar of Interaction of Neutron with Nuclei "Neutron Spectroscopy, Nuclear Structure, Related Topics, Dubna, April 27-29, 1996, E3-96-336, Dubna, 1996, 183-196.
25. S.B.Borzakov, E.Dermendjiev, A.A.Goverdovsky A.I.Kalinin, V.Yu.Konovalov, I.Ruskov, S.M.Soloviev, Yu.S.Zamyatnin. Study of Fission γ-Ray Yields from Low Energy Resonances of ^{237}Np and Searching for the (n,γ f)-Process. Yad.Fiz., 1996, 59 (7), p. 1175-1179 (in Russian).
26. S.B.Borzakov, E.Dermendjiev, A.A.Goverdovsky A.I.Kalinin, V.Yu.Konovalov, I.Ruskov, S.M.Soloviev, Yu.S.Zamyatnin. Study of Fission γ-ray Yields from Low Energy Resonances of ^{237}Np and Observation of the (n,γ f)-Process. In: Proceedings of the XIII Meeting on Physics of Nuclear Fission in the Memory of Prof. G.N. Smirenkin, Obninsk, 3-6 October, 1995, p. 41-51.

27. S.B.Borzakov, E.Dermendjiev, A.I.Kalinin, V.Yu.Konovalov, I.Ruskov, S.M.Soloviev, Yu.S.Zamyatnin. Study of Fission γ-Ray Yields from Low Energy Resonances of ^{237}Np and Observation of the $(n,\gamma f)$ - Process. Proceedings of the 3rd International Seminar on Interaction of Neutrons with Nuclei (ISINN-3): Nuclear Spectroscopy, Nuclear Structure, Related Topics p. 307-317.
28. S.B.Borzakov, E.Dermendjiev, V.Yu.Konovalov, Ts.Panteleev, I.Ruskov, Yu.S.Zamyatnin, A.Filipp, W.I.Furman. Delayed Neutron Yields from Thermal Neutron Fission of ^{235}U, ^{233}U, ^{239}Pu and ^{237}Np. In: Abstracts of IV International Seminar on Interaction of Neutrons with Nuclei: Neutron Spectroscopy, Nuclear Structure, Related Topics. JINR, E3-96-6336, Dubna, 1996, p. 66, 334.
29. S.B.Borzakov, E.Dermendjiev, V.Yu.Konovalov, Ts.Panteleev, I.Ruskov, Yu.S.Zamyatnin. Study of γ-Ray Yields from the Fission of ^{234}U Induced by Resonance Neutrons. In: Proceedings of the 3rd International Conference on Dynamical Aspects of Nuclear Fission (DANF'96), Chasta-Papernichka, Slovak Republic (to be published).
30. J.D.Bowman, E.I.Sharapov, L.Y.Lowie. Likelihood Analysis of Parity-Violating Asymmetries Measured for Compound Nuclear Resonances. Phys. Part. Nucl., 27, 398 (1996).
31. J.D.Bowman, L.Y.Lowie, G.E.Mitchell, E.I.Sharapov, Yi-Fen Yen. Analysis of Parity Violation in Neutron Resonances. Phys. Rev.C, 53, 285 (1996).
32. G.G.Bunatian, V.G.Nikolenko, A.B.Popov, G.S.Samosvat, T.Yu.Tretyakova. On the Neutron Charge Radius and the New Experiments Proposed for the Precise (n,e)-Scattering Length Measurement. JINR E3-96-79, Dubna, 1996. Yad.Fiz. v.60, N4, p.p. 1-4 (in Russian).
33. Chen Yingtang, Chen Zemin, Qi Huiquan, Li Mingtao, Tang Guo-you, Zhang Guohua, Fan Jihong, Yu.M.Gledenov, G.Khuuhenhuu. Angular Distribution and Cross Section Measurements of $^{64}Zn(n,\alpha)^{61}Ni$ for Neutron Energy 5 MeV. Chinese Journal of Nuclear Physics, v.17, No.2, 167-170, 1995.
34. Chen Yingtang, Qi Huiquan, Chen Zemin, Li Mingtao, Tang Guo-you, Qu Decheng, Yu.M.Gledenov, G.Khuuhenhuu. Gridded Ionization Chamber and Dual Parameter Measurement System for Fast Neutron-Induced Charged Particles Emission Reaction. Nuclear Electronics \& Detection Technology, v.15, No.2, 72-78, 1995 (in Chinese).
35. B.E.Crawford, N.R.Roberson, S.J.Seestrom, C.M.Frankle, J.D.Bowman, S.I.Penttila, A.Masaike, Y.Matsuda, T.Haseyama, E.I.Sharapov. Apparatus for Capture γ-Ray Studies of Parity Violation at Los Alamos. ISINN-4: JINR, E3-96-336, Dubna 1996, p.268.
36. T.L.Enik, L.V.Mitsyna, V.G.Nikolenko, A.B.Popov, G.S.Samosvat. Specifications for Deriving Neutron Electric Polarizability from the Total Cross Sections of ^{208}Pb. JINR Preprint, E3--96--102, Dubna, 1996; Yad.Fiz., 1997 (in press).
37. Fan Jihong, Cheng Jinxiang, Tang Guoyou, Shi Zhaomin, Zhang Guohui, Yu.M.Gledenov, G.Khuuhenhuu. Progress on Measurement of $^{58}Ni(n,\alpha)$ Reaction Cross Sections and Angular Distribution at 6.0 MeV and 7.0 MeV. Communication of Nuclear Data Progress, No.13, p.10-12, Beijing, 1995.
38. M.Florek et al: Natural Neutron Fluence Rate and the Equivalent Dose in Localities with Different Elevation and Latitude. Radiation Protection Dosimetry, Nuclear Technology Publishing, v.67, No.3, pp.187-192, 1996.
39. M.Florek, J.Masarik, I.Szarka, D.Nikodemova, A.Hrabovcova. Experimental and Calculated data for estimating the Back-ground from Natural Neutrons. Proceedings of IV.International Seminar on Interaction of Neutrons with Nuclei. JINR, Dubna, April 27-30, 1996.
40. M.Florek, J.Masarik, I.Szarka, D.Nikodemova, A.Hrabovcova. Natural Neutron Equivalent Dose in Middle Europe Region. Proceedings of 9 Inter. Congress on Radiation Protection (IRPA9), Vienna, April 14-19, 1996, v.2, p.271-273.
41. A.I.Frank, R.Geiler. Neutron Time Focusing. JINR Preprint, P3-96-34, Dubna, 1996 (in Russian).
42. A.I.Frank, V.G.Nosov. Dynamic Neutron Optics. International Symposiom on Advance in Neutron Optics. (Kumatory, Osaka, Japan 19-21 March 1996). To be published in Jorn.Phys.Soc.Jap., 65A,1996.
43. G.F.Gareeva, Al.Yu.Muzychka, Yu.N.Pokotilovski. Monte Carlo Simulation of Nonstationary Transport and Storage of UCN in Horizontal Neutron Guides and the Storage of UCN. NIM, A369 (1995) 180-185.
44. P.Geltenbort, Al.Yu.Muzychka, Yu.N.Pokotilovski. Search for Low-Energy Upscattering of Ultracold Neutrons from a Beryllium Surface with the Indium Foil Activation Method. JINR Comm., E3-96-349, Dubna, 1996.
45. G.P.Georgiev et al. Determination of Neutron Resonance Parameters via Gamma-Ray Multiplicity Spectrometry. Proc.Int. Conf. Capture Gamma-Ray Spectroscopy and Related Topics, 9-14 October, 1996, Budapest, Hungary.
46. G.P.Georgiev et al. Gamma-Ray Multiplicity and Neutron Resonance Parameter Measurements with the Dubna 4π Detector "Romashka". Proc. Int. Conf. Neutrons in Research and Industry, 9-15 June, Crete, Greece.
47. G.P.Georgiev et al. Neutron Resonance Parameters of ^{177}Hf. JINR Comm., E3-96-9, Dubna, 1996.

48. G.P.Georgiev, Yu.V.Grigoriev, N.A.Gundorin, N.B.Janeva, H.Stanczyk. Neutron Resonances in $^{113,115}In$ Investigations. III International Seminar on the Interaction of Neutrons with Nuclei. Dubna, 26-28 April 1995, JINR, p.170.
49. Yu.M.Gledenov, M.V.Sedysheva, Tang Guoyou, Chen Jinxiang, Shi Zaomin, Fan Jihong, Zhang Guohui, Chen Zemin, Chen Yiantan, G.Khuukhenkhuu. Angular Distribution and Cross Section of the $^{58}Ni(n,\alpha)^{55}Fe$ and $^{54}Fe(n,\alpha)^{51}Cr$ Reactions at 6 and 7 MeV. ISINN-4: Neutron Spectroscopy, Nuclear Structure, Related Topics 1996 (abstrtacts), JINR, E3-96-114, Dubna 1996, p.51.
50. Yu.M.Gledenov, V.I.Salatskii, P.V.Sedyshev, P.I.Salanski. Измерение сечения реакции $^{35}Cl(n,p)^{35}S$ для тепловых нейтронов. JINR Comm., P3-96-356, Dubna, 1996 (in Russian).
51. Yu.V.Grigoriev, A.A.Bogdzel, G.P.Georgiev, H.Faikow-Stanczyk, Hyon Seng Ho. An Instrument for Investigations of the γ-Quanta Energy Spectra of Radiative Neutron Capture and Nuclear Fission. Preprint PEI, 2558, Obninsk, 1996 (in Russian).
52. Yu.V.Grigoriev, G.P.Georgiev, H.Faikow-Stanczyk, Hyon Sung Ho. Investigations of γ-Multiplicity Spectra in the Capture of Neutrons by Iodine-127 and Lutecium-175 Nuclei.. Preprint PEI, *2553*, Obninsk, 1996 (in Russian).
53. Yu.V.Grigoriev, V.V.Sinitsa, H.Fajkow-Stanczyk, G.P.Georgiev, Hyon Sung Ho. The Measurement of the Gamma-Ray Multiplicity Spectra and the Alpha Value for Uranium-235 and Plutonium-239, IV International Seminar on the Interaction of Neutrons with Nuclei, Dubna, 27-30 April, 1996. JINR, E3-96-336, Dubna, 1996.
54. R.W.Hoff, H.G.Borner, K.Schrechenbach, G.G.Golvin, F.Hoyler, W.Schauer, T.von Egidy, R.Georgii, J.Ott, S.Schrunder, R.F.Casten, R.L.Gill, M.Balodis, P.Prokofjevs, L.Simonova, J.Kern, V.A.Khitrov, A.M.Sukhovoj, O.Bersillon, S.Joly, G.Graw, D.Hofer, B.Valnion, Nuclear Structure of ^{170}Tm from Neutron-Capture and *(d,p)*-Reaction Measurements. Phys. Rev. C, v.54, N1, p. 77-116.
55. J.Honzatko, I.Tomandle, V.A.Khitrov, A.M.Sukhovoj, Peculiarities of the ^{125}Te Compound-State Cascade Gamma-Decay. Ninth International Symposium on Capture Gamma-Ray Spectroscopy and Related Topics, Abstract Booklet, Budapest, 1996, Institute of Isotopes. p.184.
56. V.K.Ignatovich, M.Utsuro. Phys. Lett A, 7 Febr. 1997.
57. V.K.Ignatovich, D.Protopopescu, M.Utsuro. Phys. Rev. Lett., 1996, v. 77, No. 20, p. 4202.
58. V.K.Ignatovich. Uspekhi Fiz. Nauk., 1996, v. 166, No. 3, p. 303 (in Russian).
59. E.M.Iolin, E.A.Raitman, V.N.Gavrilov, B.V.Kuvaldin, L.L.Rusevich, Yu.A.Alexandrov, E.M.Galinskii, V.V.Ermakov, A.A.Loshkarev, M.Vrana, P.Mikula, P.Lukash, L.Sedlakova. The Influence of the High Frequency Ultrasound on the Parameters of Double-Crystal Spectrometers, I, Report to X-Ray Topography and High Resolution Diffraction, 2nd European Symposium, Berlin, Germany, 5-7 Sept. 1994, Abstracts, p.119.
60. E.M.Iolin, E.A.Raitman, V.N.Gavrilov, B.V.Kuvaldin, L.L.Rusevich, Yu.A.Alexandrov, E.M.Galinskii, V.V.Ermakov, A.A.Loshkarev, M.Vrana, P.Mikula, P.Lukash, L.Sedlakova. The Influence of the High Frequency Ultrasound on the Parameters of Double-Crystal Spectrometers, II, Report to XIII Symposium on the Neutrons in Solid-State Physics. Zelenogorsk, 20-25 June, 1995, Abstracts, p.112.
61. M.V.Kazarnovsky, O.A.Langer, G.K.Matushko, V.L.Matushko, V.G.Miroshnichenko, S.V.Novoselov, Yu.P.Popov, M.V.Sedysheva. A New Method for Generating in a Moderator the Maxwellian Neutron Spectra for Stellar Temperatures. Int. Symp. on Nucl. Astrophys. "Nuclei in the Cosmos", USA, 1996 (abstract).
62. V.V.Ketlerov, A.A.Goverdovski, O.T.Groudzevich, S.M.Grimes, R.C.Haight, P.E.Koehler, V.A.Khryachkov, V.F.Mitrofanov, Yu.B.Ostapenko, R.S.Smith, M.Florek. Detailed Study of the Double-Differential Cross-Sections for $^{17}O(n,\alpha)^{14}C$ Reaction. Proceedings of IV International Seminar on Interaction of Neutrons with Nuclei. JINR Dubna, April 27-30, 1996, E3-96-336, c.241.
63. V.A.Khitrov, A.M.Sukhovoj. Cascade Gamma-Decay of Compound-States: Hypotheses and Experiment. Proc. of III International Seminar of Interaction of Neutron with Nuclei "Neutron Spectroscopy, Nuclear Structure, Related Topics". Dubna, April 26-28, 1995, E3-95-307, Dubna, 1995, p.124-132.
64. V.A.Khitrov, A.M.Sukhovoj. Possible Structure of States Affectine the Gamma-Decay Process of Heavy Nuclei Below the Excitation Energy of 3-5 MeV. Nuclear Physics: Chaotic Phenomena in Nuclear Physics, Crete, Greece, 28 September - 3 October 1996, Contributions, European Reseach Conferences, p.32.
65. V.A.Khitrov, Yu.V.Kholnov, Yu.P.Popov, A.M.Sukhovoj, A.V.Voinov. The Excitation and Decay Peculiarities of the 1+ States in ^{200}Hg by Cascade Gamma-Transitions. Ninth International Symposium on Capture Gamma-Ray Spectroscopy and Related Topics, Abstract Booklet, Budapest, 1996, Institute of Isotopes, p.187.
66. V.Khryachkov, A.Goverdovski, V.Ketlerov, V.Mitrofanov, N.Semenova, M.Tarasko, A.Bogdzel, M.Florek. Large-Solid-Angle Bragg-Curve Spectrometer for Fission Fragments. Proceedings of 3 Intern. Conf. on Dynamical Aspects of Nuclear Fission. Casta-Papiernicka, Slovak Republic, 30.8.-4.9.,1996.

67. D.A.Korneev, V.Bodnarchuk, V.K.Ignatovich. Off Specular Neutron Reflection from Magnetic Media.JETP Lett., v. 63, 1996, p. 900 (in Russian).
68. S.V.Masalovich, A.I.Frank. Neutron Microscope with Phase Contrast. International Symposiom on Advance in Neutron Optics. (Kumatory, Osaka, Japan 19-21 March 1996). To be published in Jorn.Phys.Soc.Jap., 65A,1996.
69. U.Mayerhofer, T.von Egidy, J.Klora, H.Lindner, H.G.Boerner, S.Judge, B.Krusche, S.Robinson, K.Schreckenbach, A.M.Sukhovoj, V.A.Khitrov, S.T.Boneva, V.Paar, S.Brant and R.Pezer, The Nucleus ^{198}Au Investigated with Neutron Capture and Transfer Reactions: I. Experiments and Evaluation, Fizika (Zagreb) B5 (1996) p.167-198.
70. Al.Yu.Muzychka, Yu.N.Pokotilovski, Monte Carlo Simulation of Nonstationary Transport of Very Cold and Ultracold Neutrons in Vertical Neutron Guides and the Storage of UCN. Preprint JINR, E3-95-377, Dubna, 1995; NIM, A373 (1996) 81-85.
71. V.G.Nosov, A.I.Frank. Dispersion Law for Neutrons at Extremely Low Energy. III International Seminar on Interaction of Neutrons with Nuclei, ISSIN-3 (Dubna, April 26-28, 1995). JINR E3-95-307, Dubna, 1995.
72. Ts.Ts.Panteleev, V.Semkova, N.Kamburov, A.Trifonov, M.Mikhailov, V.Yu.Konovalov, A.D.Rogov. Measurements of the (*n, 2n*) Reaction Cross-section Using the Time Intervals Spectroscopy Technique. Proceedings of the IV International Seminar on Interaction of Neutrons with Nuclei, Dubna, April 27-30, E3-96-6336, Dubna, 1996, p.225.
73. Yu.P.Popov, P.V.Sedyshev, M.V.Sedysheva. New Method of Analysis of Intermediate Energy Neutron Spectra (1 keV- 100 keV). JINR Rapid Communications, **6[81]** Dubna, 1996.
74. E.I.Sharapov, H.M.Shimizu. Experimental Study of Time-Reversal Invariance in Neutron-Nucleus Interactions. Phys. Part. Nucl., 27, 1607 (1996).
75. V.R.Skoy, E.I.Sharapov, N.A.Gundorin, Yu.P.Popov, Yu.V.Prokofichev, N.R.Roberson, G.E.Mitchell. The Isotopic Identification of the Parity - Violating Neutron p-Wave Resonance at Energy E=3.2 eV in *Xe*. Phys. Rev. C 53 (1996) 2573.
76. V.R.Skoy, E.I.Sharapov, N.A.Gundorin, Yu.P.Popov, Yu.V.Prokofichev, N.Roberson, G.E.Mitchel. Isotopic Identification of the Parity-Violating Neutron p-Wave Resonance at Energy E_0=3.2 eV in *Xe*. Phys.Rev.C. **53** (1996) R2573-R2575.
77. V.R.Skoy. Analysis for an Experimental Study of Time-Reversal Violating Effects in Polarized Neutron Propagation Through a Polarized Target. Phys. Rev. D 53 (1996) 4070.
78. M.Stempinski, P.Salanski, A.Zak. Fast Ionization Chamber with a Grid Collector. JINR Comm., P3-96-352, Dubna, 1996 (in Russian).
79. A.A.Startsev, A.E.Shikanov, S.B.Borzakov. On the Question of Interpretation of Signals from Pulsed Neutron Logging. JINR Comm., 18-96-338, Dubna, 1996 (in Russian).
80. S.L.Stephenson, J.D.Bowman, S.J.Seestrom, H.Postma, E.I.Sharapov. Multiscattering Effects on (n,γ) Resonances. ISINN-4: JINR, E3-96-336, Dubna 1996, p.171.
81. A.V.Strelkov, G.N.Nekhaev, V.N.Shvetsov, A.P.Serebrov, A.G.Kharitonov, Tal'daev, M.N.Sazhin, V.E.Varlamov, V.V.Nesvizhevsky, P.Geltenbort, P.Pendlebury, K.Schreckenbach. Preliminary Results on Searching the Weak Upscattering of UCN's from the Cold Beryllium Surface. Intenational Seminar on Interaction of Neutron with Nuclei, ISINN-4 proceedings, E3-96-336, Dubna 1996, p.p.299-304.
82. J.J.Szymanski, W.M.Snow, J.D.Bowman, B.Cain, B.E.Crawford, P.P.Delheij, R.D.Hartman, T.Haseyama, C.D.Keith, J.N.Knudson, A.Komives, M.Leuschner, L.Y.Lowie, A.Masaike, Y.Matsuda, G.E.Mitchell, S.I.Penttila, H.Postma, D.Reich, N.R.Roberson, S.J.Seestrom, E.I.Sharapov, S.L.Stephenson, Y.F.Yen, V.W.Yuan. Observation of a Large Parity Nonconserving Analyzing Power in Xe. Phys. Rev.C, 53, R2576 (1996).
83. Tang Guo-you, Bai Xin-hua, Shi Zhao-min, Cheng Jin-xiang, Yu.M.Gledenov, G.Khuuhenhuu. Measurement of Angular Distribution and Cross Sections for $^{58}Ni(n,\alpha)$ Reaction at 5.1 MeV. Chinese Journal of Nuclear Physics, v.17, No.1, 45-48, 1995 (in Chinese).
84. Tang Guoyou, Qu Decheng, Zhong Wenguang, Cao Wentian, Bao Shanglian, Chen Zemin, Chen Yingtang, Qi Huiquan, Yu.M.Gledenov, G.Khuuhenhuu. Angular Distribution and Cross Section Measurements for the Reaction $^{40}Ca(n,\alpha)^{37}Ar$ Using Gridded Ionization Chamber. Nuclear Techniques, v.17, No.3, 129-135, 1994.
85. Tang Guoyou, Shi Zhaomin, Cheng Jinxiang, Yu.M.Gledenov, G.Khuuhenhuu. Measurement of Angular Distribution and Cross Sections for $^{58}Ni(n,\alpha)$ Reaction at 5.1 MeV. High Energy Physics and Nuclear Physics, v.10, No.3, 223-228, 1995 (in Chinese).
86. T.Yu.Tretyakova, D.E.Lanskoy, Structure of Λ-Hypernuclei with Neutron Halo. Few-Body Systems Suppl. 9, pp.272-276, 1995.

87. T.Yu.Tretyakova. Electromagnetic Structure of Neutron. Overview of Modern Dynamical Models. IV Intern. Seminar on Interaction of Neutron with Nuclei., Dubna, April 27-30, 1996, JINR E3-96-336, p.211, Dubna, 1996.
88. E.V.Vasilieva, A.V.Voinov, A.M.Sukhovoj, V.A.Khitrov, Yu.V.Kholnov. Investigations of the Peculiarities of the Cascade γ-Decay of the Compound State of ^{170}Tm Excited in Thermal Neutron Capture. Izv. RAN, ser. fiz., 1996, v.60, N11, p.36-51 (in Russian).
89. E.V.Vasilieva, A.V.Voinov, A.M.Sukhovoj, V.A.Khitrov, Yu.V.Kholnov. Gamma-Transition Cascades Following Thermal Neutron Capture in ^{199}Hg. Izv. RAN, ser. fiz., 1996, v.60, N11, p.52-57 (in Russian).
90. E.V.Vasilieva, A.V.Voinov, A.M.Sukhovoj, V.A.Khitrov, Yu.V.Kholnov Two-Quanta Cascades Following Thermal Neutron Capture in ^{113}Cd. Izv. RAN, ser.fiz. 1996, v.60, N11, p.58-67 (in Russian).
91. V.A.Vesna, Yu.M.Gledenov, I.S.Okunev, Yu.P.Popov, E.V.Shulgina. Search of Parity-Violation Effects in Reactions $^{6}Li(n,\alpha)^{3}H$ and $^{10}B(n,\alpha)$ with Polarized Thermal Neutrons. Sov. J. Nucl.Phys. **51** (1996) 23-32.
92. V.A.Vesna, Yu.M.Gledenov, I.S.Okunev, Yu.P.Popov, E.V.Shulgina. Searching of P-Odd Effects in the $^{6}Li(n,\alpha)^{3}H$ and $^{10}B(n,\alpha)^{7}Li$ Reactions with Polarized Thermal Neutrons. Yad.Fiz., 1996, v.59, p.23-32 (in Russian).
93. V.A.Vesna, YU.M.Gledenov, P.V.Lebedev, I.S.Okunev, A.V.Sinyakov, Yu.M.Tchuvilskii, E.V.Shulgina. Investigations of P-Parity Violation for the γ-Quanta E_γ=0.478 MeV in the Output Channel of the $^{10}B(n,\alpha)^{7}Li^{*} \rightarrow\gamma(M1)\rightarrow {}^{7}Li$ Reaction. Preprint PNPI, NP-19-1996, 2111, Gatchina, 1996 (in Russian).
94. A.V.Voinov. Test of the E1 Gamma-Ray Strength Function and Level Density Models by the $^{155}Gd(n,2\gamma)^{156}Gd$ Reaction. Ninth International Symposium on Capture Gamma-Ray Spectroscopy and Related Topics, Abstract Booklet, Budapest, 1996, Institute of Isotopes, p.40.
95. A.V.Voinov. Test of the E1 Radiative Strength Function and Level Density Models by $^{155}Gd(n,2\gamma)^{156}Gd$ Reaction Proc. of IV International Seminar of Interaction of Neutron with Nuclei: "Neutron Spectroscopy, Nuclear Structure, Related Topics". Dubna, April 27-29, 1996, E3-96-336, Dubna, 1996, p.197.

Theory

1. S.G.Kadmensky, V.V.Lyuboshitz, A.A.Shaikina. The Generalized Hartree-Fock Potential for Finite Nuclei Based on Realistic Nucleon-Nucleon Forces. Yad.Fiz., 1995, v.58, p.982 (in Russian).
2. S.G.Kadmensky, V.V.Lyuboshitz, A.A.Shaikina. The Spin-Orbital Optical Potential of Nucleons as a Hartree-Fock Potential. Yad.Fiz., 1995, v.58, p.1222 (in Russian).
3. S.G.Kadmensky, V.V.Lyuboshitz, A.A.Shaikina. The Structure of the Real Part of the Optical Potential of Nucleons. Yad.Fiz., 1995 v.58, p.1606 (in Russian).
4. S.G.Kadmensky, V.V.Lyuboshitz. The Gradient Term and Surface Absorption in the Nuclear Optical Model. "Nuclear Spectroscopy and Nuclear Structure". Book of Abstracts of the 45th International Meeting. St.-Petersburg, "Nauka", 1995. p.148 (in Russian).
5. S.G.Kadmensky, V.V.Lyuboshitz. The Relation between Shell and Optical Models of the Nucleus and the Role of Gradient Terms. Yad.Fiz., 1996 v.59 p.239 (in Russian).
6. S.G.Kadmensky, V.V.Lyuboshitz. The Relation between the Optical and Shell Potential and the New One Quasiparticle Basis.. "Nuclear Spectroscopy and Nuclear Structure". Book of Abstracts of the 45th International Meeting. St.-Petersburg, "Nauka", 1995. p.147 (in Russian).

NEUTRON SOURCES

1. V.I.Lushikov, A.V.Vinogradov. "Applied Research at the IBR-2 Fast Pulsed Reactor". International Seminar on Enhancement of Utilization of Research & Test Reactors, Bombay, India, 11-15 March, 1996.
2. A.K.Popov. "Analysis of the Stability of IBR-2 Operation for the Nine-Parameter Feedback Model". JINR Comm., P13-96-297, Dubna, 1996 (in Russian).
3. R.Narain, V.L.Lomidze. "An Analytical Evaluation of Super-Prompt Transients with a Triangular Reactivity Pulse". Congresso Geral de Energia Nuclear CGEN-VI, Rio de Janeiro, 27.10.-01.11.1996.

M.V.Frontasyeva, V.P.Chinaeva, A.A.Volokh, E.Steinnes, K.A.Rahn. Study of Trace Elements in Annual Segments of Moss Biomonitors by Using Epithermal Neutron Activation Analysis. Link with Atmospheric Aerosol. French-Russian Seminar on the Use of Neutrons and Synchrotron Radiation (June 24-July 2, 1996, Baikal, Russia). Book of Abstracts.

2. M.V.Frontasyeva. Neutron Activation Analysis for Investigations of Antropogenic Pollution with Heavy Metals in the Oka Basin. Proceedings of the First Regional School-Seminar "Monitoring of Aqua-Objects" (5-10 August 1996, Dubna, Russia). Moscow, Roskomvod, 1996, p. 356-368 (in Russian).
3. M.V.Frontasyeva, F.I.Tiutiunova, E.M.Grachevskaia, A.T.Savichev, S.F.Gundorina, T.M.Ostrovnaia, V.P.Chinaeva. Monitoring of the Heavy Metal Pollution of Aqual Landscapes in the Oka Basin. International Congress "Water: Ecology and Technology" (17-21 September 1996, Moscow). Book of Abstracts (in Russian).
4. M.V.Frontasyeva, E.Steinnes. Epithermal NAA for Studying the Environment. International Symposium on Harmonization of Health Related Environmental Measurements Using Nuclear and Isotopic Techniques (4-7 November, 1996, Hyderabad, India). Book of Synopsis, p. 176.
5. M.V.Frontasyeva and E.Steinnes. A Comparison of INAA and ICP-MS for the Determination of Trace Elements in Peat. Workshop on Peat Bog Archived of Atmospheric Metal Deposition (October 1-3, 1996, Berne, Switzerland). Book of Abstracts.
6. O.M.Gorshkova, M.V.Frontasyeva. Distribution of *Fe, Mn, Co* and *Ni* with Organic Colloids in Sea and Pore Water from Pacific Ocean *Fe-Mn* Nodule Fields. VIII Pacific Science Inter-Congress (Suva, Fiji Island, July 13-19, 1997).
7. K.P.Koutzenogii, E.N.Valendik, N.S.Bufetov, G.A.Ivanova, V.F.Peresedov. The Nuclear Physics Methods for the Study of the Aerosol Production in Forest Fires in Siberia. IV Russian-French Seminar on the Applications of Neutrons and Synchrotron Radiation for Condensed Matter Investigation. Novosibirsk-Irkutsk, Russia, June 25-July 3, 1996. JINR, E14-96-191, Dubna 1996.
8. K.P.Koutzenogii, S.P.Efremov, T.T.Efremova, V.F.Peresedov. The Neutron Activation Analysis for the Study of the Multielemental Composition and the Stratigraphy of the Siberian Peat Deposit. Ibid.
9. K.P.Kutzenogii, G.A.Ivanova, V.F.Peresedov. Multielement Composition of Forests Inflammable Materials. Regional Use of Natural Resources and Ecological Monitoring. The Institute of Aqua- and Ecological Problems, Siberian Branch RAS, Barnaul 1996, p.248-251 (in Russian).
10. V.F.Peresedov, A.D.Rogov. Simulation and Analysis of Neutron Energy Spectra from Irradiation Channels of the IBR-2 Reactor. JINR Rapid Communications, No.1[75]-96, Dubna 1996; Journ. of Radioanal. and Nucl. Chem. 1996 (in print).

V.F.Peresedov et al. Analysis of Soil and Pine-Needle Data From Northern Terrestrial Ecosystems. Journ. of Radioanal. and Nucl. Chem., Vol.207, No.2, 1996, p.295-302; JINR Rapid Communications, No.5[79]-96, Dubna, 1996.

12. V.F.Peresedov, V.P.Chinaeva, S.F.Gundorina, T.M.Ostrovnaia. Activation Analysis for Monitoring of Northern Ecosystems. Proceedings of the First Regional School-Seminar "Monitoring of Aqua-Objects" (5-10 August 1996, Dubna, Russia). Moscow, Roskomvod, 1996.
13. V.A.Sarin, M.V.Frontasyeva, V.F.Peresedov, I.V.Alekseev. Recent Developments of Radioanalytical Methods and Their Applications to Interscience Studies at the IBR-2 Pulsed Fast Research Reactor. International Seminar of Developments on Enhancement of Research Reactor Utilization. Trombay/Bombay, India, 11-15 March 1996. Part II: Extended Synopses.
14. V.A.Sarin, V.L.Aksenov, T.E.Galinskaya, I.V.Lutsenko, V.F.Peresedov, M.V.Frontasyeva. NAA and Irradiation Research of Topazes. Third European Meeting Spectroscopic Methods in Mineralogy. Program and Abstracts, 10-13 September 1996, Kiev, Ukraine, p.35.
15. V.A.Sarin, V.L.Aksenov, T.E.Galinskaya, V.F.Peresedov, M.V.Frontasyeva. NAA and Radiation Research of Some Minerals. Third European Meeting Spectroscopic Methods in Mineralogy. Program and Abstracts, 10-13 September 1996, Kiev, Ukraine, p.35.
16. V.A.Sarin, E.E.Rider, D.Hohlwein, W.Depmeier, H.Bessert, F.Frey, K.Hradil, A.M.Balagurov, A.I.Beskrovny, T.E.Galinskaya, V.L.Levashvili. Neutron and *X*-ray Bragg and Diffuse Scattering Investigation of Defect Structure of ZrO_2-Y_2O_3 (Y_2O_3 - 3, 12, 30 mol%) Single Crystals. ECNS'96, 8-11 October 1996, Interlaken, Switzerland, F63.

M.V.Avdeev, A.A.Bogdzel, F.V.Levchanovsky. Multi-Ring Position-Sensitive Detector for Registering Small-Angle Neutron Scattering. Report at the 4th International Conference on Position-Sensitive Detectors, University of Manchester, September 9-13, 1996, (to be published in Nucl. Instr. Meth.).

2. M.V.Avdeev, A.M.Balagurov, A.I.Beskrovnyi, A.A.Bogdzel, S.A.Kutuzov, F.V.Levchanovsky, V.G.Tishin. Two-Dimensional Detector with a Delay Line Readout for the DN-2 Neutron Diffractometer at the IBR-2 Pulsed Reactor. Report at the 4th International Conference on Position-Sensitive Detectors, the University of Manchester, September 9-13, 1996.
3. V.A.Ermakov. Module Computer-Based Systems for Experiment Automation for Time-of-Flight Measurements. Author's abstract of dissertation, JINR, 13-96-474, Dubna, 1996 (in Russian).
4. M.L.Korobchenko, F.V.Levchanovsky, V.I.Prikhodko, V.E.Rezaev. Architecture of Unified VME-Based Data Registration and Accumulation Equipment for the Spectrometers at the IBR-2 Reactor. International Workshop LPSS, Berlin, June 24-27, 1996.
5. E.I.Litvinenko. Interactive Data Analysis for Neutron Spectrometers Data Based on Visual Numerics' PV-WAVE Software Package". Proceedings of the International Workshop AIHENP'96, Lausanne, September 2-6, 1996 (to be published in Nucl. Instr. Meth.).
6. E.I.Litvinenko. Hypertext Infosystem for Pulsed Neutron Sources and Scientific Investigations Based on these Sources. Proceedings of the International Workshop on Advances in Databases and Information Systems (ADBIS'96). Moscow, September 10-13, 1996, v.2: Extended Abstracts (pp. 42-46). Moscow: MEPhI, 1996.

4. PRIZES

JINR Prizes:

For Methodical and Engineering Research:

Second Prize:

V.L.Aksenov, A.M.Balagurov, V.G.Simkin, V.A.Trounov, P.Hiismaki. "Neutron High Resolution Fourier Diffractometer at the IBR-2 Pulsed Reactor"

FLNP Prizes:

In Nuclear Physics:

First Prize:

W.I.Furman, A.A.Bogdzel, P.Geltenbort, N.N.Gonin, M.A.Guseinov, J.Kliman, Yu.N.Kopach, L.K.Kozlovsky, L.V.Mikhailov, A.B.Popov, G.Postma, N.S.Rabotnov, D.I.Tambovtsev. "Investigations of the Energy Dependence of the Angular Anisotropy of Fission Fragments from the Fission of ^{235}U Induced by Resonance Neutrons"

Second Prize:

A.I.Frank, V.G.Nosov, D.B.Amanzholova. "Quantum Nonstationary Phenomena Arising as a Result of Periodic Action on the Neutron Wave"

V.R.Skoy, E.I.Sharapov, N.A.Gundorin, Yu.P.Popov, Yu.V.Prokofichev, G.Mitchell, N.Roberson. "Isotope Identification of a Parity Violating 3.2 eV Resonance in Xenon"

In Condensed Matter Physics:

First Prize:

V.I.Bodnarchuk, L.S.Davtyan, D.A.Korneev. "Geometrical Phase Effects in Neutron Optics

D.A.Korneev, V.I.Bodnarchuk, L.S.Davtyan. "Observation of Nonadiabatic Geometrical Effects in a Time-of-Flight Experiment with Polarized Neutrons"

L.S.Davtyan. "Geometry of Adiabatic Changes (General Analysis)"

Second Prize:

V.L.Aksenov, A.M.Balagurov, V.V.Sikolenko, V.G.Simkin et al. "Precision Neutron Diffraction Study of the High-T_c Superconductor $HgBa_2Cu_{4+d}$"

D.A.Korneev, V.I.Bodnarchuk, V.K.Ignatovich. "Off-Specular Neutron Reflection from Magnetic Media with Nondiagonal Reflectivity Matrices"

Third Prize:

A.M.Balagurov, V.Yu.Pomjakushin, V.G.Simkin, A.A.Zakharov. "Neutron Diffraction Study of Phase Separation in La_2CuO_{4+d} Single Crystals"

In Applied Physics:

First Prize:

Yu.M.Gledenov, G.Khuukhenkhuu, M.V.Sedysheva et al. "Investigation of the Fast Neutron Induced (n,α) Reaction (Experimental Techniques)"

Second Prize:

V.B.Zlokazov. "AUTOX-A Program for Autoindexing Reflections from Multiphase Polycrystals"

Third Prize:

A.D.Bozhko, A.P.Kobzev, D.A.Korneev, L.P.Chernenko, D.M.Shirokov. "Complete Profile Analysis of Diamond-Like Films"

The JINR young scientists contest in condensed matter and nuclear physics with neutrons:

First Prize:

V.V.Sikolenko. "Neutron Diffraction Studies of the Magnetic Structure of a UPd_2Ge_2 Compound"

Second Prize:

Yu.N.Kopach. "Experimental Studies of the Energy Dependence of the Angular Anisotropy of Fission Fragments from the Resonance Neutron induces Fission of ^{235}U"

V.G.Cherezov. "Proof of the Entropy Contribution to the Intermembrane Interaction"

Encouraging Prize:

N.Kardzhilov. " Study of Stresses in a Al-Bi-Al Sandwich"

5. NEUTRON SOURCES

5.1. THE IBR-2 PULSED REACTOR

In 1996, the reactor operated for 2450 hours in 10 cycles for physical experiments. Detailed information on the operation of the reactor is presented in Tables 1 and 2.

Table

State of the reactor (as of December 1, 1996)

№	Parameter (from the start of reactor operations)	Value
1	Total operation time for physical experiments, hrs.	31136
2	Total energy generated, MW/hrs.	59081
3	PO-2R total operation time, hrs. (inclusive of operating time during tests)	5234
4	Maximum fluence on the reactor jacket in the center of the active core: (10^{22} n/cm^2) for $E_n > 0.8$ MeV for $E_n > 0.1$ MeV	 1.11 2.58
5	Maximum fuel burning, (%)	4.77
6	Total number of emergency shutdowns	367

Table 2

IBR-2 reactor operation characteristics for 1996 (9 cycles)

Cycle №	Start and completion dates of cycles	Operation time for physical experiments, $T_{ph.e.}$	MR operation time, T_{MR}	Number of emergency shutdowns, N_{ES}	Causes of emergency shutdowns (malfunction classification according to RD-04-10-94)					Number of operating beams
					Voltage drops (MR8)	Equipment break-downs (MR7)	Electronic equipment break-downs (MR7)	Personnel errors (MR5)	Scheduled emergency shutdowns	
1	15.01—27.01	241	275							12
2	12.02—23.02	219	2	1		1			1	12
3	11.03—22.03	238	27	4	1		2	1		12
4	01.04—20.04	409	441	3	2		1			12
5	14.05—25.05	250	287	4	1		3			12
6	03.06—17.06	301	333	3	2		1			12
7	14.10—25.10	231	266	4	1		2	1		12
8	11.11—23.11	244	290	2	1				1	12
9	02.12—15.12	273	311	3			1	1	1	12
Total:		**2406**	**2750**	**24**	**8**	**0**	**10**	**3**	**3**	**12**

The fuel-element assemblies (FEA) were successfully reloaded to achieve equal fuel burning in the succeeding years of reactor operation. Seven central FEAs with maximum burning, were moved to the periphery of the active zone and two FEAs were taken out of the reactor for investigations in a specialized laboratory. The current state of the active zone after reloading the FEAs is illustrated in Fig.1.

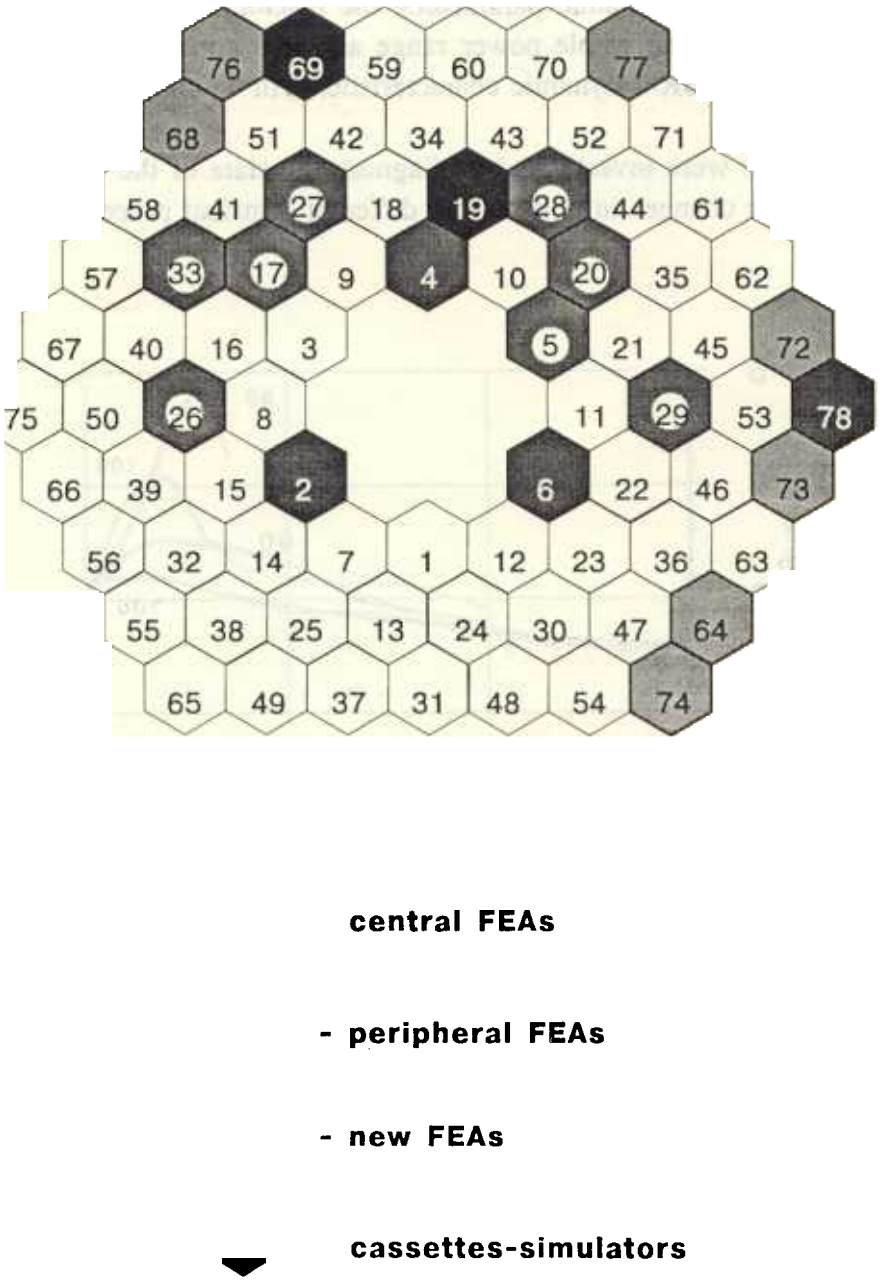

Fig.1. Cartogram of loading the cassettes into the cells in 1996

The dynamic characteristics of the IBR-2 reactor were studied in connection with the instability of the reactor operation which was noticed at the end of 1995 in the power range

1.6 – 1.8 MW and at a coolant flow rate of 90 m^3/h. At the power rating of 2 MW, the operation of the reactor was stable. By increasing the flow of sodium to 100 m^3/h, the instability was removed. The change in the dynamic characteristics is caused by variation of the "fast" component of the power coefficient of reactivity, which is either a result of the change in thermal conditions causing the FEAs to bend (reloaded in 1993) or is due to fuel burn-out.

The reactor dynamics were studied following the reloading in 1996. The preliminary results have shown that in its dynamic parameters, the reactor corresponds to its early stage of operation and is steady over the whole power range and at a coolant flow rate from 80 to 100 m^3/h. Measurements of the IBR-2 dynamic characteristics will be continued in 1997.

The reactor noises were investigated to diagnose the state of the operating reactor and to study the character of the changes in noises from different transient processes (see Figs.2 and 3).

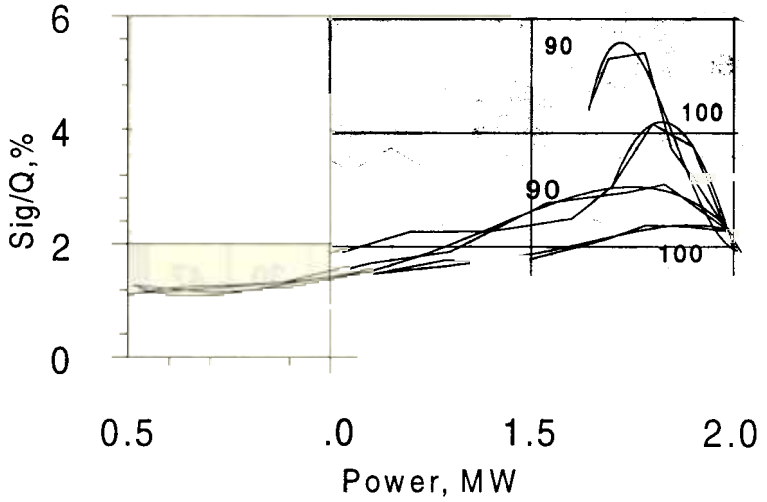

Fig.2. Change in the root-mean-square deviations of the energy of power pulses in the low-frequency region of the spectrum (0.01 – 0.4 Hz) upon increasing the power up to 2 MW and decreasing from 2 MW at the sodium flow rate in Contour I of 90 and 100 m^3/h. These measurements were conducted in 1996 at a pulse repetition frequency of 5 s^{-1}. Figures indicate the flow rate of sodium. The oscillations increased with the increase in power over 1 MW at a frequency of 0.103 Hz (9.7 sec period). The two upper curves were measured with decreasing power.

In 1996, the airtightness of the TVELs (fuel elements) was monitored by the gamma-activity of gaseous fission products (mainly Xenon-135) in the argon cavity of the expansion tank of Contour I. The activity was measured at the end of each reactor cycle at a power of 2 MW with a Na(I) scintillation detector. The observed activity of Xenon-135, amounting to an average of 6000 Bq/l, is caused by surface contamination of the TVELs by plutonium and it remained constant over the whole period of observations. The results of the measurements in the reported year are given in Table 3.

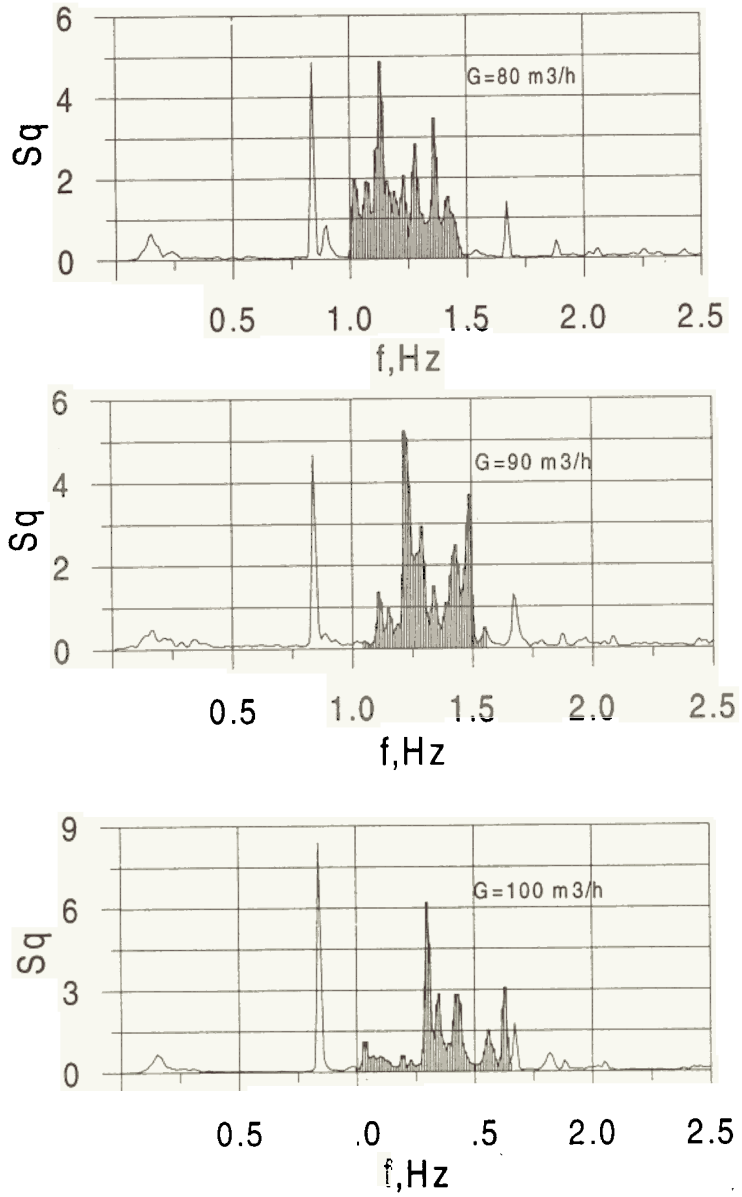

Fig.3. Spectral density of oscillations in the pulse energy at a mean power of 2 MW for different values of the sodium flow rate in Contour I (80, 90, 100 m^3/h). The shaded region indicates the spectrum area which is not correlated with the vibrations of the movable reflector. One can clearly see the shift of the peaks toward higher frequencies as the sodium flow increases.

Table 3

Cycle №	Date	Activity of Xe-135 (Bq/l)
8	29.12.95	8300
1	26.01.96	4500
2	23.02.96	6000
3	22.03.96	4800
4	19.04.96	6600
5	26.05.96	5500
6	17.06.96	6200
7	25.10.96	4900
8	22.11.96	7800

The low and steady level of activity (less than 10 kBq/l) points to the fact that the TVEL cases are hermetically sealed.

The control of admixtures in the sodium coolant gives additional information on the airtightness of the TVELs (by the occurrence of nonvolatile fission fragments) and on the processes of corrosion in the sodium Contour (by the emergence of admixtures of iron, nickel, chromium, etc.).

The main long-lived activity of the sodium samples from Contour I (after the decay of sodium-24) is due to sodium-22, which has remained constant at a level of 3–6 kBq/g since 1989.

The results of the measurement of possible activity in the sodium samples from Contour I, taken before the summer shutdown on July 17, 1996, are presented in Table 4.

Table 4

№	Radioactive Nuclide	Activity Bq/g
1.	Sodium-22	$2.7 \cdot 10^3$
2.	Cesium-137	<1
3.	Manganese-54	<1
4.	Cobalt-58	<1
5.	Cobalt-60	<1
6.	Zinc-65	3.0

As can be seen from the Table, the control admixtures of sodium practically have not been detected at the sensitivity level of the control techniques used. As of the beginning of 1997, the sodium in Contour I is free of fission products and corrosion admixtures.

In 1996, work to construct a cryogenic moderator (CM) for the IBR-2 reactor continued in accordance with the work schedule. Unfortunately, because of the financial difficulties, the plant-manufacturer was shut down in November 1996. As of December 30, 1996, the cryogenic moderator is 50% complete.

In the framework of the IBR-2 modernization project, the "Agreement on Realization of the Plan for Upgrading the IBR-2 Reactor in 1996-2005" has been drawn up and approved by the main contractors NIKIET, GSPI, and VNIINM as to the dates and amount of work to be done. Tables 5 and 6 present schedule of the work for the IBR-2 modernization.

In 1996, in accordance with the Agreement, the following documents were drawn up:

1. technical proposal for IBR-2 modernization, where the basic technical solutions are specified;
2. design specification for the modernization of the PO-3 movable reflector of IBR-2;
3. design specification for the TVELs.

Contracts for drawing up the technical projects for the modernization of IBR-2 and the production of TVELs, as well as for working drawings for the PO-3, were concluded.

Unfortunately, deficit financing and delays in funding the IBR-2 modernization project (about 25% of the plan) resulted in the suspension of work in all areas of the modernization project.

Table 5

Schedule of work for the IBR-2 reactor modernization (stage I)

№	Type of work	1995	1996	1997	1998	1999	2000	2001
1.	IBR-2 operation for physical experiments							
2.	Active zone (new loading):							
	– design							
	– manufacture							
	– assembly							
	– tests							
3.	PO-3 movable reflector:							
	– design							
	– manufacture							
	– tests							
4.	Main equipment (reactor jacket, CES, stationary reflectors, etc.):							
	– design							
	– manufacture							
5.	Cryogenic moderator:							
	– manufacture							
	– tests							
6.	GPP-2 reserve control desk:							
	– assembly							

Table 6

Schedule of work for the IBR-2 reactor modernization (stage II)

№	Type of work	2002	2003	2004	2005
1.	Unloading the active zone				
2.	Dismantling used equipment				
2.1.	Reactor jacket				
2.2.	PO-2R				
2.3.	Control and emergency systems (CES)				
3.	Assembly of the new equipment:				
3.1.	Reactor jacket				
3.2.	PO-3				
3.3.	CES				
4.	Physical startup				
5.	Power startup				
6.	Operation for physical experiments				

5.2. THE IREN PROJECT

The project status. Following the recommendations of the JINR Plenipotentiary Committee (March 1993) the JINR Directorate adopted the decision, approved at the 76th Session of the JINR Scientific Council June 1994), to construct the new modern source of resonance neutrons for investigations in fundamental nuclear physics. The completion date (physical startup date) is the end of 1997 - the beginning of 1998. The IBR-30 analogous scheme, i.e., the combination of a powerful linear electron accelerator and a subcritical multiplying target, was chosen for the new neutron source. The new IREN facility will permit the neutron energy resolution to be increased by an order of magnitude at a double increase in luminosity.

In 1996, because of deficit financing, a considerable delay in fulfilment of the IREN project has to be noted. Nevertheless,

- manufacture of TVELs was started at the MAJAK Industrial Enterprise – the cores have been made and worked with a high degree of precision from metallic plutonium, the VNIINM produced 25% of inserts from tungsten diboride;

  project of the IBR-30 disassembly has been completed for the most part;

  design specification for the LUE-200 equipment complex has been drawn up and agreed to with GSPI;

- progress has been achieved in creating a full-scale stand of the LUE-200 accelerator, – the M-350 modulator created on the basis of the OLIVIN station has been assembled, the first signals from the modulator to a load simulator were obtained (July 1996); further work was suspended because of the shortage of funds on electric energy;

- at the LUE-40 accelerator the elements of the beam diagnostics and thermostatic control systems for the LUE-200 accelerator were tested;

- general scheme of the LUE-200 vacuum system and a full-scale stand has been developed in collaboration with VAKUUM (Prague, Czech Republic); the manufacture of the vacuum equipment for the electron gun and the LUE-200 stand, which is to be shipped to FLNP in February 1997 on account of the Czech dues to JINR, has been agreed to and started;

- in the FLNP Design Bureau the drawings of a draft arrangement of LUE-200 including the first section with a buncher, an intermediate segment and the second section have been elaborated;

  the 6th Session of the Program Advisory Committee on Nuclear Physics recommended to prolong theme 06-4-0993-94/96 till 1999 and to adjust the work schedule of the IREN project to the completion date at the end of 1999.

6. MEASUREMENT AND COMPUTATION COMPLEX

Research within the theme was carried out in full accordance with the project "Development of the FLNP Information and Computation Complex".

In 1996, the main efforts of the department's specialists and financial resources were directed toward developing the FLNP local computing network (LCN). The network equipment and software necessary to switch over to data-transfer rates of up to 100 Mbit/s in the main LCN segments, and primarily in the segment of the IBR-2 experimental setups, were purchased. A number of X-terminals were bought, in addition to those already available. This will make it possible to significantly increase the efficiency of the servers and workstations of the SUN-cluster.

Main work to design, construct, and put into operation the VME measuring systems at the NERA-PR, HRFD, and NSVR spectrometers has been performed. At the majority of the spectrometers, standard equipment for regulating the temperature of the samples under study was put into service. Development of the detector and unified electronics of the data acquisition and accumulation systems in VME standard for the position-sensitive detectors (PSD) at the YuMO and DN-2 spectrometers has been completed. At present, the equipment is being constructed and adjusted. Financial difficulties, however, have seriously reduced the pace of executing work. Since September 1996, there have been no funds to manufacture multilayer printed circuit boards, to pay the concluded contracts, and for current expenses. This has automatically resulted in corresponding delays in the introduction of new developments.

Nevertheless, in 1996, we ensured the steady running of the experiment automation systems at IBR-2 and IBR-30, and made significant progress in all directions in the creation of new measuring and control systems for the spectrometers and in the development of the information and computation infrastructure of the Laboratory.

Detector electronics. In 1996, a large amount of work to create electronic blocks for PSDs, helium neutron counters, and semiconductor detectors was performed:

- A stand for studying gas PSDs with high-resistance wires was designed and constructed on the basis of a personal computer. It consists of two spectrometric tracks, two ADCs, and a KK-009 CAMAC crate-controller. The software that makes it possible to accumulate amplitude spectra from each ADC and spectra of the sum of two signals (also in the chosen window), as well as to calculate the position codes and accumulate position spectra with several values for the maximum number of channels, was developed for the stand. Work for studying the characteristics of the annular PSD at the YuMO spectrometer was carried out with this stand, and the starting data to design electronics were obtained. At present, the design of the charge-sensitive preamplifier and spectrometric amplifier has been completed and, at the moment, sixteen blocks of this kind are being constructed for eight wires of the detector. A mechanical construction for mounting the preamplifiers onto the case of the annular PSD was designed. But because of still unclarified problems with the detector, we failed to obtain satisfactory amplitude spectra and the required angular resolution for all wires of the detector. For lack of financing, the contract for the manufacture of a set of eight two-channel ADCs has not been fulfilled.
- The prototype of the two-channel time-to-digital converter (TDC) using hybrid microcircuits ("charge-to-time converter") was constructed for the two-dimensional PSD of the DN-2 spectrometer, which is based on a multi-wire proportional chamber with a cathode

delay line readout. The TDC digitizes the time intervals between the formed anode signal and the cathode signal from the end of the delay line and, in this way, determines neutron coordinates. This TDC is constructed in the form of a double two-channel device with ranges of: 500 ns with a scale for 512 channels to determine the x coordinate of the neutron and 250 ns with a scale for 256 channels to determine the y coordinate. In 1996, using this equipment, physical measurements with the two-dimensional chamber were conducted on beam 6 of the IBR-2 reactor. The following results were obtained:

- integral nonlinearity of both TDCs < 0.2%;
- intrinsic resolution over the whole range is 1 channel, i.e., 0.5 mm over the volume of the chamber;
- conversion time for the x coordinate ≈ 5 μs, and for the y coordinate ≈ 2.5 μs.

At present, the standard block of the TDC-2 with the indicated parameters has been constructed and tested. The TDC-2 block has two data outputs: one to the connector on the front panel, and one in parallel to the CAMAC bus.

♦ The engineering specifications were prepared for the manufacture of the one-channel TDC-1 for four ranges of measurement: 50 ns, 100 ns, 512 ns and 1000 ns, for time measurements with the spectrometers of the Scientific Department of Nuclear Physics.

For the X-ray PSD, the analog processor block from the industrial device RKD-1 was adapted to CAMAC construction and adjusted. The AK-1024 ADC was also constructed and adjusted. The interface to connect it to the VME crate is presently being designed.

♦ The detector equipment of the NERA-PR spectrometer, which includes 50 channels of electronics for picking up signals from the helium neutron counters, and the NIM-TTL converter blocks with a light diode display, have been put into operation. Each channel contains a charge-sensitive preamplifier, an amplifier with active signal shaping, a comparator, and a NIM driver.

♦ Thirty similar detectors equipped with electronics have been adjusted for the SKAT setup.

♦ The prototype of the 8-channel preamplifier for the 128-component detector system of the DN-12 spectrometer has been designed, constructed, and tested. The characteristics of the detector were measured with a neutron source. Using the results of the measurement, the detector electronics for DN-12 were constructed and tested on the stand with a neutron source.

♦ Work to modernize the detector electronics of the ROMASHKA setup has been performed.

♦ Ten preamplifiers for the *Si*-detectors of the setup with polarized nuclei have been designed and are being constructed.

♦ Work to adjust the electronics of the anti-Compton spectrometer is in progress. The electronics for the 16-channel neutron detector of the UGRA setup are being designed and constructed.

♦ The prototypes of new ADCs (two types) with 1024 and 4096 channels have been constructed. The main characteristics have been measured and the engineering specifications for production samples are being drawn up.

Data acquisition and accumulation systems. The architecture of the unified systems in VME standard for acquiring and accumulating data from the IBR-2 spectrometers has been developed. These systems are based on a limited but functionally complete set of identical (from

the viewpoint of hardware) blocks used for registering and accumulating data, which realize distinctions in parameters and in the correction and preliminary data processing procedures, that are specific to each spectrometer. This is accomplished by means of microprograms, electronic tables, etc.

For any spectrometer, the data acquisition and accumulation system has four basic blocks.

Interface block: intended to receive data from PSDs, add the neutron time-of-flight code to the position code, synchronize read/write processes, and provide intermediate data storage in the FIFO memory and further data transfer to the processor block, etc.

Block for encoding the point detector number: writes the detector number by parallel position codes into the intermediate FIFO memory, followed by determination of the binary code of the detector using the priority encoder.

Processor block: calculates position codes (using ADC codes from both ends of the high-resistance wires of the annular detectors), corrects for the geometric location of the detectors, forms addresses for the histogram memory, executes control over VETO signals, and counts the number of pulses from monitor detectors, etc. This block is based on the high performance TMS320C40 signal processor with a large address space (32 bits), floating-point arithmetic (execution time is 40 ns), six communication ports with a data-transfer rate of 20 Mbytes/s, two internal buffers with dual-port access, two independent buses to connect the external memory, and so on. The processor block includes two buffers with a capacity of 1 Mbyte which store all of the data from the spectrometer detectors from one cycle of the reactor. Thus, for example, the data in the current reactor cycle are written to buffer 1, while the data from the previous cycle are copied from buffer 2 to the DSP internal memory for computations and for transferring the processed data to the histogram memory. In this case, the processor is not involved in data input/output; these operations are executed via communication ports and built-in DMA co-processors. In the processor block, the function of encoding the neutron time-of-flight (the number of channels to 64 K and the number of time scales to 4; the channel width is entered in table form and can be chosen for any scale from 50 ns to 128 μs, graduated in 50 ns) is realized.

Histogram memory: has a two-port configuration to provide access for both the processor block and the VME bus. The storage capacity can be increased from 2 Mbytes (which is sufficient for the majority of spectrometers) to 64 Mbytes (this volume is necessary for DN-2) by building in additional memory chips or by using several blocks. Both the address space and memory depth (up to 32 bits) can be enhanced. The memory has an embedded program-adjustable table for page addressing. The memory access time is not more than 500 ns, the modes of operation are: +1 to the content of the memory cell or +1 to the current address.

The following work has been carried out at the IBR-2 spectrometers:

- In the reported year, at the NSVR spectrometer, the VME-standard data acquisition system was in successful operation. Work to develop this system, specifically in the framework of the EPSILON and SKAT projects, has been performed.
- The equipment and software for the data acquisition and accumulation system in VME standard has been put into service at the NERA-PR spectrometer.
- At the HRFD spectrometer, the equipping of the VME-system has been completed. The subsystem for registering low-resolution spectra (including the TCC-6 time-to-code converter, histogram memory with a capacity of 2 Mbyte, block for encoding the detector number with 16 inputs, software, etc.), has been fully adjusted. Four DSPTMS320C51-based

RTOF-analyzers were constructed and adjusted, and tests for accumulating high-resolution spectra were conducted. In the near future, the system will be put into operation.

- Equipment in VME standard has been designed and constructed for the SAX X-ray diffractometer. In October 1996, the system was turned over to the programmers to adjust the software. The multi-parameter measuring system for the ionization chamber with two grids, used in experiments at IBR-30, was adjusted and put into operation.

Sample environment control systems. The control equipment of the step motors for goniometers, neutron scanners, shutters, devices for changing samples, etc., is an important part of the above-mentioned VME-systems at the NSVR, NERA-PR and HRFD spectrometers. This equipment is based on the developed unified power amplifier blocks and standard input/output registers.

The system for acquiring analog parameters for different types of sensors has been developed and tested.

The prototype of the block for controlling the neutron choppers, which is based on the K1816 BE31 microprocessor controller, was constructed. The microprograms for the controller and the service software for the PC of the operating personnel were written. At present, tests on the beam are nearing completion and the preparations for the manufacturing of these blocks for all choppers are being made.

The Euroterm standard temperature regulators were put into operation at the YuMO, SPN, DIN-2, and DN-2 spectrometers. The low-level software to connect the Euroterm regulators to the PCs and VME-based equipment was designed. At a number of spectrometers, these temperature regulators have been mounted and are ready for operation. The delays are caused by the acute shortage of programmers.

The system for correlation analysis of the power pulses of the IBR-2 reactor and for measuring the vibrations of the movable reflector has been completed. Work to create a system for monitoring the power pulses of the reactor and the condition of the shutters has been performed. The operation of this system is being tested.

Software for data accumulation and control systems of the spectrometers. The PC software for a number of spectrometers has been upgraded.

The low-level software was designed for the VME system at the NERA-PR spectrometer. It comprises modules for the motor control equipment, for exercising control over the data accumulation system, the parameters of the spectrometer and the devices for controlling and maintaining a constant temperature at the samples (Euroterm-902/906, LTC-60). These programs make it possible to control the experiment in interactive and automatic modes. The automatic mode is realized by creating a command file and executing it by the standard interpreter of the OS-9 – Shell operating system.

At the HRFD spectrometer, the low-level software for the equipment for accumulating low-resolution spectra and equipment for controlling the motors of the mechanical units of the diffractometer was designed for the VME-based system.

The software of the NSVR spectrometer has been considerably developed and upgraded.

The prototype of the unified control system for the spectrometers was developed for the VME-based systems under the OS-9 real-time operating system. This makes it possible to configure the control software of a specific spectrometer from the set of control and interface modules realized according to certain rules. The program manager plays a key role in this software. It provides the connection between the interface and control modules by means of the

Sockets mechanism using TCP/IP protocol, synchronizes access to the control modules, controls the state of the elements of the spectrometer, and checks the access to them for correctness. It also controls the user's rights to operate the system, manages the system configuration (inclusion or exclusion of spectrometer devices from the working configuration), and provides information on the state of the system as a whole and specific devices or subsystems.

The developed technique for programming the control modules allows one to use the same modules for the control systems of different spectrometers without making any changes, but only adjusting them to the specific configuration and parameters of the devices and subsystems. The new modules design does not require that the modules written previously be changed. The software as designed enables one to use the modules in both interactive and automatic modes. For this purpose, we use standard solutions accepted by the UNIX and OS-9 operating systems that make the realized solutions compatible with other platforms and operating systems, since the software is available in all modern operating systems.

The interface program modules are realized on the SUN SPARCStation 2 (20) and make it possible to control the system in interactive mode. They also can be used as commands to design the interpreted program for measurements in automatic mode. In the future, this new software will allow us to realize a graphic user interface on SUN SPARCStation. The TCL/TK package is to be used for this purpose.

Development of the SUN-cluster and network infrastructure. In the reported year, work to install, support, and service the hardware and software of PCs and workstations was carried out. In particular, the system software was reinstalled or corrected on more than 80 PCs. Disks where defects were detected were excluded from the SUN-cluster configuration and new disks with larger capacities were included by correcting the system configuration on the SUN stations accordingly.

Six X-terminals were adjusted and integrated into the SUN-cluster. A number of them were not only integrated into the local network, but were also put into service as the console terminals of VME-systems. The system programs of the SUN-cluster were modernized or corrected to provide better protection of the system against unsanctioned access, as well as new versions of a number of program products (MAKE, GHOSTSCRIPT, EMACS, TCK/TK, PEARL, etc.) were installed. The software for the network printers was upgraded on the basis of the experience gained during a year of service. The software supporting the terminal mode and the mode of IP connection via the PPP protocol was designed to obtain remote access to the SUN-cluster machines via modems.

New commercial software packages (PV-WAVE v.6.04, POWERVIEW, XILINX) were installed on the SUN-cluster machines and software support of the above-mentioned products is being provided. For the PV-WAVE package, freely distributed additional libraries were installed. These libraries make it possible to save images created by PV-WAVE as files in the standard graphic formats (specifically, GIF), which can be used to create files in the HTML format for the Web.

On the basis of the PV-WAVE package, software to access, visualize, and treat neutron spectra accumulated at different spectrometers of the IBR-2 reactor was developed. In particular, software to import neutron spectra was designed for 14 spectrometers. In addition, a general data format for neutron spectra was developed, which also includes the parameters saved along with the spectra by the different data acquisition programs running at these spectrometers. The parameters are divided into two groups: the so-called spectrum parameters (used directly in the

treatment of spectra) and the comments to the spectra (an extendible set of text parameters). Also among the component parts of this format are the spectrum statistic errors and the current accumulation of X-coordinates, which can assume the values of time-of-flight channels, wavelengths, transfer momenta, etc. While importing spectra from any of the 14 spectrometers into the PV-WAVE package medium, the data structure is formed in accordance with the developed data format, which is transparent to treatment procedures and can be saved on disk (and read out later) when exporting data in the general format. The proposed data format can be considered as an intermediate between the formats available at the IBR-2 spectrometers and the HADES (NEXAS) international neutron data format under discussion at the present time. The developed set of 24 procedures for treating spectra includes arithmetic and special operations, specifically, the conversion of spectra to different coordinate systems. Each operation is accompanied by a recalculation of the statistical errors for the resulting spectrum.

The designed software is available to any user of the FLNP SUN-cluster via the graphic user interface of PV-WAVE Point&Click 2.20 and the command interface of PV-WAVE Advantage 5.5 and 6.0. Short illustrated userguides for the packages of the PV-WAVE family and the developed software are available on the Web at:

http:/nfdfn.jinr.ru/flnph/pv/pv_info.html.

The information system on the activity of the Laboratory, as well as the means of presenting information materials on Web, were also further developed.

The channels of the IBR-30 reactor (IREN) and the spectrometers of the Scientific Department of Nuclear Physics were connected to the Ethernet network. The project to change the FLNP "backbone" network over to the Fast Ethernet standard with data-transfer rates of up to 100 Mbit/s was worked out. Based on the purchased network commutators CISCO 5000 and CISCO 2800, as well as the network adapters (10/100 Mbit/s) for SUN-type machines, work to switch over the "backbone" and servers to the Fast Ethernet standard has begun. The completion of the first stage of this work will significantly improve the intra-laboratory traffic and decrease the response time of computers of the Laboratory SUN-cluster.

It should also be noted that traffic to LCTA and on to the outside world will remain as before because the project to switch the JINR "backbone" over to the ATM standard was not financed in 1996.

7.1. STRUCTURE OF LABORATORY AND SCIENTIFIC DEPARTMENTS

Directorate:
Director:
V.L.Aksenov
Deputy Directors:
A.V.Belushkin
W.I.Furman
Scientific Secretary:
V.V.Sikolenko

Reactor and Technical Departments
Chief engineer: V.D.Ananiev
IBR-2 reactor
Chief engineer: A.V.Vinogradov
IBR-30 booster + LUE-40
Head: S.A.Kvasnikov
Nuclear physics and pulsed neutron sources sector
Head: V.L.Lomidze
Mechanical maintenance division
Head: A.A.Belyakov
Electrical engineering department
Head: V.P.Popov
Design office
Head: V.I.Konstantinov
Construction
Head: A.N.Kuznetsov

Scientific Departments and Sectors
Condensed matter department
Head: A.M.Balagurov
Nuclear physics department
Head: V.N.Shvetsov
Department of electronics, computers and networks
Head: V.I.Prikhodko
Department of IREN
Head: A.K.Krasnykh
Activation analysis and radiation research sector
Head: V.A.Sarin
Applied research sector
Head: V.I.Luschikov

Administrative Services
Deputy Director: S.V.Kozenkov
Secretariat
Finances
Personnel

Scientific Secretary Group
Translation
Graphics
Photography
Artwork

THE CONDENSED MATTER DEPARTMENT

Sub-Division	Title	Head
Group No.1	HRFD	V.Yu.Pomjakushin
Group No.2	DN-2	A.I.Beskrovnyi
Group No.3	DN-12	B.N.Savenko
Group No.4	NSVR	K.Ullemeyer
Group No.5	YUMO	M.A.Kiselev
Group No.6	SPN-1	Yu.V.Nikitenko
Group No.7	REFLEX	D.A.Korneev
Group No.8	NERA-PR	I.Natkaniec
Group No.9	KDSOG	A.Yu.Muzychka
Group No.10	EG-5	A.P.Kobzev
Group No.11	Automatization	E.S.Kuzmin

THE NUCLEAR PHYSICS DEPARTMENT

Sub-Division	Title	Head
Group No.1	Polarized neutrons and nuclei	V.P.Alfimenkov
Group No.1	Neutron spectroscopy	A.B.Popov
Group No.3	Nuclear reactions	Yu.S.Zamyatnin
Group No.4	Properties of the neutron	Yu.A.Alexandrov
Group No.5	Proton and α-decay	Yu.M.Gledenov
Group No.6	Properties of γ-quanta	A.M.Sukhovoy
Group No.7	Radiation capture of neutrons	G.P. Georgiev
Group No.8	Ultra-cold neutrons	V.N.Shvetsov
Group No.9	Neutron structure	G.S.Samosvat
Group No.10	Rare reactions	Yu.N.Pokotilovsky

7.2. USER POLICY

The IBR-2 reactor usually operates 10 cycles a year (2500 hrs. total) to serve the experimental programme. A cycle is established as of 2 weeks of operation for users, followed by a one week period for maintenance and machine development. There is a long shut-down period between the end of June and the middle of October.

All experimental facilities of IBR-2 are open to the general scientific community. The User Guide for neutron experimental facilities at FLNP is available by request from the Laboratory's Scientific Secretary.

Condensed matter studies at IBR-2 have undergone some changes in accordance with the experience gained during the last several years. It was found to be necessary to establish specialized selection committees formed of independent experts in their corresponding fields of scientific activities. The following four committees were organized:

1. Diffraction *Chairman* - V.A.Somenkov - Russia	3. Neutron optics *Chairman* - A.I.Okorokov - Russia
2. Inelastic scattering *Chairman* - J.Janik - Poland	4. Small angle scattering *Chairman* - L.Cser - Hungary

Dr. Vadim V. Sikolenko, Scientific Secretary of FLNP, is responsible for the user policy. Two deadlines for proposal submission are: May 16 - for the experimental period from October through February; and October 16 - for the period from March through June.

Scientific Secretary is responsible for:

- distribution of "Application for Beam Time" forms to potential users;
- registration of submitted proposals;
- reviewing of the proposals by instrument scientists to estimate the technical feasibility of the proposed experiment;
- sending of the approved proposals to Members of Selection Committees and registration of their comments and recommendations.

The IBR-2 beam schedules are drawn up by the head of the Condensed Matter Department together with instruments responsibles on the basis of experts recommendations and are approved by the FLNP Director or Deputy Director for condensed matter physics. The schedules are sent to Chairmen of Selection Committees.

After the completion of experiments, "Experimental Report" forms are filled out by experimenter(s) and submitted to the Scientific Secretary.

The Application Form and other information about FLNP are available by WWW: http://nfdfn.jinr.ru/~sikolen/usepol.html

Contact address:
***Dr. V.Sikolenko**, Frank Laboratory of Neutron Physics*
Joint Institute for Nuclear Research
141980 Dubna, Moscow region, Russia
Tel.: (+7)-095-926-22-53, (+7)-09621-65096, Fax: (+7)-09621-65085; (+7)-09621-65882;
E-mail: sikolen@nf.jinr.ru

7.3. CONFERENCES AND MEETINGS

In 1996, FLNP organized the following meetings:

1.	IV International Seminar on Interaction of Neutrons with Nuclei (ISINN-4)	April 27-30.	Dubna
2.	International Seminar on Relaxor Ferroelectrics	May 21-23	Dubna
3.	International Seminar "Polarized Neutrons in Condensed Matter Investigations	June 18-20	Dubna
4.	IV Russian-French Seminar on the Application of Neutron and Synchrotron Radiation for Condensed Matter Investigations	June 24 - July 2	Novosibirsk-Irkutsk

In 1997, FLNP will organize the following meetings

1.	International Seminar "Structure and Properties of Crystalline Materials" SPCM	March 4-7	Dubna
2.	V International Seminar on Interaction of Neutrons with Nuclei (ISINN-5)	May 13-16	Dubna
3.	National Conference on X-ray, Synchrotron, and Neutron Investigations (RSN-97)	May 26-29	Dubna-Moscow
4.	International Workshop on Data Acquisition Systems for Neutron Experimental Facilities (DANEF'97)	June 2-4	Dubna
5.	International Seminar "Neutron Analysis of Textures and Stresses NTSA,	June 23-27	Dubna

7.4. COOPERATION

List of Visitors from Non-Member States of JINR in 1996

Name	Organization	Country	Dates
K.Walther	FRZ, Rossendorf	Germany	10/01-16/02
G.Bottger	PSI, Villigen	Switzerland	18/01-27/01
H.Barthel	Wacker-Chemie GmbH, Burghausen	Germany	22/01-26/01
P.Spalthoff	TU Clausthal	Germany	29/01-16/02
J.-H.Schreiber	Ins. f. zerstoerungsfr. Pruef., Dresden	Germany	07/02-22/02
H.-G.Brokmeier	TU Clausthal	Germany	07/02-09/02
S.Haile	University of Washington, Seattle	USA	10/03-22/03

V.Passiouk	ILL, Grenoble	France	11/03-22/03
H.J.Lauter	ILL, Grenoble	France	15/03-22/03
K.Walther	FRZ, Rossendorf	Germany	22/03-26/04
T.Gutberlet	University, Leipzig	Germany	31/03-04/04
M.Rudalics	University, Linz	Austria	28/03-28/04
B.Meftah	CRN, Draria	Algeria	01/04-30/04
M.Azzoune	CRN, Draria	Algeria	01/04-30/04
M.Hempel	Ins. f. zerstoerungsfr. Pruef., Dresden	Germany	09/04-21/04
J.-H.Schreiber	Ins. f. zerstoerungsfr. Pruef., Dresden	Germany	11/04-14/04
J.Kalus	University, Bayreuth	Germany	13/04-17/04
M.-G.Roetlein	University, Bayreuth	Germany	13/04-17/04
H.J.Lauter	ILL, Grenoble	France	17/04-19/04
D.Reefman	NPB, Eindhoven	The Netherlands	11/05-17/05
M.L.Mestres Vila	University of Barcelona	Spain	12/05-24/05
K.Walther	FRZ, Rossendorf	Germany	14/05-24/05
J.-H.Schreiber	Ins. f. zerstoerungsfr. Pruef., Dresden	Germany	19/05-27/05
H.J.Lauter	ILL, Grenoble	France	04/06-14/06
V. Passiouk	ILL, Grenoble	France	04/06-14/06
O.Schaerph	ILL, Grenoble	France	17/06-23/06
E.Steinnes	University of Trondheim	Norway	13/06-17/06
K.Rahn	Univ. of Rhode Island	USA	18/06-25/06
H.-W.Schaeben	TU, Aachen	Germany	07/07-19/07
O.Verdie	Ecole Centrale	France	22/07-24/07
Mohamed Mounir Saad El-Din	Cairo University	Egypt	15/08-12/09
Jonghwa Chang	AERI, Seoul	South Korea	18/08-21/08
Guinyun Kim	Pohang Univ. of Science and Tech.	South Korea	18/08-21/08
D.D.Surmeli	University, Magdeburg	Germany	18/08-25/08
E.Steiness	Trondheim University	Norway	11/09-15/09
S.Ahmad	PLEVSOUND Ltd., London	UK	17/09-18/09
D.Schmidt	TU, Claustahl	Germany	13/10-30/10
T.Bhatia	LANL, Los Alamos	USA	24/10-25/10
M.Betzl	FRZ, Rossendorf	Germany	04/11-15/11
W.Boede	FRZ Rossendorf		04/11-15/11
P.Reichel	FRZ, Rossendorf	Germany	04/11-15/11
K.Walther	FRZ, Rossendorf		04/11-15/11
T.Gutberlet	University, Leipzig	Germany	10/11-17/11
J.-H.Schreiber	Ins. f. zerstoerungsfr. Pruef., Dresden	Germany	11/11-21/11

S.Skirl	TU, Darmstadt	Germany	11/11-21/11
C.Muench	University, Bayreuth	Germany	11/11-22/11
P.Spalthoff	TU, Clausthal	Germany	11/11-30/11
H.-G.Brockmeier	TU, Clausthal	Germany	12/11-17/11
M.A.Ali	NRC-AEA, Cairo	Egypt	14/11-14/02/97
M.R.El-Asser	NRC-AEA, Cairo	Egypt	14/11-04/12
K.Walther	FRZ, Rossendorf	Germany	25/11-05/12
C.Scheffzuek	GeoFRZ, Potsdam	Germany	25/11-10/12
H.Barthel	Wacker-Chemie GmbH, Burghausen	Germany	27/11-01/12

7.5. EDUCATION

The University Centre (UC) affiliated with the Joint Institute for Nuclear Research and based on the faculties of the Moscow State University and Moscow Engineering Physics Institute admits, for continuation studies, undergraduate students of the last two years of study in higher education institutions who have attended introductory specialized courses or lectures in the following topics: particle physics, nuclear physics, investigation of condensed matter at nuclear reactors and accelerators, radiation biology. The second and third specializations are in line with research performed at FLNP, which has at its disposal a good experimental base for both sectors comprising the the IBR-2 reactor and the IBR-30 booster pulsed neutron sources.

The education courses and practical training for the students affiliated with FLNP have been organized, to a large extent, to prepare specialists in neutron physics for both the Laboratory and for other Russian neutron centres.

As an example illustrating this aim, we present the list of courses taught by lecturers of the Condensed Matter Physics Chair of the UC (Head: Prof.V.L.Aksenov):

- theoretical methods in condensed matter physics
- methods of investigation of condensed matter at nuclear reactors and accelerators
- fundamentals of neutron physics and neutron sources
- methods for structure analysis of ideal and real crystals
- synchrotron radiation spectroscopy of solid matter
- influence of radiation on solid-state properties
- methods of experimental data processing.

A number of leading FLNP scientists take part in delivering these courses. Each student is allowed access to the Laboratory's computer network. An obligatory condition for successful completion of the 4th year is the capability to use modern personal computers. Earlier, students were included in the research groups led by their instructors, which made it possible for undergraduate students working on their theses to take part in preparing or performing experiments.

In 1996, the teaching process at UC continued successfully. Ten students who had their UC training course at FLNP were employed by JINR or other scientific centers in Russia.

The Condensed Matter Physics Chair gave graduation certificates to its fourth group of students in the reported year. This group had 9 students, making the total number of students

who have graduated from the Chair, 39. Two of them have been employed by FLNP and who have renewed the staff of the FLNP Scientific Department of Condensed Matter Physics to a noticeable degree.

7.6. PERSONNEL

Distribution of the Main Staff Personnel per Department as of 31.12.96

Departments	Permanent personnel			Contracts			Trainees
	S.	E. & T.	St.	S.	E. & T	St.	
Nuclear Physics Department			1	34.5	7	5.5	5
Personnel of the Directorate				15	1		
Condensed Matter Physics Department	2	1		39.5	8	6	2
Personnel of the Directorate				23	2		
Physical and Technical Research Sector	5	2		2		1	
Activation Analysis Sector	2	5			3		
Personnel of the Directorate				5	1		
Department of Electronics, Computers and Networks				17	25	9	
Personnel of the Directorate				1			
IREN Department	4			3	5	3	
Personnel of the Directorate				2	1		
Nuclear Safety Sector				6	1	1	
IBR-30 Department					17	3	
IBR-2 Department					40	7	
Technical services:							
Mechanical and Technical Department					12	48	
Electric and Technical Department		1	2		11	22	
Personnel of the Directorate					1		
Central Experimental Workshops,			5		6	31	
Design Bureau,		3			8		
Tool and Cleaning Services			7		1		
Management Services			1		17	8	
Personnel of the Directorate					1		
	41 (7.8%)			483.5 (92.2%)			
Total	**524.5 (100%)**						

Comment: S. - Scientists, E. & T - Engineers & Technicians, St. - Staff.

Personnel of the Directorate as of 31.12.96

Country	People
Azerbaijan	3
Armenia	1
Bulgaria	3
Germany	2
Georgia	4
KPDR	2
Kazakhstan	1
Mongolia	2
Poland	9
Romania	5
Russia	13
Slovakia	1
Ukraine	1
United States	1
Vietnam	2

7.7. FINANCE

Financing of the FLNP Scientific Research Plan in 1996

No.	Theme	Financing plan, $ th.	Expenditures for 12 months, $ th.	In % of FLNP budget
I	**Condensed matter physics**	**3731.9**	**3169.9**	**84**
	-0864-	2002.9	2020.2	100
	-0851-	1242.1	600.7	48
	-1012-	399.5	437.9	109
	-0975-	87.4	111.1	127
II	**Neutron nuclear physics**	**1034.1**	**1199.0**	**115**
	-0974-	548.8	598.1	109
	-0993-	485.3	600.9	123
III	**Elementary particle physics** -1007-	**5.6**	**13.2**	**235**
IV	**Relativistic nuclear physics** -1008-	**38.1**	**13.7**	**36**
V	**TOTAL:**	**4809.7**	**4395.8**	**91**

The part of the JINR budget assigned to FLNP (%)

Year	Plan	Fact
1992	21.70	13.30
1993	16.70	14.70
1994	16.80	13.00
1995	19.01	18.20
1996	19.9	18.7

Celebration of the 40th anniversary of JINR. Director of the Frank Laboratory of Neutron Physics V.L.Aksenov (right) and Director of the Flerov Laboratory of Nuclear Reactions Yu.Ts.Oganessian (left) presented with the Officer's cross, the order of merit of Poland.

FLNP Deputy Directors W.I.Furman (left) and A.V.Belushkin (right).

Prof. G.Bauer prepares for the neutron scattering experiment.

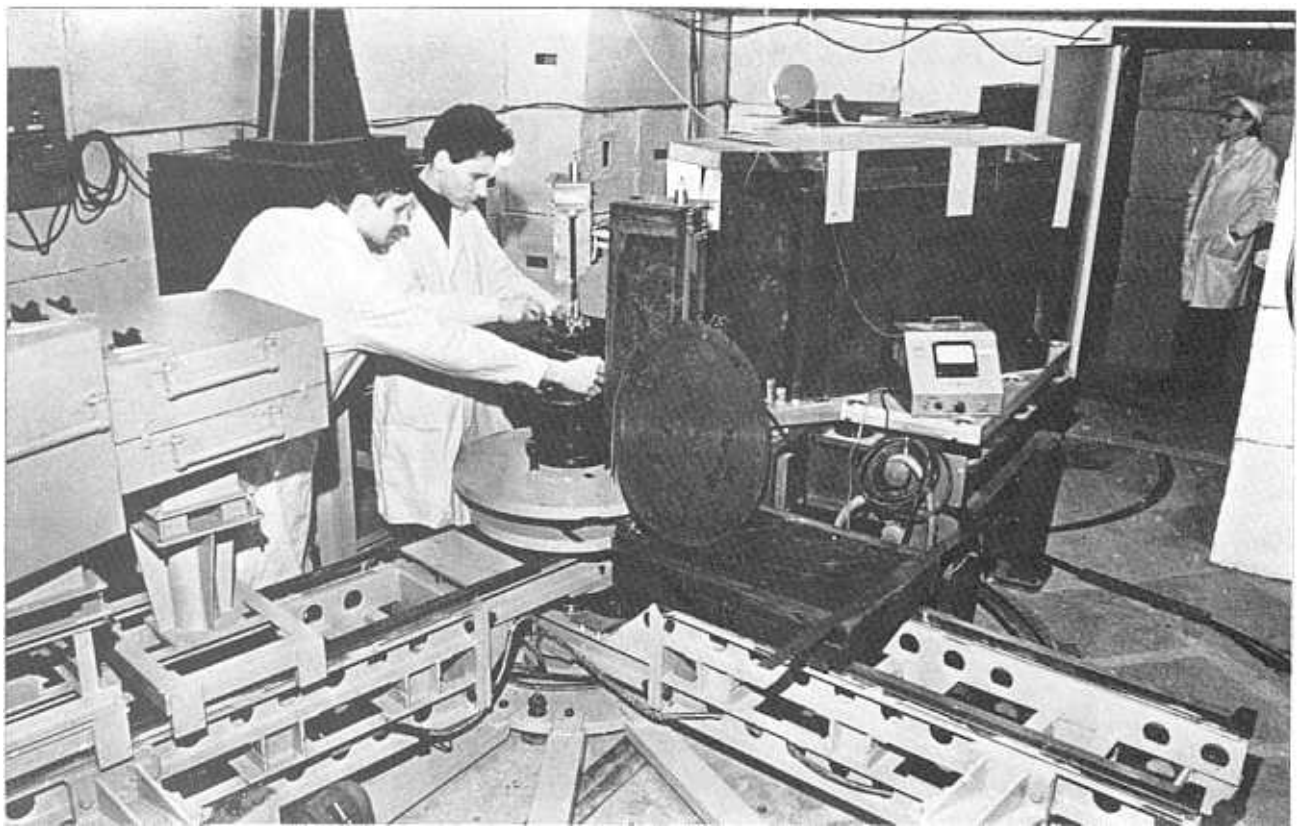

G.Bokuchava and V.Sikolenko adjust the sample on the HRFD diffractometer.

The REFLEX-P spectrometer commissioned in 1996.

Prof. V.Somenkov demonstrates the high pressure cells for the DN-12 spectrometer.

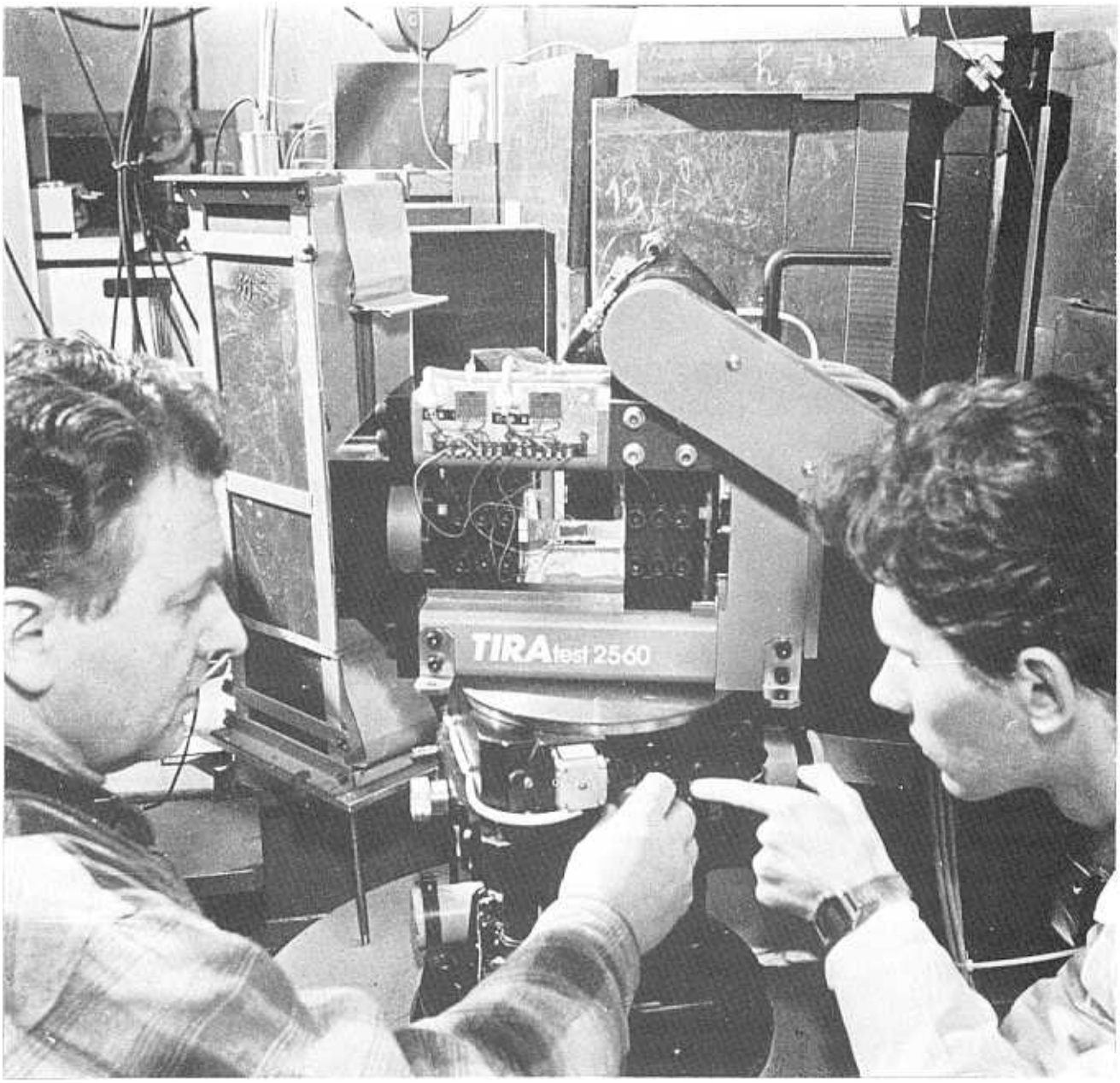

Prof. J.Schreiber and G.Bokuchava adjust the loading machine.

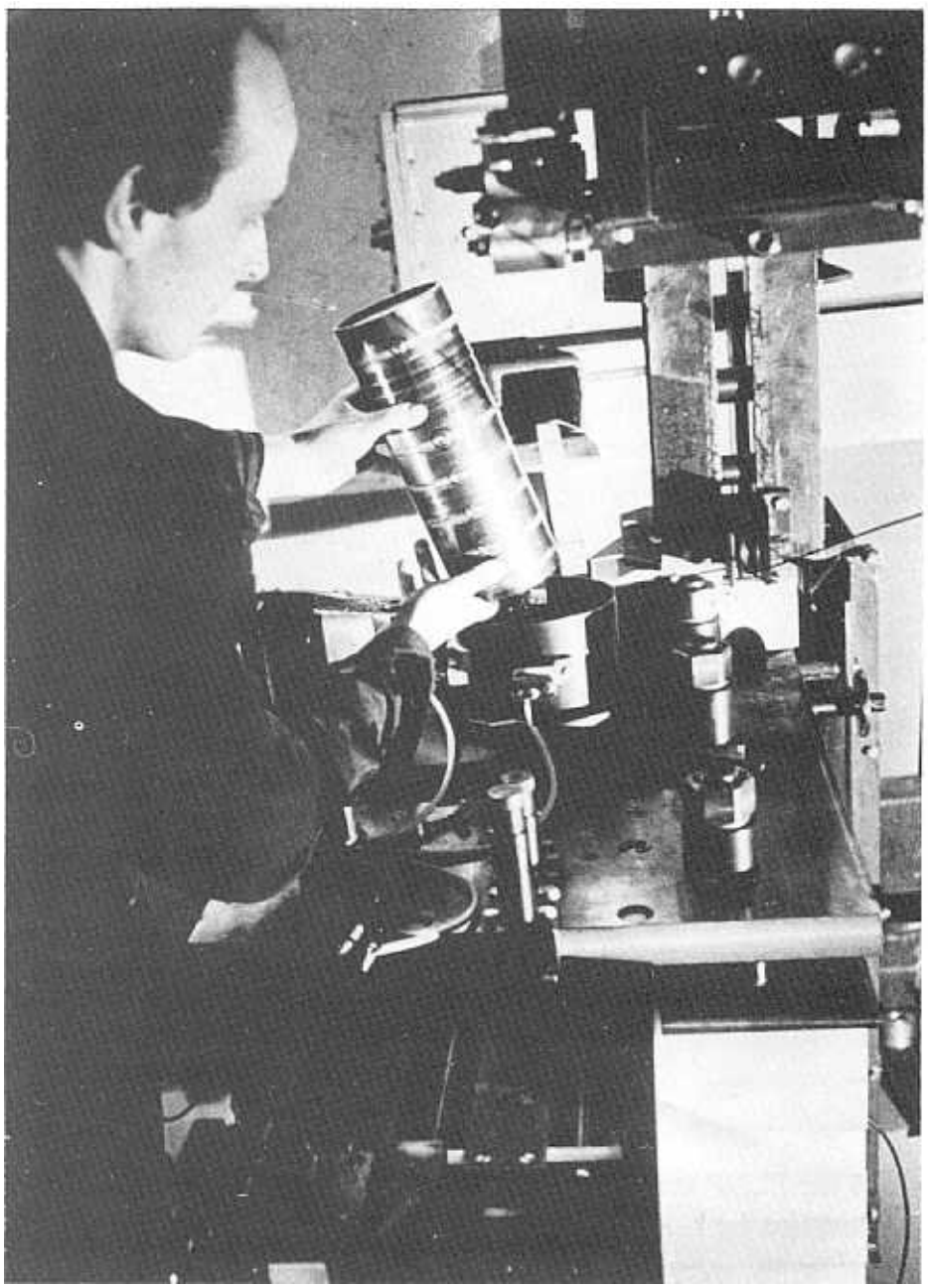

G.Nekhaev installs the container for ultracold neutron.

The performance of the FLNP amateur theater devoted to the 40th anniversary of JINR.
The scenario and direction by L.K.Kulkin.